MOLECULAR CHARACTERIZATION OF β-HEXOSAMINIDASE A DEFICIENCY IN A LATE-ONSET G_{M2} GANGLIOSIDOSIS TYPE I PATIENT

BY

EMMANUEL PETROULAKIS

A Thesis
Submitted to the Faculty of Graduate Studies
in Partial Fulfilment of the Requirements
for the Degree of

MASTER OF SCIENCE

Department of Biochemistry and Molecular Biology
University of Manitoba
Winnipeg, Manitoba

ISBN 0-612-16231-1

Name _____

Dissertation Abstracts International and *Masters Abstracts International* are arranged by broad, general subject categories. Please select the one subject which most nearly describes the content of your dissertation or thesis. Enter the corresponding four-digit code in the spaces provided.

SUBJECT TERM

MOLECULAR BIOLOGY

SUBJECT CODE 0307 UMI

Subject Categories

THE HUMANITIES AND SOCIAL SCIENCES

COMMUNICATIONS AND THE ARTS
Architecture 0729
Art History 0377
Cinema 0900
Dance 0378
Design and Decorative Arts 0389
Fine Arts 0357
Information Science 0723
Journalism 0391
Landscape Architecture 0390
Library Science 0399
Mass Communications 0708
Music 0413
Speech Communication 0459
Theater 0465

EDUCATION
General 0515
Administration 0514
Adult and Continuing 0516
Agricultural 0517
Art 0273
Bilingual and Multicultural 0282
Business 0688
Community College 0275
Curriculum and Instruction 0727
Early Childhood 0518
Elementary 0524
Educational Psychology 0525
Finance 0277
Guidance and Counseling 0519
Health 0680
Higher 0745
History of 0520
Home Economics 0278
Industrial 0521
Language and Literature 0279
Mathematics 0280
Music 0522
Philosophy of 0998
Physical 0523
Reading 0535
Religious 0527
Sciences 0714
Secondary 0533
Social Sciences 0534
Sociology of 0340
Special 0529
Teacher Training 0530
Technology 0710
Tests and Measurements 0288
Vocational 0747

LANGUAGE, LITERATURE AND LINGUISTICS
Language
- General 0679
- Ancient 0289
- Linguistics 0290
- Modern 0291
- Rhetoric and Composition 0681

Literature
- General 0401
- Classical 0294
- Comparative 0295
- Medieval 0297
- Modern 0298
- African 0316
- American 0591
- Asian 0305
- Canadian (English) 0352
- Canadian (French) 0355
- Caribbean 0360
- English 0593
- Germanic 0311
- Latin American 0312
- Middle Eastern 0315
- Romance 0313
- Slavic and East European 0314

PHILOSOPHY, RELIGION AND THEOLOGY
Philosophy 0422
Religion
- General 0318
- Biblical Studies 0321
- Clergy 0319
- History of 0320
- Philosophy of 0322

Theology 0469

SOCIAL SCIENCES
American Studies 0323
Anthropology
- Archaeology 0324
- Cultural 0326
- Physical 0327

Business Administration
- General 0310
- Accounting 0272
- Banking 0770
- Management 0454
- Marketing 0338

Canadian Studies 0385
Economics
- General 0501
- Agricultural 0503
- Commerce-Business 0505
- Finance 0508
- History 0509
- Labor 0510
- Theory 0511

Folklore 0358
Geography 0366
Gerontology 0351
History
- General 0578
- Ancient 0579
- Medieval 0581
- Modern 0582
- Church 0330
- Black 0328
- African 0331
- Asia, Australia and Oceania 0332
- Canadian 0334
- European 0335
- Latin American 0336
- Middle Eastern 0333
- United States 0337

History of Science 0585
Law 0398
Political Science
- General 0615
- International Law and Relations 0616
- Public Administration 0617

Recreation 0814
Social Work 0452
Sociology
- General 0626
- Criminology and Penology 0627
- Demography 0938
- Ethnic and Racial Studies 0631
- Individual and Family Studies 0628
- Industrial and Labor Relations 0629
- Public and Social Welfare 0630
- Social Structure and Development 0700
- Theory and Methods 0344

Transportation 0709
Urban and Regional Planning 0999
Women's Studies 0453

THE SCIENCES AND ENGINEERING

BIOLOGICAL SCIENCES
Agriculture
- General 0473
- Agronomy 0285
- Animal Culture and Nutrition 0475
- Animal Pathology 0476
- Fisheries and Aquaculture 0792
- Food Science and Technology 0359
- Forestry and Wildlife 0478
- Plant Culture 0479
- Plant Pathology 0480
- Range Management 0777
- Soil Science 0481
- Wood Technology 0746

Biology
- General 0306
- Anatomy 0287
- Animal Physiology 0433
- Biostatistics 0308
- Botany 0309
- Cell 0379
- Ecology 0329
- Entomology 0353
- Genetics 0369
- Limnology 0793
- Microbiology 0410
- Molecular 0307
- Neuroscience 0317
- Oceanography 0416
- Plant Physiology 0817
- Veterinary Science 0778
- Zoology 0472

Biophysics
- General 0786
- Medical 0760

EARTH SCIENCES
Biogeochemistry 0425
Geochemistry 0996
Geodesy 0370
Geology 0372
Geophysics 0373
Hydrology 0388
Mineralogy 0411
Paleobotany 0345
Paleoecology 0426
Paleontology 0418
Paleozoology 0985
Palynology 0427
Physical Geography 0368
Physical Oceanography 0415

HEALTH AND ENVIRONMENTAL SCIENCES
Environmental Sciences 0768
Health Sciences
- General 0566
- Audiology 0300
- Dentistry 0567
- Education 0350
- Administration, Health Care 0769
- Human Development 0758
- Immunology 0982
- Medicine and Surgery 0564
- Mental Health 0347
- Nursing 0569
- Nutrition 0570
- Obstetrics and Gynecology 0380
- Occupational Health and Safety 0354
- Oncology 0992
- Ophthalmology 0381
- Pathology 0571
- Pharmacology 0419
- Pharmacy 0572
- Public Health 0573
- Radiology 0574
- Recreation 0575
- Rehabilitaion and Therapy 0382
- Speech Pathology 0460
- Toxicology 0383

Home Economics 0386

PHYSICAL SCIENCES
Pure Sciences
Chemistry
- General 0485
- Agricultural 0749
- Analytical 0486
- Biochemistry 0487
- Inorganic 0488
- Nuclear 0738
- Organic 0490
- Pharmaceutical 0491
- Physical 0494
- Polymer 0495
- Radiation 0754

Mathematics 0405
Physics
- General 0605
- Acoustics 0986
- Astronomy and Astrophysics 0606
- Atmospheric Science 0608
- Atomic 0748
- Condensed Matter 0611
- Electricity and Magnetism 0607
- Elementary Particles and High Energy 0798
- Fluid and Plasma 0759
- Molecular 0609
- Nuclear 0610
- Optics 0752
- Radiation 0756

Statistics 0463

Applied Sciences
Applied Mechanics 0346
Computer Science 0984
Engineering
- General 0537
- Aerospace 0538
- Agricultural 0539
- Automotive 0540
- Biomedical 0541
- Chemical 0542
- Civil 0543
- Electronics and Electrical 0544
- Environmental 0775
- Industrial 0546
- Marine and Ocean 0547
- Materials Science 0794
- Mechanical 0548
- Metallurgy 0743
- Mining 0551
- Nuclear 0552
- Packaging 0549
- Petroleum 0765
- Sanitary and Municipal 0554
- System Science 0790

Geotechnology 0428
Operations Research 0796
Plastics Technology 0795
Textile Technology 0994

PSYCHOLOGY
General 0621
Behavioral 0384
Clinical 0622
Cognitive 0633
Developmental 0620
Experimental 0623
Industrial 0624
Personality 0625
Physiological 0989
Psychobiology 0349
Psychometrics 0632
Social 0451

THE UNIVERSITY OF MANITOBA

FACULTY OF GRADUATE STUDIES

COPYRIGHT PERMISSION

MOLECULAR CHARACTERIZATION OF B-HEXOSAMINIDASE A DEFICIENCY IN A LATE-ONSET G_{M2} GANGLIOSIDOSIS TYPE I PATIENT

BY

EMMANUEL PETROULAKIS

A Thesis/Practicum submitted to the Faculty of Graduate Studies of the University of Manitoba in partial fulfillment of the requirements for the degree of

MASTER OF SCIENCE

Dedication

To my Mother and Father

Acknowledgements

I extend my gratitude to Dr. Barbara Triggs-Raine who has helped me realize a career goal in science. I sincerely appreciate the time you made to guide me through scientific problems, to share your wisdom, and provide enthusiasm, confidence, and priceless criticism in my work. I feel fortunate to have had an exceptional supervisor, mentor, and friend. I am especially grateful that you were able to provide funding for my entire graduate program and for the opportunity to attend several scientific conferences. I feel indebted to you.

A very special thanks to Zhimin Cao for his comradery and for working with me on time-consuming and exhausting experiments. It was a very rewarding experience working with you, and I wish you a successful clinical post-doctoral fellowship.

To the members of my thesis committee, Dr. R.D. Gietz and Dr. D. Litchfield who have been valuable resources during my studies. I extend my appreciation for the effort of Dr. S. Pind who replaced Dr. Litchfield (now with the University of Western Ontario) upon short notice.

To the Department of Biochemistry and Molecular Biology for providing an excellent setting for graduate studies.

To my dearest friend, Deborah, for always being there from the beginning to experience with me every learning curve I've been through during my studies, for being there to share common goals and problems, and for understanding me.

Tim Salo, thanks for always providing humour and technical assistance as we worked at the bench together.

Helmut Dotzlaw, thank you for your technical advice.

To the past and most recent members of Dr. Triggs-Raine's lab, Brandy Wicklow, Brian Mark, Steve Wayne, Dr. Rick Hemming, Gillian Knells, Melanie Richard-Psooy, Cheryl Jerome, Kerri Wyant, and Adam Cheng, you have all left me with cherishable memories.

TABLE OF CONTENTS

LIST OF FIGURES

LIST OF TABLES

LIST OF ABBREVIATIONS

α	-	Alpha
A	-	Adenosine or adenine; also alanine
A_{260}	-	Absorbance at 260 nm 1 A_{260} unit=50 μg of double-stranded DNA 1 A_{260} unit=40 μg of single-stranded RNA 1 A_{260} unit=37 μg of single-stranded DNA
AEBSF	-	4-(2-aminoethyl)-benzenesulfonyl fluoride
Asn	-	Asparagine
ATP	-	Adenosine-5'-triphosphate
β	-	Beta
BSA	-	Bovine serum albumin
C	-	Cytosine or cytidine; also cysteine
°C	-	Degrees celsius
$CaCl_2$	-	Calcium chloride
cDNA	-	Complementary DNA
Ci	-	Curie=37 gigabecquerels
cm	-	Centimetre
cm^2	-	Square centimetres
CPB	-	Citrate phosphate buffer
cpm	-	Counts per minute
CO_2	-	Carbon Dioxide
D	-	Aspartic acid
dATP	-	Deoxyadenosine 5'-triphosphate
dCTP	-	Deoxycytosine 5'-triphosphate
dGTP	-	Deoxyguanosine 5'-triphosphate
D-MEM	-	Dulbeco's minimal essential medium
DMSO	-	Dimethylsulfoxide
DNA	-	Deoxyribonucleic acid
DTT	-	Dithiothreitol
dTTP	-	Deoxythymidine 5'-triphosphate
E	-	Glutamic acid
EDTA	-	Ethylenediamine tetraacetic acid
ER	-	Endoplasmic reticulum
FBS	-	Fetal bovine serum
g	-	Gram
G	-	Guanine or guanosine; also glycine
GalNAc	-	N-acetylgalactosamine
Glc	-	Glucose
GlcNAc	-	N-acetylglucosamine
GM2A	-	Human G_{M2} activator gene
H_2O	-	Water
H_3PO_4	-	Phosphoric acid

HCl	-	Hydrochloric acid
HEXA	-	Human *HEXA* gene
HEXB	-	Human *HEXB* gene
Hexa	-	Murine *Hexa* gene
Hexb	-	Murine *Hexb* gene
Hex A	-	β-hexosaminidase A
Hex B	-	β-hexosaminidase B
Hex S	-	β-hexosaminidase S
I	-	Current
IgG	-	Immunoglobulin G
IGF	-	Insulinlike growth factor
IVS	-	Intervening sequence
K	-	Lysine
kb	-	Kilobase
KCl	-	Potassium chloride
kDa	-	Kilodalton
KH_2PO_4	-	Potassium phosphate, dibasic
kV	-	Kilovolt
LB	-	Luria-Bertani
μCi	-	Microcurie
μL	-	Microlitre
M	-	Molar
mA	-	Milliamp
MCB	-	Membranous cytoplasmic bodies
mCi	-	Millicurie
mg	-	Milligram
$MgCl_2$	-	Magnesium chloride
Mg_2SO_4	-	Magnesium sulfate
mL	-	Millilitre
mm	-	Millimetre
mM	-	Millimolar
MOPS	-	3-(*N*-Morpholino) propanesulfonic acid
MPR	-	Mannose-6-phosphate receptor
M6P	-	Mannose-6-phosphate
4-MU	-	4-methylumbelliferone
4-MUG	-	4-methylumbelliferyl-2-acetamido-2-deoxy-β-D-glucopyranoside
4-MUG-β-gal	-	4-methylumbelliferyl-β-D-galactoside
4-MUGS	-	4-methylumbelliferyl-β-D-*N*-acetylglucosamine-6-sulfate
MWCO	-	Molecular weight cut-off
N	-	Amino-terminus; also asparagine
Na_2CO_3	-	Sodium carbonate
Na_2HPO_4	-	Sodium phosphate, dibasic
NaCl	-	Sodium chloride

NaH_2PO_4	-	Sodium phosphate, monobasic
NaN_3	-	Sodium azide
NaOH	-	Sodium hydroxide
NaP_i	-	Sodium phosphate
NeuAc	-	N-acetylneuraminic acid
NH_4Cl	-	Ammonium chloride
ng	-	Nanogram
nm	-	Nanometre
nmol	-	Nanomole
NP40	-	Nonidet-P40
OD	-	Optical density
Ω	-	Ohms
P	-	Phosphorus; also proline
pI	-	Isoelectric point
%	-	Percent
PAGE	-	Polyacrylamide gel electrophoresis
PBS	-	Phosphate buffered saline
PCR	-	Polymerase chain reaction
PEG	-	Polyethylene glycol
pfu	-	Plaque forming units
pmol	-	Picomole
RER	-	Rough endoplasmic reticulum
RNA	-	Ribonucleic acid
RNase	-	Ribonuclease
RT-PCR	-	Reverse transcription-polymerase chain reaction
rpm	-	Revolutions per minute
rRNA	-	Ribosomal RNA
S	-	Sulphur; also serine
s.a.	-	Specific activity
SA	-	Sialic acid
SAP	-	Sphingolipid activator protein
SD	-	Sandhoff disease
SDS	-	Sodium dodecyl sulphate
Ser	-	Serine
SRP	-	Signal recognition particle
SSC	-	Sodium citrate buffer solution
SSCP	-	Single-stranded conformational polymorphism
ssDNA	-	Single-stranded DNA
T	-	Thymidine
T_U	-	Upper threshold
T_L	-	Lower threshold
Taq	-	DNA dependent DNA polymerase from *Thermus aquaticus*
TBE	-	Tris borate/EDTA buffer
TBS	-	Tris buffered saline

TBS-T	-	Tris buffered saline with Tween-20
TEMED	-	N,N,N',N'- tetramethylethylenediamene
Tris	-	Tris (Hydroxymethyl) aminomethane
TSD	-	Tay-Sachs disease
U	-	Units
UDP	-	Uridine diphosphate
V	-	Volts
v/v	-	Volume/volume ratio
W	-	Watts; also tryptophan
w/v	-	Weight/volume ration
x	-	Times
x g	-	Times gravity

SUMMARY OF CONTRIBUTIONS

The work presented in this thesis is a compilation of work presented in abstracts. The work presented here has not been published as a research article at the present time. Work contributed by persons other than myself is acknowledged in the text.

ABSTRACT

A proband diagnosed with subacute G_{M2} gangliosidosis, Type I (late-onset Tay Sachs disease) was found to be compound heterozygous at the *HEXA* locus for a common 4-bp insertion and a novel G1422C transversion. The G1422C mutation, which results in a W474C amino acid substitution in the α-subunit protein of Hex A, was found to be responsible for partial Hex A activity in the proband. The mutation was characterized at the DNA, protein, and RNA levels.

The G1422C mutation was found to segregate through the father to both of his affected sons. Transient expression of the mutant α-subunit in Cos-7 cells demonstrated that this mutation could result in low levels of enzyme activity and mature α-subunit when it was co-expressed with the normal β-subunit to produce Hex A ($\alpha\beta$). This observation was consistent with the low levels of enzyme activity detected in proband fibroblasts and with the late-onset phenotype.

Pulse-chase analysis was used to demonstrate that the mutant α-subunit was synthesized in the rough endoplasmic reticulum, but it was not processed to its mature lysosomal form in proband fibroblasts. An early processing defect is suspected to be the cause of Hex A deficiency in the proband because the α-subunit was not phosphorylated on its high mannose oligosaccharide chains, a prerequisite for targeting of Hex A to the lysosome.

Northern blot analysis of total proband RNA detected an abnormally large *HEXA* mRNA species. Since the G1422C mutation occurred at the first nucleotide of exon 13, this mutation may cause abnormal splicing of *HEXA* mRNA.

It was concluded that the G1422C mutation is responsible for late-onset TSD phenotype in the proband and his brother. The mutation affects α-subunit protein processing and abnormal splicing may also account for a portion of the α-subunit deficiency associated with this mutation.

1 INTRODUCTION

1.1 Historical overview

Tay-Sachs disease (TSD) is an autosomal recessive genetic disorder that has been studied extensively for more than one century. Its name pays tribute to two scientists, Warren Tay, a British ophthalmologist, and Bernard Sachs, an American neurologist, who independently brought the general clinical manifestations to attention. A cherry-red spot in the retina of a 1-year-old mentally and physically retarded patient (Tay, 1881), and distended cytoplasm due to storage material in the neurons of affected patients particularily of Jewish origin (Sachs, 1887), were recognized as classic characteristics of TSD.

Initial biochemical studies of tissues from Tay-Sachs disease patients led to the identification (Klenk, 1935; Klenk, 1939; Klenk, 1942), and structural characterization (Svennerholm, 1962; Makita & Yamakawa, 1963; Ledeen & Salsman, 1965) of the storage material, G_{M2} ganglioside, in neuronal ganglion cells of affected patients. The absence of a hydrolase, hexosaminidase, that was preventing further breakdown of G_{M2} ganglioside was believed to be the cause of its accumulation.

Two forms of hexosaminidase were identified in spleen using electrophoretic analysis. One was a heat labile acidic protein called Hex A, and the second was a heat-stable basic protein called Hex B (Robinson & Stirling, 1968). The biochemical basis for TSD was better understood when the absence of Hex A was demonstrated in Jewish TSD patients, indicating Hex A deficiency was the underlying cause of TSD (Okada &

O'Brien, 1969 and Sandhoff, 1969). Both Hex A and Hex B were later shown to be absent in some atypical TSD patients and this was called Sandhoff disease (Sandhoff *et al.*, 1968; Sandhoff *et al.*, 1971). The difference in the thermal properties of Hex A and Hex B were essential in the development of a simple enzyme assay for the detection and quantification of Hex A in patient tissues (Kaback, 1972).

The availability of an assay to detect Hex A deficiency proved to be useful for identifying TSD carriers, particularly in Jewish familes where there was a high-incidence (1/3600) of TSD. The frequency of the disease has been drastically reduced since screening programs were implemented (Kaback, 1993).

Identification of Hex A as a heterodimer of one α- and one β-subunit, was essential in understanding that this enzyme was the product of two genes, *HEXA* and *HEXB*. It also provided the basis for the study of subunit association and other post-translational modifications that were essential for normal Hex A processing and function (reviewed in Gravel *et al.*, 1995). This knowledge was essential for demonstrating that the molecular basis of Hex A deficiency, in most cases, was significantly different in Jewish and non-Jewish patients.

Before the end of the 1980s, the α- and β-subunit genes of Hex A, *HEXA* and *HEXB*, respectively, were mapped in the human genome (Takeda *et al.*, 1990; Fox *et al.*, 1984), and their cDNAs were isolated (Korneluk *et al*, 1986; Proia & Soravia, 1987; Proia, 1988). The availability of this information was essential for identifying the mutations responsible for Hex A deficiency in TSD patients.

The identification of common TSD mutations and others associated with variants

of the disease had a significant impact in prenatal and carrier screening programs and in the clinical diagnosis of TSD. The clinical heterogeneity associated with the various forms of TSD attracted a considerable effort to establish genotype-phenotype relationships for mutations. These studies would be most useful for providing more reliable genetic counselling for carrier couples because some mutations have been found to be polymorphisms that do not result in disease.

A large number of mutations in the *HEXA* gene and their effects at the mRNA and protein levels have been examined (Gravel *et al.*, 1994). Now, there is evidence that mutations in the *HEXA* gene affect *HEXA* mRNA processing and targetting of Hex A to the lysosome.

By 1996, the disruption of both murine *Hexa* and *Hexb* genes (Yamanaka *et al.*, 1994; Yamanaka *et al.*, 1994; Sango *et al.*, 1995; Cohen-Tannoudji *et al.*, 1995; Taniike *et al.*, 1995; Phaneuf *et al.*, 1996), has provided animal models that could lead to therapeutic approaches for correcting the metabolic defect that causes TSD.

1.2 The G_{M2} gangliosidoses

1.2.1 "Classic" G_{M2} gangliosidosis

Catabolism of G_{M2} ganglioside (figure 1) catabolism is a well characterized biochemical process where a blockage at almost any point in the pathway (figure 2), corresponds to the accumulation of storage material such as G_{M2} ganglioside and a corresponding lysosomal storage disease (reviewed in Neufeld, 1991) such as Tay-Sachs (TSD) or Sandhoff disease (SD). The massive accumulation of G_{M2} ganglioside and other

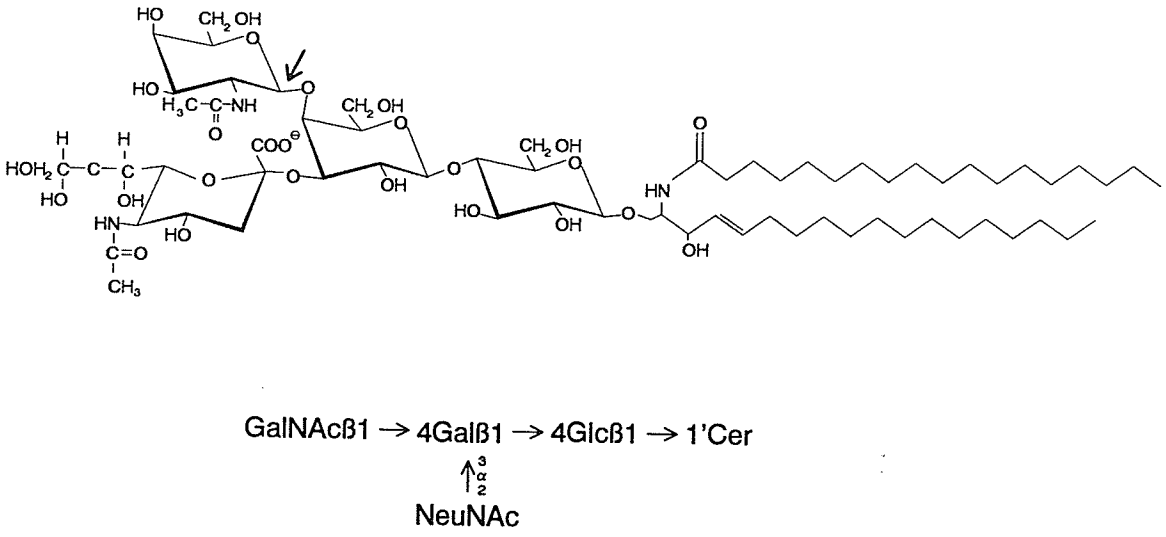

Figure 1 ***Structure of G_{M2} ganglioside.*** The arrow indicates the bond that is cleaved by β-hexosaminidase A. N-acetylgalactosamine in $\beta 1 \rightarrow 4$ linkage is removed.

related compounds, particularly in the neurons of patients, results in the development of membranous cytoplasmic bodies (MCBs) (Terry & Weiss, 1963). This became known as G_{M2} gangliosidosis, a term coined by Suzuki & Chen, 1967, that was due to a defeciency of the lysosomal hydrolase β-hexosaminidase A (Hex A).

Mutations in Hex A or Hex B, the two most abundant hexosaminidase isoenzymes, result in G_{M2} gangliosidosis (reviewed in Gravel *et al.*, 1995). Hex A is a heterodimer ($\alpha\beta$) comprised of an α- and a β-subunit, and Hex B ($\beta\beta$) is a homodimer comprised of β-subunits. Hex S ($\alpha\alpha$), a homodimer comprised of α-subunits, accounts for a small proportion of total hexosaminidase. The α- and the β-subunit are encoded by the *HEXA* and *HEXB* genes, respectively. Mutations in the *HEXA* gene result in TSD (G_{M2} gangliosidosis, Type I) and is also referred to as variant B because only active Hex B remains in these patients. Mutations in the *HEXB* gene result in Sandhoff disease (G_{M2} gangliosidosis, Type II) and is referred to as variant O because they result in a deficiency of both Hex A ($\alpha\beta$) and Hex B ($\beta\beta$). Variant AB is a third form of the disease that is caused by mutations in the G_{M2} activator, a small thermostable protein that is required for G_{M2} ganglioside hydrolysis by Hex A (Hechtman, 1977; Conzelmann & Sandhoff, 1978). Although a simple biochemical assay can detect the absence of either enzyme, TSD and SD are clinically indistinguishable and are collectively referred to as infantile acute G_{M2} gangliosidosis.

Figure 2 Ganglioside metabolism. The metabolic breakdown of G_{M1} ganglioside to ceramide is summarized. G_{M2} ganglioside is hydrolyzed by β-hexosaminidase A (Hex A) in the presence of the G_{M2} activator protein to produce G_{M3} ganglioside. An absence of Hex A results in Tay-Sachs disease. Similarily, an absence of almost any enzyme involved in ganglioside metabolism results in a lysosomal storage disorder (indicated in figure; reviewed by Neufeld, 1991).

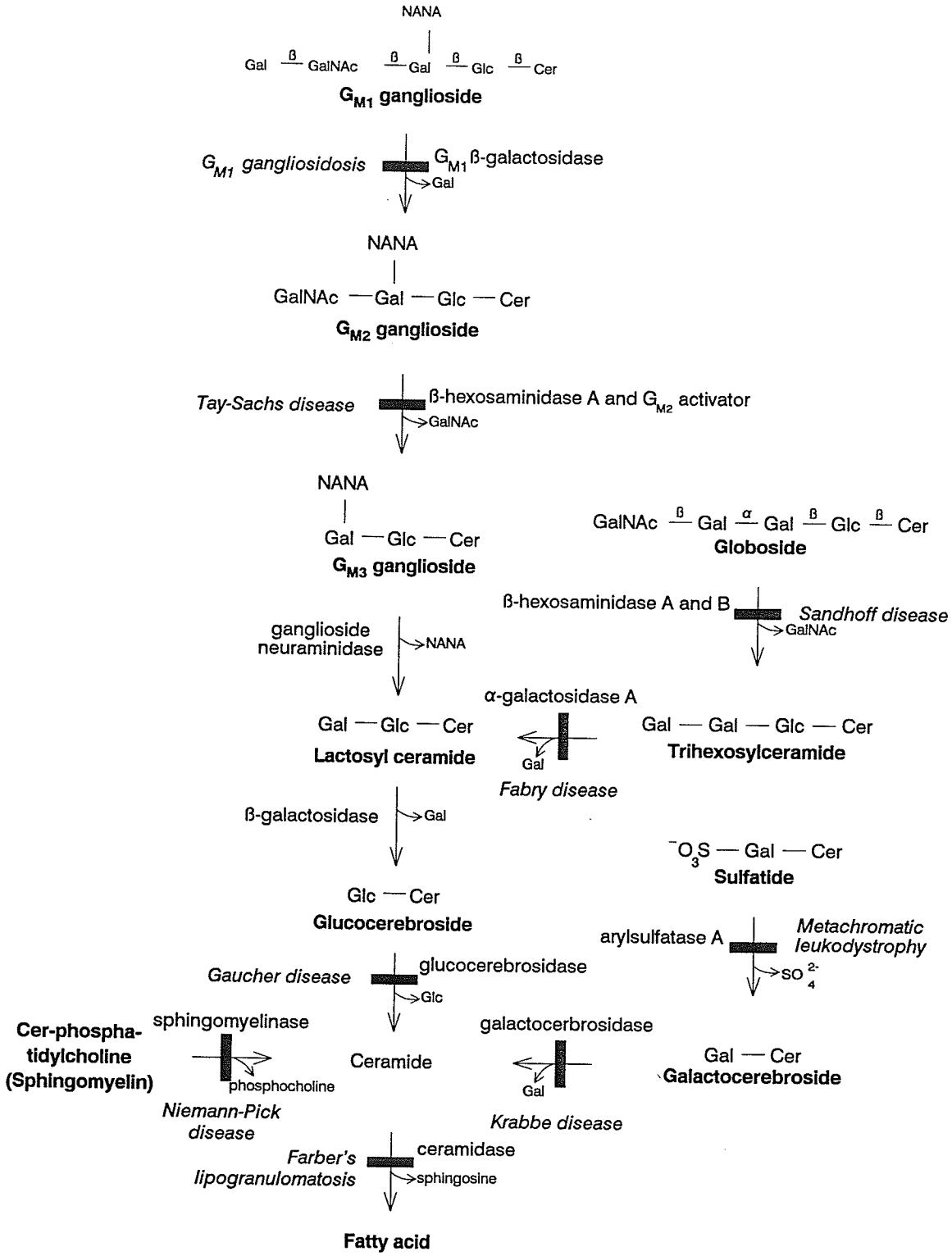
NANA
Gal ß GalNAc ß Gal ß Glc ß Cer
G$_{M1}$ ganglioside
G$_{M1}$ gangliosidosis
G$_{M1}$ ß-galactosidase
Gal
NANA
GalNAc — Gal — Glc — Cer
G$_{M2}$ ganglioside
Tay-Sachs disease
ß-hexosaminidase A and G$_{M2}$ activator
GalNAc
NANA
Gal — Glc — Cer
G$_{M3}$ ganglioside
GalNAc ß Gal α Gal ß Glc ß Cer
Globoside
ß-hexosaminidase A and B
Sandhoff disease
GalNAc
ganglioside neuraminidase
NANA
α-galactosidase A
Gal — Glc — Cer
Lactosyl ceramide
Gal
Gal — Gal — Glc — Cer
Trihexosylceramide
Fabry disease
ß-galactosidase
Gal
$^{-}O_3S$ — Gal — Cer
Sulfatide
Glc — Cer
Glucocerebroside
arylsulfatase A
Metachromatic leukodystrophy
SO_4^{2-}
Gaucher disease
glucocerebrosidase
Glc
sphingomyelinase
Cer-phospha-tidylcholine (Sphingomyelin)
phosphocholine
Ceramide
galactocerbrosidase
Gal
Gal — Cer
Galactocerebroside
Niemann-Pick disease
Krabbe disease
Farber's lipogranulomatosis
ceramidase
sphingosine
Fatty acid

1.2.2 Infantile acute, subacute, and chronic G_{M2} gangliosidosis

The clinical course of infantile TSD and SD (reviewed in Gravel *et al.*, 1995) is quite rapid and is characterized by symptoms classic of those described by Warren Tay and Bernard Sachs (Tay, 1881 and Sachs, 1887). After 8 to 10 months of age, affected infants present with progressive weakness, hypotonia, and loss of gross motor skills. The immediate sign of TSD is the prominence of the fovea centralis, the infamous cherry-red spot, under ophthalmoscopic examination. Although indistinguishable from Sandhoff disease, a Jewish heritage in the patient usually suggests TSD. Today, three common TSD mutations (see 1.5.1) are routinely screened for in Jewish carriers identified using a biochemical assay to detect Hex A deficiency. The presence of other non-neurological manifestations such as organomegaly, skeletal abnormalities, oligosaccharidurıa and storage cells in bone marrow are usually characteristic of Sandhoff disease.

Subacute and chronic G_{M2} gangliosidosis (late-onset TSD) are characterized by a less severe clinical course with more heterogeneous manifestations and a variable age onset (reviewed in Gravel *et al.*, 1995). Phenotypic variability is notable among siblings despite a similar genotypic basis for the disease (Navon, 1991). The mutations that cause late-onset TSD (see 1.4), appear to allow for small amounts of Hex A activity, delaying the neurological defects caused by accumulating G_{M2} ganglioside. Before mutations in the *HEXA* gene were known, the extent of Hex A deficiency as measured in fibroblasts with its natural substrate, G_{M2} ganglioside, was shown to be inversely correlated with the severity or onset of the disease (Conzelmann & Sandhoff, 1983). A recent study using a fluorescent ganglioside, sulforhodamine-G_{M1}, demonstrated a similar relationship *in vivo*

where significant differences between substrate metabolism in fibroblasts or white blood cells from adult-onset and infantile TSD patients were observed (Agmon *et al.*, 1996). Interestingly, the genetic basis of late-onset and infantile disease in the tissues used in the latter study were limited to the adult-onset mutation, G805A nucleotide substitution, and the 4-bp insertion, respectively (see 1.4). Therefore, the relationship of other allelic mutations to these studies remain to be explored. The relationship between Hex A levels and the severity of disease has recently been demonstrated in a mammalian transfection system (Brown and Mahuran, 1993). Expression of α-subunit mutants associated with late-onset TSD, resulted in higher levels of Hex A activity compared to mutants associated with infantile disease. For diagnostic purposes, two classes of late-onset TSD have been described (reviewed in Gravel *et al.*, 1994), (i) subacute G_{M2} gangliosidosis that includes late-infantile and juvenile-onset TSD, and (ii) chronic G_{M2} gangliosidosis, or adult-onset TSD.

Subacute G_{M2} gangliosidosis generally manifests between 1 and 9 years of age, and patients usually die in their midteens. Developmental regression, dementia, increasing spasticity, and psychomotor retardation are common symptoms. This phenotype has been described in patients with mutations in the *HEXA* or *HEXB* genes, including the B1 variant that is due to an α-subunit mutation that affects the catalytic activity of the Hex A enzyme (reviewed in Suzuki and Vanier, 1991).

Chronic G_{M2} gangliosidosis (adult-onset TSD), is generally indistinguishable from the subacute form but is classified based on a much later onset. It is less severe, usually affects patients in their second or third decade of life, and they usually survive to late

adulthood. Lower-motor-neuron, pyramidal tract and cerebellar deterioration are common characteristics, and in at least 50% of cases, stuttering and/or dysarthria are prominent features. Weakness, clumsiness, and gait disturbance (unsteady, wide-based walking) that appear in 50 to 60% of cases are important clues to the presence of a metabolic disorder. Movement disorders, including dysarthria and dyskinesia, have been described in similar proportions.

Psychosis usually precedes neurological abnormalities in 50% of cases (Navon *et al.*, 1981). Treatment for late-onset TSD is usually oriented toward treating the psychiatric disturbances despite the poor and unpredictable prognosis that is associated with the disease. The failure of anti-psychotic medicine probably reflects a lack of appreciation that metabolic disorders are associated with psychiatric disturbances.

The diagnosis of a metabolic disorder such as TSD may be impeded by other factors including an unawareness of a patient's cognitive decline or an insufficient reassessment of patients that are resistant to psychiatric drug therapy (Rosebush *et al.*, 1995). In the former, little evidence supports a correlation between TSD and cognitive decline. However, affected patients are often considered as being "slow learners" or as "always being this way." In the latter, the adequacy or appropriateness of the treatment is usually questioned and other diagnoses are usually considered before evidence for an underlying metabolic disorder is pursued.

1.3 The *HEXA* and *HEXB* genes and their cDNAs

The most striking features of the *HEXA* and *HEXB* genes are their high degree

of homology and structural similarity. There is over 50% coding sequence identity and both have 14 exons and 13 introns (figure 3) whose junctions are in corresponding positions, suggesting that they arose from a common ancestral gene (Proia, 1988).

The *HEXA* gene is approximately 35 kb in length and maps to chromosome 15q23→q24 (Takeda *et al.*, 1990). It has a GC-rich promoter region that contains possible TATA and CAAT box motifs (Proia & Soravia, 1987). The *HEXB* gene maps to chromosome 5q13 (Fox *et al.*, 1984). It is about 45 kb in length, and also has a GC-rich promoter region that contains several GC box-like and other consenus sequences matching those of various promoter elements (Neote *et al.*, 1988). The promoter regulatory elements responsible for both *HEXA* and *HEXB* expression were recently studied (Norfulus *et al.*, 1996).

An alignment of the primary structure of the α- and β-subunit proteins demonstrates several regions of identity (figure 4) that have been exploited in mutation studies to understand the structural and functional roles of particular amino acid residues in the α-subunit protein. The two most definitive studies were used to identify the α-subunit active site and to demonstrate that the G269S amino acid substitution, associated with late-onset TSD (Paw *et al.*, 1989), affects α-subunit stability (Brown & Mahuran, 1993). Moreover, mutation studies have suggested that conserved amino acids in the C-terminal region of both α- and β-subunit proteins are important for protein processing through the endoplasmic reticulum (Zokaeem *et al.*, 1987; Lau *et al.*, 1989; Paw *et al.*, 1990a; Paw *et al.*, 1991). The availability of sequences from other cloned hexosaminidases, particularily those of the murine *Hexa* (Beccari *et al.*, 1992) and *Hexb*

Figure 3 Genomic structure of the *HEXA* and *HEXB* genes. A comparison of the structural organization of the *HEXA* and *HEXB* genes (adapted from Proia, 1988). Exons are indicated by vertical bars and are separated by introns. Polyadenylation signals are indicated.

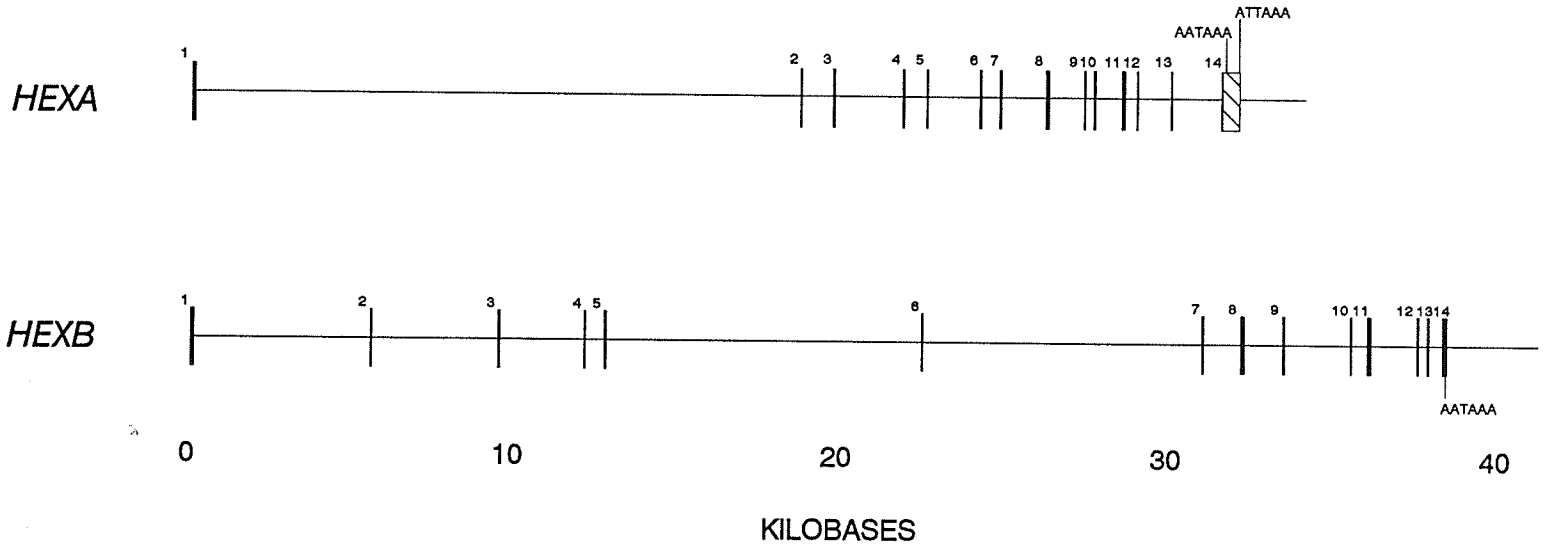
HEXA
1
2 3
4 5
6 7
8
9 10
11 12
13
14
AATAAA
ATTAAA
HEXB
1
2
3
4 5
6
7
8
9
10 11
12 13 14
AATAAA
0
10
20
30
40
KILOBASES

Figure 4 Alignment of the α- and β-subunit primary structures. Alignment of the α- and β-subunit proteins (adapted from Mahuran *et al.*, 1988). Amino acid identity is indicated by "*". The signal peptides are shaded and N-glycosylation sites are outlined (□) for each polypeptide. The location of introns in both proteins are found in corresponding positions.

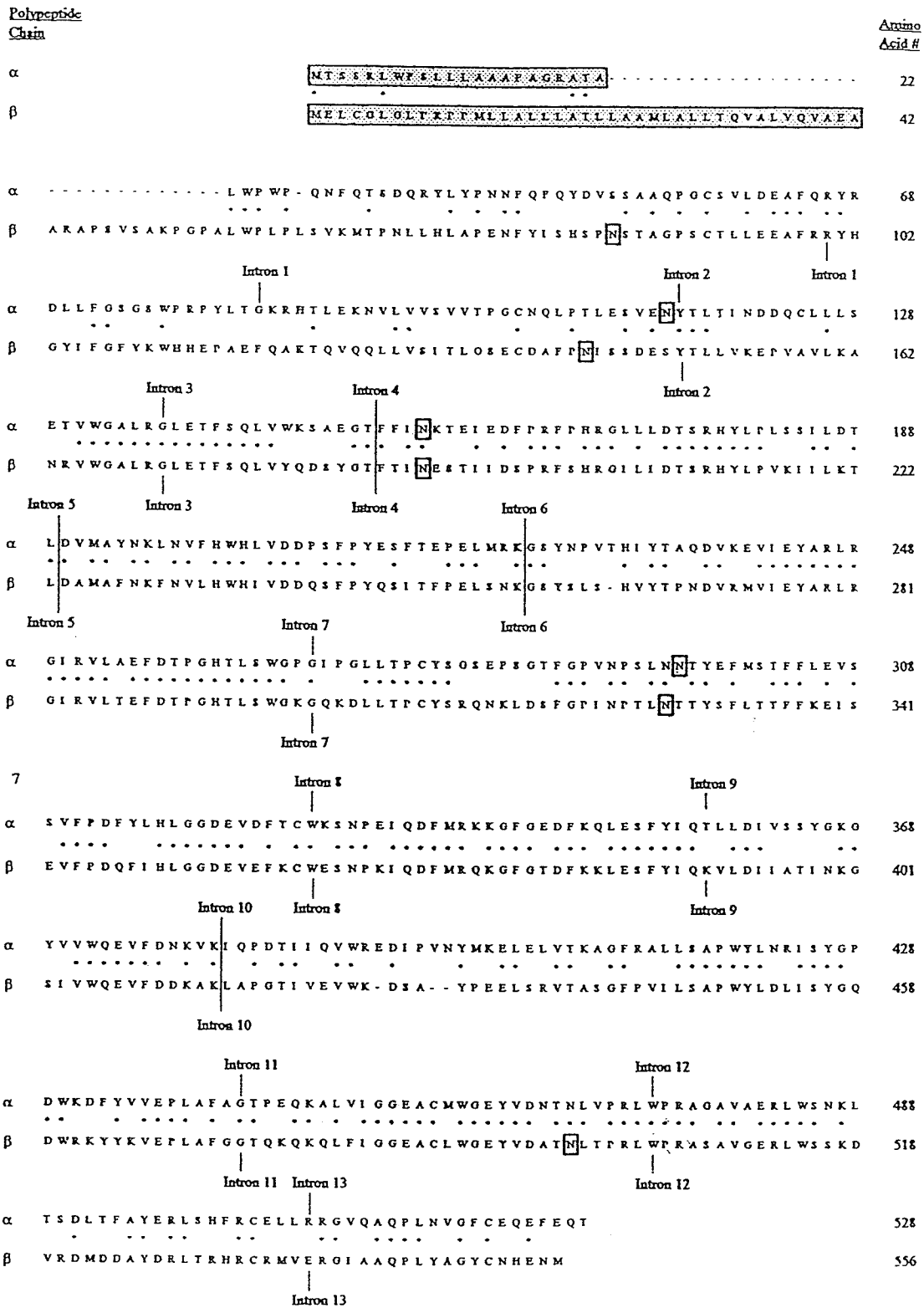
Polypeptide Chain
Amino Acid #
α
β
Intron 1
Intron 2
Intron 3
Intron 4
Intron 5
Intron 6
Intron 7
Intron 8
Intron 9
Intron 10
Intron 11
Intron 12
Intron 13

(Triggs-Raine *et al.*, 1994) genes and those of lower organisms have been useful for predicting the importance of particular amino acids based on their conservation. The structure and physical properties of the α- and β-subunits of hexosaminidase are best understood through an analysis of their biosynthetic and post-translational modification events that are described below.

1.4 Biochemistry of hexosaminidases

1.4.1 Biosynthesis and post-translational modifications

1.4.1.1 Biosynthesis and signal peptide cleavage of the α- and β-subunits of Hex A

Lysosomal proteins are synthesized on the ribosomes of the rough endoplasmic reticulum (RER). Their fate as glycoproteins is ensured by an N-terminal hydrophobic signal peptide (pre-sequence) (reviewed in Von Heijne, 1990), typically between 15 and 30 amino acids in length, that is cleaved by signal peptidase as newly synthesized proteins translocate to the lumen of the RER. During the synthesis of the α- and β-subunits, cleavage of the signal peptide is the first of two major proteolytic events. A second event occurs in the lysosome to give rise to a mature Hex A isoenzyme. Hence, newly-synthesized α- and β-subunit proteins translocating to the ER are referred to as pre-pro α- and β- subunits. The biological function of the signal peptide is to form a complex with the signal recognition particle (SRP) that forms a complex with the SRP-receptor (docking protein) at the surface of the rough endoplasmic reticulum (reviewed in Rapoport, 1992).

The signal peptide of the pre-pro-α-subunit is 22 amino acids in length and

exposes leucine-23 as the N-terminus following cleavage (Little *et al.*, 1988) (figure 4). The signal peptide of the pre-pro-β-subunit is 42 amino acids and exposes alanine-43 as the N-terminus (Quon *et al.*, 1989). The unusually large signal peptide of the β-subunit has been a subject for debate because there are three AUG codons upstream of the signal peptidase cleavage site that could be used as initiation codons. Although putative cleavage sites predict that translation could be initiated at methionine-26, initiation occurs preferentially at methionine 1 and 13 in a cell free translation system to give rise to an atypically large signal peptide (Quon *et al.*, 1989). Similarly, the lysosomal enzyme β-glucocerebrosidase has an atypically large signal peptide of 39-amino acids, although there are two initiation (AUG) codons that could be used *in vitro* (Sorge *et al.*, 1987).

1.4.1.2 Glycosylation in the endoplasmic reticulum

Co-translational glycosylation of newly-synthesized unfolded peptides occurs in the lumen of the RER. A dolichol intermediate that carries a common oligosaccharide block (figure 5) is transferred to an elongating polypeptide at Asn-X-Ser/Thr sequences, where X can be any amino acid except for Pro or Asp (reviewed Kornfeld and Kornfeld, 1985). The pro-α chain has 3 possible glycosylation sites at Asn 115, 157, 295 (Weitz & Proia, 1992). The pro-β chain has 5 possible sites, Asn 84, 142, 190, 327, and 497, although only the first four are preferentially glycosylated (O'Dowd *et al.*, 1988; Sonderfeld-Fresko & Proia, 1989; see Hirschberg and Snider, 1987 for a review of glycosylation reactions). Oligosaccharide trimming proceeds almost immediately by glucosidase I followed by trimming by action of glucosidase II, and subsequently by α1,2-mannosidase. N-linked oligosaccharide side chains play many roles, particularly

Figure 5 N-glycosylation and oligosaccharide processing. Transfer of the dolichol intermediate by oligosaccharyl-transferase to an Asn residue is shown. Modifications by enzymes and their location in the ER or particular Golgi compartments are indicated. Proteins destined for the lysosome attain an exposed phosphate (action of phosphodiesterase) that is recognized by a mannose-6-phosphate receptor. Other proteins are targetted toward the secretory pathway. M=mannose; G=glucose; GlcNAc=N-acetylglucosamine; Asn=asparagine; Gal=galactose; SA=sialic acid; Fuc=fucose; P=phosphate.

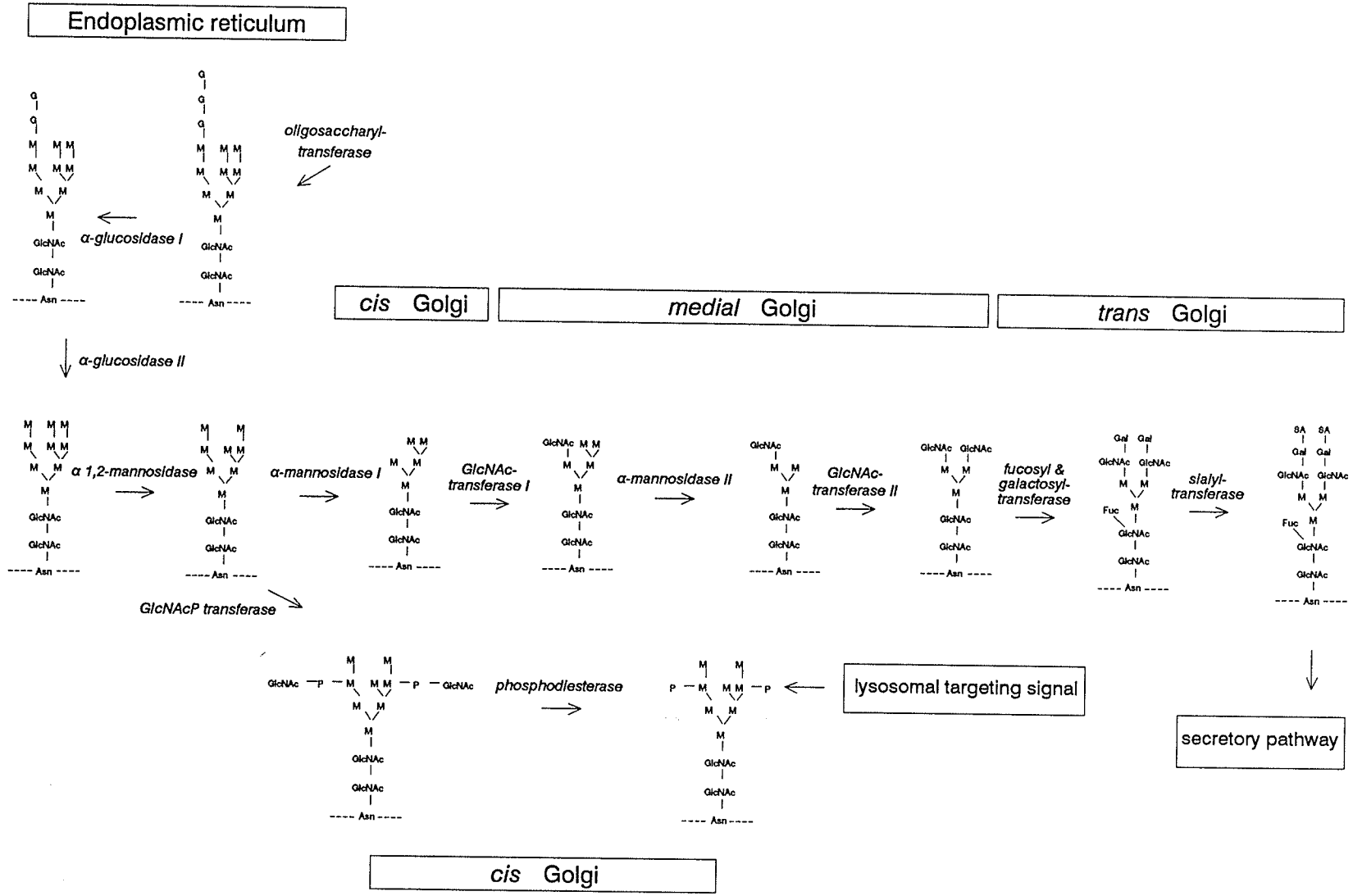
Endoplasmic reticulum
oligosaccharyl-transferase
α-glucosidase I
α-glucosidase II
cis Golgi
medial Golgi
trans Golgi
α 1,2-mannosidase
α-mannosidase I
GlcNAc-transferase I
α-mannosidase II
GlcNAc-transferase II
fucosyl & galactosyl-transferase
sialyl-transferase
GlcNAcP transferase
phosphodiesterase
lysosomal targeting signal
secretory pathway
cis Golgi

in mediating correct folding of the nascent polypeptide (reviewed in Helenius, 1994 and Fielder and Simons, 1995).

Proteins destined for the Golgi cisternae for further post-translational modification need to acquire an "exit-competent", or folded state, in the ER/salvage compartments where folding and oligomerization of most proteins is believed to occur. Correct folding in the lumen of the ER is mediated by a large number of chaperones and folding factors that are resident in the endoplasmic reticulum (reviewed in Gething and Sambrook, 1992 and Helenius *et al.*, 1992). One of these factors, BiP, has been shown to be involved with the retention of misfolded mutant proteins. However, the involvement of specific components of the folding machinery with the folding of normal or mutant α- and β-subunits has not been described. Once proper folding (and often oligomerization) has occurred, proteins are transported to the Golgi for further modifications. The mechanisms of protein sorting from the ER to the Golgi and subsequent sorting have been reviewed (Rothman & Wieland, 1996).

1.4.1.3 Phosphorylation of high-mannose chains in the Golgi cisternae

Soluble lysosomal proteins acquire phosphorylated mannose residues on oligosaccharide side chains that function as lysosomal sorting signals (reviewed in Kornfeld, 1990). Phosphorylation occurs in one or two events (figure 5). The first may occur in the ER/salvage compartment and is mediated by UDP-GlcNAc:lysosomal enzyme N-acetylglucosamine-1-phosphotransferase (phosphotransferase) that acts on the α-1,6 linked branch of the oligosaccharide and where it transfers GlcNAc-1-phosphate from UDP-GlcNAc. The second critical step in phosphorylation occurs at a later Golgi

compartment where the phosphomannosyl marker is exposed by the action of N-acetylglucosamine-1-phosphodiester-α-N-acetylglucosaminidase.

In the Golgi, oligosaccharide side chains undergo further trimming via α-mannosidase II, an enzyme that appears to have its highest activity in the mid-cisternae of the Golgi complex. Mannosidase II activity is followed by the addition of GlcNAc, galactose, and sialic acid. Since these modifications prevent phosphorylation, these proteins are targeted to the secretory pathway.

The significance of mannose-phosphorylation is illustrated by I-cell disease (mucolipidosis II) and pseudo-Hurler syndrome (mucolipidosis III) where a deficiency of N-acetylglucosamine transferase leads to a massive secretion of most lysosomal enzymes, resulting in a deficiency of lysosomal enzymes that require sorting in a mannose-6-phosphate-dependent fashion (Hasilik *et al.*, 1981; Reitman *et al.*, 1981). In contrast, non-lysosomal proteins have almost undetectable levels of phosphorylated mannose chains. Of all newly synthesized soluble lysosomal enzymes, phosphate has been found to be present in the high mannose chains of secreted proteins. In addition, a large proportion of lysosomal enzymes escape lysosomal sorting despite the presence of a phosphorylation sorting signal.

The extent of mannose phosphorylation may also determine the efficiency of sorting to the lysosome. A protein with two phosphomannosyl side chains, for example, has a higher affinity for the mannose-6-phosphate receptor in comparison to a protein with only one phosphomannossyl side chain (Hoflack *et el.*, 1987). Similarly, a diphosphorylated oligosaccharide side chain can be compensated by two singly

phosphorylated side chains. Taken together, not all newly-synthesized proteins are phosphorylated uniformly.

1.4.1.4 Sorting by mannose-6-phosphate receptors

Mannose-6 phosphate receptors (MPRs) ensure the targeting of newly-synthesized lysosomal enzymes harbouring phosphorylated mannose chains (reviewed in Kornfeld, 1992 and Hille-Rehfeld, 1995). Ligands likely bind the receptor in the *trans*-Golgi and are then trasported to the lysosome where the dissociation of the ligand-receptor complex is dependent on the reduced pH of the lysosome. Once dissociation occurs, the receptors could be recycled for further sorting of newly-synthesized proteins. Dissociation of receptor-ligand complexes *in vivo* could be prevented in cell culture by incubating tissues in the presence of a weak amine, such as NH_4Cl, that would increase the pH of the late-endosomal/pre-lysosomal compartments (Seglen, 1983). Eventually, all MPR ligand-binding sites become occupied and newly-synthesized lysosomal proteins would be missorted toward the secretory pathway.

Two MPRs, MPR46 and MPR300 (type I membrane proteins), that have apparent molecular masses of 46 kDa and 300 kDa, respectively, have been described as having unique functions (reviewed in Hille-Rehfeld, 1995). Phosphorylated ligands bind to the extracytoplasmic domain of MPR46 that is homologous to each of the repeating units of the extracytoplasmic domain of MPR300. MPR300 is also known to bind IGFII; however, its relationship to signal transduction events is still unclear. Although each MPR has a distinct function, they do share complementary roles in sorting of newly-synthesized proteins toward the lysosome or the secretory pathway (Pohlmann *et al.*,

1995). For example, the cellular uptake of extracellular ligands has been found to be possible through MPR300 (reviewed in Hille-Rehfeld, 1995).

The biological basis for two MPRs has never really reached a consensus. Pohlmann and colleagues suggested that if ligands bind both MPRs in the trans-Golgi network, then the distinct complementation in sorting may be due to several possible structures of mannose-6 phosphate markers that would give rise to several structural forms of soluble lysosomal enzymes (Pohlmann *et al.*, 1995). In combination with a preferential structure for binding, each MPR has a limited capacity and affinity for all ligands. Thus, the presence of both MPRs may ensure sufficient retention in the Golgi and sufficient targeting. Furthermore, the concise sorting of lysosomal from non-lysosomal enzymes in combination with various degrees of phosphorylation may have proven to be more efficient during evolution with two MPRs.

1.4.1.5 Limited proteolysis and other modifications in the lysosome

The α- and β-subunits undergo significantly different proteolytic modifications to produce their mature forms (figure 6). The mature α-subunit is approximately 54 kDa, it has leucine-90 exposed as its N-terminus (Little *et al.*, 1988). In addition, the mature α-subunit undergoes a change in molecular mass from 56 kDa to 54 kDa that cannot be accounted for by the removal of a 2 kDa peptide; this is caused by trimming of oligosaccharide side-chains and the removal of sialic acid (O'Dowd *et al.*, 1988). The mature β-subunit has been described as a tripeptide that is maintained by sulfhydryl bonds. Three peptides, "a", "b", and "c" are covalently bound in that order as observed from the C-terminus. The nomenclature for the "a" and "b" peptides was based on their

relative pIs; the more acidic peptide was termed the "a" peptide (pI=4.5-5), the more basic peptide was termed the "b" peptide (pI=5.3-6) (Mahuran *et al.*, 1988). For simplicity, the third peptide was termed as the "c" peptide.

The "a" peptide is 29 kDa and has lysine-315 exposed as its N-terminus (Mahuran *et al.*, 1988; Quon *et al.*, 1989). However, when the β-subunit is associated with the α-subunit to make Hex A, leucine-316 is exposed. The biological basis for a different N-terminus in either isoenzyme is not well understood.

The "b" peptide is a composite of a triplet of 16, 22, and 24 kDa peptides, all having threonine-122 exposed as the N-terminus (Mahuran *et al.*, 1988; Quon *et al.*, 1989). However, upon treatment with endoglycosidase H, only one peptide is apparent, demonstrating the presence of a heterogeneous group of oligosaccharide side chains on the "b" peptide. Similarily, glycosylation gives the "c" peptide an apparent molecular mass of 11 and 12 kDa that has valine-48 exposed at the N-terminus (Quon *et al.*, 1989).

The biological basis for proteolytic modifications in the lysosome is not well understood. The rationale for limited proteolysis is obscured because the unprocessed secreted forms of hexosaminidase are active toward synthetic substrates *in vitro* (Zühlsdorf *et al.*,1983).

1.4.2 Substrate specificity

Hexosaminidase hydrolyzes a broad range of substrates, including glycolipids, glycoproteins, and glycosaminoglycans. The specific hydrolytic reaction occurs at terminal non-reducing GlcNAc or GalNAc residues in β-linkage (reviewed in Gravel et., 1995).

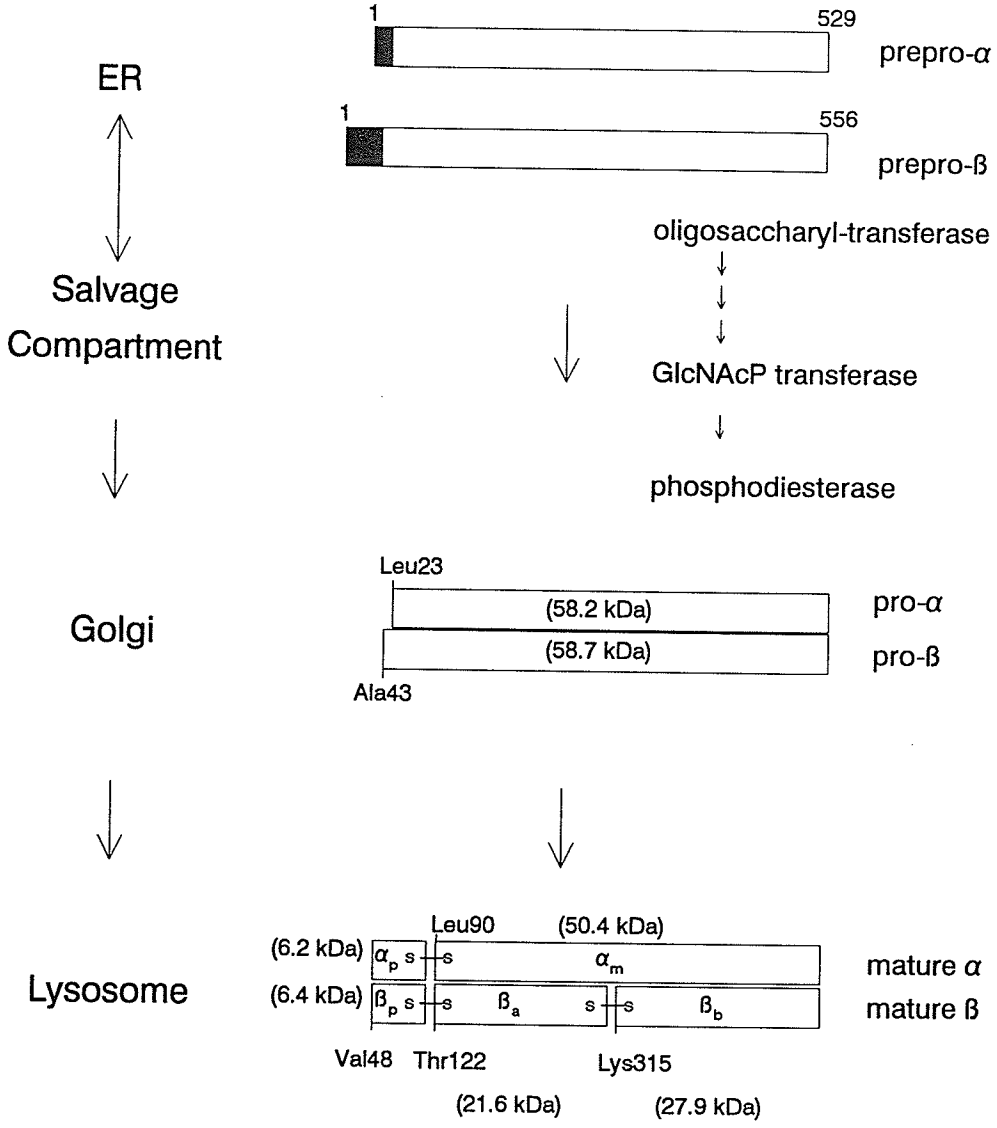

Figure 6 ***Proteolytic processing of the α- and β-subunits.*** The prepro, pro, and mature forms as they are processed from the ER to the lysosome are shown. The signal peptide (shaded) is removed by signal peptidase upon translocation to the lumen of the RER. The N-terminus of each peptide is indicated at each level of processing. The mature subunits in the lysosome are represented as being held together by disulfide bonds (S-S). The location of these bonds are not known. The sizes of the peptides indicated in the figure are taken from Mahuran (1995). See figure 5 for a summary of the oligosaccharide modifications that occur at each stage of processing.

Hex A, but not Hex B, requires the G_{M2} activator protein for catalytic activity *in vivo*. The G_{M2} activator is believed to solublize G_{M2} ganglioside and present it to Hex Afor hydrolysis (reviewed in Gravel *et al.*, 1995). The requirement for an activator protein is similar for other lysosomal hydrolases that require the sphingolipid activating protein complex (Furst and Sandhoff, 1992; reviewed in Sandhoff *et al.*, 1995). Although hydrolysis by Hex A requires the presence of the G_{M2} activator *in vivo*, Hex A activity can be measured *in vitro* using synthetic substrates in the absence of the G_{M2} activator.

4-MUG (4-methylumbelliferyl-2-acetamido-2-deoxy-β-D-glucopyranoside) is the β-GlcNAc derivative of the fluorogenic compound 4-methylumbelliferone. 4-MUG is the most commonly used substrate for the assay of hexosaminidase activity and it is hydrolyzed by Hex A and Hex B at identical pH optimums of 4.4 and nearly identical Km/Vmax values of 0.91 mM/$1.8x10^{-4}$ mol/min/mg and 0.90 mM/$4.4x10^{-4}$ mol/min/mg, respectively (Wenger *et al.*, 1972; Tallman *et al.*, 1974; Wiktorowitcz *et al.*, 1977; Conzelmann *et al.*, 1978). Because Hex A is heat-labile, and Hex B is heat-stable, the proportion of total hexosaminidase contributed by Hex A could be determined by the difference between an untreated and a heat-inactivated sample.

4-MUGS (4-methylumbelliferyl-β-D-*N*-acetylglucosamine-6-sulfate) is the sulfated derivative of 4-MUG. 4-MUGS is used specifically for the assay of α-subunit-containing dimers, Hex A ($\alpha\beta$) and Hex S ($\alpha\alpha$) (Bayleran *et al.*, 1984). The negatively charged sulfate moiety of 4-MUGS appears to mimic the negative charged of substrates such as G_{M2} ganglioside. The specificity of 4-MUGS for Hex A is illustrated by a Km that is ten-fold higher for Hex B. Although the specificity for 4-MUGS lies in the α-subunit, the

specific activity for Hex S is approximately one-fifth of that of Hex A. Recently, a method for identifying the substrate specificity of the active site in the α-subunit of Hex A was described (Hou *et al.*, 1996), and D196 in the β-subunit was identified as an active residue in the catalytic site of β-hexosaminidase (Tse *et al.*, 1996).

The hydrolysis of G_{M2} ganglioside by Hex A is specific and only GalNAc in $\beta 1 \rightarrow 4$ linkage is hydrolyzed. Even with an available sialic acid moiety on G_{M2} ganglioside, human sialidase does not hydrolyze sialic acid from G_{M2} ganglioside, probably due to steric hinderance by surrounding oligosaccharides. In contrast, the murine sialidase and Hex B enzymes are believed to be capable of G_{M2} ganglioside metabolism, suggesting two mechanisms that could be used by *Hexa* -/- mice to overcome the neurological symptoms associated with the human TSD phenotype (Sango *et al.*, 1995; Phaneuf *et al.*, 1996).

The availability of sequences from cloned hexosaminidases of other species have proved to be useful for predicting the structure of the human Hex A isoenzyme. A recent high resolution three-dimensional structure of chitobiase (Tews *et al*, 1996), which shows 26% identity to the catalytic domain of hexosaminidases, has provided a means of interpreting the secondary structures that may be affected by mutations in the human α-subunit, and predicting how these might affect its structure in infantile, subacute, and chronic G_{M2} gangliosidosis, and in Hex A pseudodeficiency. These studies, combined with those conducted in the *Hexa* -/- mice to understand Hex A function in the neuron, should prove to be useful in understanding the molecular defects associated with human Hex A activity.

1.5 Mutations in the *HEXA* gene

1.5.1 Common mutations

Hex A deficiency in the majority of cases has been attributed to a small number of mutations in the *HEXA* gene. The first mutation to be identified was a 7.6 kb deletion at the 5' end of the gene of a French Canadian TSD patient (Myerowitz & Hogikyan, 1986; Myerowitz & Hogikyan, 1987). However, the prevalence of TSD in the Ashkenazi Jewish population prompted the identification and elucidation of the frequencies of three common TSD-causing mutations in the *HEXA* gene that accounted for up to 98% of TSD alleles in this ethnic group (Paw *et al.*, 1990b; Triggs-Raine *et al.*, 1990; Grebner & Tomczak, 1991; Landels *et al.*, 1991; Fernandes *et al.*, 1992a). The 4-bp insertion ($+TATC_{1278}$) is the most common mutation (Myerowitz and Costigan, 1988), accounting for 75-80% of mutant *HEXA* alleles in the Ashkenazi Jewish population. A mutation in intron 12 (+1 IVS-12 G→C) (Myerowitz, 1988) accounts for approximately 15% of Jewish carriers. The least frequent of the three common mutations is the G805A mutation (Navon *et al.*, 1990; Paw *et al.*, 1989) that accounts for 3% of Jewish TSD carriers. The G805A nucleotide substitution causes a G269S amino acid substitution that is associated exclusively with chronic TSD when it is found in the homozygous state or heteroallelic with one of the two most common TSD-causing mutations. The adult-onset mutation has also been detected in non-Jewish patients (Navon *et al.*, 1990). Other late-onset TSD associated mutations also exist, but are likely to be low in frequency and allelic with one of the two most common mutations.

In the non-Jewish population, the 4-bp insertion and the adult-onset mutation

account for approximately 20% and 5% of carriers, respectively (Kaback, 1993). However, the intron 12 mutation has never been identified in the non-Jewish population. In contrast, a +1 IVS-9 (G→A) mutation has been found in 15% of non-Jewish carriers and has yet to be described in the Jewish population (Kaback *et al.*, 1993). The prevalence of three mutations in the Jewish population and the isolation of mutations such as the +1 IVS-9 mutation in the non-Jewish population suggests that identifying mutations in this population would be valuable for understanding the interaction of ethnic-specific or environmental factors that may influence α-subunit expression at the mRNA and protein processing levels.

1.5.2 Mutations affecting mRNA processing

TSD is most commonly associated with mutations that affect α-subunit mRNA stability and/or splicing. The two most common mutations in the Ashkenazi Jewish population are classic examples of mutations that result in a complete deficiency of *HEXA* expression and are associated with the most severe, infantile, form of TSD. The insertion mutation results in a premature stop codon, and therefore an unstable mRNA that is quickly degraded (Boles & Proia, 1995). Such a profound deficiency of *HEXA* mRNA is typical of the +1 IVS-12 G→C mutation that results in skipping of intron 12, or retention of intron 12, resulting in a cryptic termination codon (Ohno and Suzuki, 1988). The defects associated with the +1 IVS-9 G→A mutation are similar (Akerman *et al.*, 1992). The G805A adult-onset mutation, that causes a G269S amino acid substitution, may also affect mRNA stability because it occurs at the most 3' nucleotide of exon 7 (Paw *et al.*, 1989). This suggests that it may affect normal splicing by influencing the

5' acceptor splice-site of exon 7.

Mutations that affect normal mRNA splicing, and are associated with late-onset disease, must allow for a small proportion of normal mRNA species in order to provide low levels of Hex A expression, resulting in some G_{M2} ganglioside hydrolysis and a delayed clinical course. Two such mutations have been described for the α-subunit (Akli *et al.*, 1990; Richard *et al.*, 1995). Similarily, three mutations that result in late-onset or asymptomatic Sandhoff (Hexosaminidase Paris) disease patients have been identified in the 3' end of the *HEXB* gene (Dlott *et al.*, 1990; Nakano & Suzuki, 1989). Hexosaminidase Paris is characterized by Hex B deficiency and some detectable Hex A (Dreyfus *et al.*, 1977), suggesting that the mutation affects β-subunit homodimerization, but heterodimerization to make Hex A ($\alpha\beta$) is less affected.

1.5.3 Mutations affecting protein processing

The effect of an amino acid substitution on the processing of the α-subunit is unpredictable. Mutations that prevent newly-synthesized α-subunits from reaching the lysosome can have one of two major effects. First, an early processing defect could cause newly synthesized proteins to be retained in the endoplasmic reticulum and/or salvage compartments where they would be subsequently degraded. Second, a mutation that causes a later processing defect could allow for the α-subunit to move from the salvage compartment to the Golgi and to become phosphorylated, however, the resulting $\alpha\beta$ dimer may be unstable.

Two well characterized early processing α-subunit mutations are a G250D amino acid substitution in exon 7 that is associated with late-onset disease (Trop *et al.*, 1992),

and a E482K amino acid substitution in exon 13 that is associated with infantile disease (Nakano *et al.*, 1988). Although the E482K and G250D mutations result in similar biochemical phenotypes, they are distant in the primary structure and are associated with distinctly different clinical phenotypes. Therefore, the relationship between the linear position of a mutation in the α-subunit and its effect on the biochemical or clinical phenotype is unclear.

The association of a mutation with late-onset TSD could be assessed in a Cos-7 cell overexpression system. Late-onset and infantile TSD-causing mutations could be differentiated by the formation of mature Hex A only by the mutants associated with the less severe forms of the disease (Brown and Mahuran, 1993). Late-onset disease-causing mutations are believed to affect α-subunit folding, although to a lesser extent in comparison to those associated with infantile disease (Brown and Mahuran, 1993). This has been suggested for only two late-onset TSD-causing mutations, G250D and G269S (Trop *et al.*, 1992 and Brown *et al.*, 1993). These observations still need to be substantiated with the study of other α-subunit mutations associated with late-onset TSD.

The second class of α-subunit processing mutations include those that allow mutant α-subunits to become phosphorylated in the salvage compartments or the Golgi, but do not reach the lysosome (d'Azzo *et al.*, 1984). The adult-onset disease-causing amino acid substitution, G269S, falls in this class and was initially described as an association-defective mutant. However, recent studies have suggested that the α-subunit does not associate because of an instability of the protein due to misfolding (Brown & Mahuran, 1993). Interestingly, a mutation in exon 1 that is also associated with late-

infantile TSD, and therefore affects patients at an earlier stage, also falls into the class of late-processing mutants (Harmon *et al.*, 1993). Once again, there is no correlation between the linear position of a mutation and the biochemical or clinical phenotype.

Interestingly, a cluster of mutations toward the C-terminus of the α-subunit, particularly in exon 13 and surrounding sequences, result in processing defects. In exon 13, seven mutations have been reported. Three of these, R499H (Paw *et al.*, 1991), R499C (Mules *et al.*, 1991), and R504H (Paw *et al.*, 1990a), are associated with juvenile-onset G_{M2} gangliosidosis. The others, including E482K (Paw *et al.*, 1991), W485R (Akalin *et al.*, 1992), ΔC1510 (Paw *et al.*, 1991), and R504C (Akli *et al.*, 1991; Paw *et al.*, 1991), result in the infantile form (TSD). Analysis of some of the mutant enzymes has suggested that the C-terminal sequence of the α-subunit is important for its association with the β-subunit (d'Azzo *et al.*, 1984; Paw *et al.*, 1990a). Similarily, mutations found toward the C-terminus of the β-subunit are also believed to affect β-subunit processing (Nakano & Suzuki, 1989; Kuroki *et al.*, 1995). One of the major efforts in the study of Hex A is to understand the parameters necessary for normal enzyme processing using mutant α-subunit as models of processing defects.

1.6 Current study

This study describes the molecular basis of Hex A deficiency that was identified in a non-Jewish proband diagnosed with subacute G_{M2} gangliosidosis, Type I. A novel mutation in the *HEXA* gene was characterized. Transient expression of the mutant α-subunit in Cos-7 cells was also used to demonstrate that this change is responsible for

Hex A deficiency in the proband. The effect of the mutation on α-subunit protein levels, processing of newly-synthesized mutant α-subunits, and *HEXA* mRNA levels were examined.

2 MATERIALS AND METHODS

2.1 Steady-state analysis of human fibroblast β-hexosaminidase A

2.1.1 Fibroblast maintenance

Materials

α-MEM (Gibco/BRL)

Fetal bovine serum (FBS) (Gibco/BRL)

Freezing medium-dimethyl sulfoxide (DMSO) (Gibco/BRL)

Trypsin (0.25%)-EDTA-4•Na (1 mM) (Gibco/BRL)

Penicillin (10, 000 U/mL)/Streptomycin (10, 000 μg/mL) (Gibco/BRL)

Phosphate buffered saline (PBS):

NaCl	137 mM
Na_2HPO_4	4.3 mM
KCl	2.7 mM
KH_2PO_4	1.47 mM
pH 7.3	

2.1.1.1 Growth

Human fibroblast lines were maintained in α-MEM supplemented with 10% fetal bovine serum and penicillin (100 U/mL)/streptomycin (100 μg/mL). Cell lines were grown on NUNCLON^R tissue culture dishes, or SARSTED or CORNING polystyrene disposable tissue culture flasks in a tissue culture incubator containing 5% CO_2 at 37°C.

2.1.1.2 Subculture

Confluent cultures were subcultured. The monolayer was rinsed with 2 to 3 mL of trypsin-EDTA, and then harvested in 3 mL of trypsin-EDTA by tapping the plate to aid in the release of the cells. α-MEM was added to a final volume of 10 mL. This was

divided among three to ten-20 x 100 mm culture dishes in a final volume of 20 to 30 mL of α-MEM containing FBS and antibiotics.

2.1.1.3 Storage

Fibroblasts were grown to 80% of confluence in 150 mm x 20 mm tissue culture dishes. They were lifted from culture dishes by trypsinization (2.1.1.2), transferred to a 50 mL polypropylene screw-capped tube in an excess of α-MEM, and pelleted in a table-top clinical centrifuge for 10 minutes at 2, 000 rpm. Each pellet, corresponding to one dish of cells, was resuspended in 2.5 mL of freezing medium, and 0.5 mL aliquots were frozen overnight at -80°C in 1.8 mL Nunc CryoTubes. The following day, the samples were placed in a liquid nitrogen storage tank for long term storage. When a sample was replated from storage, it was thawed quickly at 37°C and transferred to a tissue culture flask (75 cm^2) containing 40 mL of α-MEM that was pre-warmed to 37°C.

2.1.2 Cell lines

2.1.2.1 Normal

MCH065 fibroblasts were obtained from the The Repository for Mutant Human Cell Strains, Montreal, PQ. They are abdomen skin fibroblasts from a healthy 3.5 year-old white Finnish female.

WP09 deltoid fibroblasts from a healthy German male were obtained from the University of Manitoba, Winnipeg, MB.

2.1.2.2 Tay-Sachs disease

WG1881 human fibroblasts were obtained from The Repository of Mutant Human Cell Strains, Montreal, PQ. They are deltoid fibroblasts from a 1.5 year-old French-

Canadian male with Tay-Sachs disease. This cell line was homozygous for the 7.6 kb deletion at the 5' end of the *HEXA* locus that is common among French-Canadians (Myerowitz & Hogikyan, 1987), and was therefore a useful negative control for studies of Hex A activity and *HEXA* mRNA expression.

2.1.2.3 Sandhoff disease

GM00294 fibroblasts, that were obtained from the Human Genetic Mutant Cell Repository (Camden, NJ, USA), were from a 2 year-old caucasian affected with Sandhoff disease. This cell line was homozygous for the common 16 kb deletion that extended from the promoter, through exons 1 to 5, and part of intron 5 of the *HEXB* gene (Neote *et al.*, 1990), and was therefore a useful negative control for studies of Hex B activity and *HEXB* mRNA expression. This cell line was previously used as a negative control by Srivastava *et al.*, 1975, Rattazzi *et al.*, 1976, Wood, 1978, Macleod *et al.*, 1977, Wood & MacDougall, 1976, O'Dowd *et al.*, 1986, and Miranda *et al.*, 1988.

2.1.2.4 Late-onset G_{M2} gangliosidosis

HSC3236 fibroblasts were provided by Dr. Joe Clarke (Hospital for Sick Children, Toronto). They were obtained from a patient who was diagnosed with juvenile-onset G_{M2} gangliosidosis, Type 1. This cell line was found to be compound heterozygous at the *HEXA* locus for a common 4-bp insertion (+TATC) in exon 11 (Myerowitz & Costigan, 1988) and a G1422C transversion (Triggs-Raine, unpublished data). The molecular defects associated with this mutation were characterized in this thesis.

2.1.3 Preparation of cell lysates

Materials

PBS (see 2.1.1)

TEN buffer: 40 mM Tris-HCl, pH 7.5
1 mM EDTA
150 mM NaCl

Resuspension buffer: 20 mM Tris-HCl, pH 7.5

The medium was aspirated from confluent fibroblast cultures. The cells were rinsed twice with 5 to 10 mL of PBS, and the culture dishes were placed on ice. Cells were harvested by scraping into 1 mL of TEN buffer and transferred to a microcentrifuge tube. The cells were pelleted by centrifugation at 4°C for 2 minutes at maximum speed (> 10,000 x g). The cell pellet was resuspended in 200 μL of 20 mM Tris-HCl, pH 7.5, followed by freezing in an ethanol-dry ice bath and thawing in a 37°C water bath. Freezing and thawing was repeated three times. The lysate was finally cleared by centrifugation at 4°C for 10 minutes at maximum speed (> 10,000 x g), and the supernatant was stored in a separate tube at -45°C or -80°C (depending on the availability of storage space).

2.1.4 Assay of protein concentration

Protein concentrations were determined using a Bio-Rad protein assay kit that was based on the method of Bradford (1976). A standard curve was plotted with relative absorbance at 595 nm versus the gamma-globulin concentration (μg/mL). Six points were plotted where the concentration of gamma-globulin was 2, 4, 8, 12, 16, and 20 μg per mL. If the experimental samples were in a buffer that altered the colour formation of the BioRad protein assay reagent, then the standard was made in the presence of an equal volume of that buffer. The standard curve was routinely prepared in duplicate, and the

unknowns were prepared in duplicate, or in triplicate. The amount of unknown sample assayed was adjusted to read between relative absorbances equivalent to 6 μg to 13 μg of gamma-globulin per mL.

2.1.5 Hexosaminidase assay

Materials

Citrate phosphate buffer (CPB): 6 mM citric acid
10 mM Na_2HPO_4
pH 4.4

0.3% bovine serum albumin (BSA) in CPB

3 mM 4-MUG (Toronto Research Chemicals) in CPB

3.5 mM 4-MUGS (Toronto Research Chemicals) in CPB

Glycine carbonate: 170 mM glycine
170 mM Na_2CO_3
adjusted to pH 10.0 with 5 M NaOH

1 μM 4-MU (4-methylumbelliferone) (Toronto Research Chemicals) in glycine carbonate

2.1.5.1 Assay of Hex A activity using 4-MUG

Quantitation of Hex A activity in fibroblasts using 4-MUG as a substrate, in combination with the heat denaturation step, was done essentially as described by (Kaback, 1977). The use of control lysates from normal, TSD, and SD cell lines (see 2.1.2) was essential. Cell lysates (50 μg of protein) were added to CPB to give a final concentration of 5 μg/μL, in the presence of 0.3% BSA. It was important that the level of Hex activity in the BSA was pre-determined to be low because even different batches of BSA from the same company may have different levels of Hex activity that may contribute to misleading results, particularly in the lower ranges of Hex A activity

(Kanfer & Spielvogel, 1973).

One half of the sample to be assayed was transferred to a separate tube and incubated at 52°C for two hours. The remaining sample was kept on ice for the same duration. The heated-treated samples were then briefly centrifuged and placed on ice. If a precipitate formed (presumably due to the presence of BSA), it was resuspended by pipetting.

For both the heated-treated and non-treated samples, a 10 μL aliquot was incubated with 20 μL of 3 mM 4-MUG at 37°C for 30 minutes. The reaction was stopped by adding 970 μL of glycine carbonate. Each sample was prepared in duplicate or triplicate at every stage of manipulation. Hex activity was determined as described in 2.1.5.3.

2.1.5.2 Assay of Hex A using 4-MUGS

To assay specifically for Hex A, 4-MUGS was used as a substrate (Bayleran *et al.*, 1984). Cell lysate, (25 μg of protein), was added to CPB to give a final volume between 10 and 50 μL. The sample was incubated with two volumes of 4-MUGS for 30 minutes at 37 °C. The reaction was stopped in a final volume of 1 mL with glycine carbonate. The activity in the samples was measured as described in 2.1.5.3.

2.1.5.3 Measurement of activity

An aliquot of the stopped reaction was diluted in glycine carbonate buffer to give a final volume of 1 mL, and the fluorescence was measured using a Hitachi F-2000 Fluorescence Spectrophotometer that was set at an excitation of 353 nm and emission of 448 nm. Dilutions of a 1 μM 4-MU stock were made to give the following concentrations

for the standard curve: 20, 50, 100, 250, 500, and 800 pmol per mL.

2.1.5.4 Calculation of Hex A activity

The specific activity in each sample was predicted by the extent of 4-MU liberated during the reaction. The concentration of 4-MU in each sample was determined from the standard curve, and the specific activity in each sample was determined by the following calculation:

Specific activity (nmol substrate hydrolyzed/mg protein/hour) =

$$\frac{\text{pmol 4-MU}}{\mu\text{g protein}} \times \frac{\text{dilution factor}}{\text{time (hours)}} \times \frac{\text{1 nmol}}{10^3 \text{ pmol}} \times \frac{10^3\ \mu\text{g}}{\text{1 mg}}$$

If 4-MUG was used in combination with the heat denaturation step (see 2.1.5.1), the proportion of Hex A activity was expressed as a percentage of total Hex activity using the following calculation:

$$\frac{[\text{Specific activity (before heat)} - \text{Specific activity (after heat)}]}{\text{Specific activity (before heat)}} \times 100\% = \%\ \text{Hex A}$$

If 4-MUGS was used, then the proportion of Hex A activity was expressed as a percentage of Hex A activity observed in the normal cell line.

2.1.6 Western blot analysis

Materials

Sodium dodecyl sulfate (SDS) polyacrylamide gel:

a) Separating gel:	Distilled water	7.9 mL
	30% acrylamide:bisacrylamide (30:1)	6.7 mL
	1.5 M Tris-HCl, pH 8.8	5.0 mL
	10% SDS	0.2 mL
	10% ammonium persulfate	0.2 mL
	TEMED (ICN Pharmaceuticals, Inc)	10 μL

b) Stacking gel:	Distilled water	6.0 mL
	30% acrylamide:bisacrylamide (30:1)	1.3 mL
	1.0 M Tris-HCl, pH 6.8	2.5 mL
	10% SDS	0.1 mL
	10% ammonium persulfate	0.1 mL
	TEMED	10 μL

4 X running buffer: 200 mM Tris, 1.5 M glycine, 4% SDS

Western Transfer Buffer: 25 mM Tris, 190 mM glycine, 20% methanol

5 X Tris-Buffered saline (TBS): 100 mM Tris, 2.5 M NaCl

Skim milk solution: 5% (w/v) skim milk powder in 1 X TBS

TBS-Tween-20 (TBS-T): 0.5% (v/v) Tween-20 (BioRad) in 1 X TBS

Anti-rabbit IgG, horseradish peroxidase linked whole antibody (from donkey) (Amersham)

NitroPlus nitrocellulose transfer membrane, 0.45 micron (Micron Separations Inc.)

REFLECTION™ autoradiography film (NEN Research Products)

REFLECTION™ chemiluminescence enhancing screen

2.1.6.1 Sodium dodecyl sulfate polyacrylamide gel electrophoresis (SDS-PAGE)

SDS-PAGE of cell extracts was performed according to Laemmli, 1970. The gels were prepared on a BioRad Mini-PROTEAN™ II Cell apparatus. SDS-polyacrylamide gels (0.75 to 1.5 mm in thickness) were composed of a lower separating gel (5.5 cm in height) and an upper stacking gel (approximately 2 cm). The separating gel was poured with a pipette, covered with 95% ethanol to produce an even surface, and allowed to

polymerize for at least 30 minutes. The ethanol was then poured off and the top of the separating gel was gently rinsed with distilled water; any residual water was absorbed with gel blotting paper. The stacking gel was then mixed and poured on top of the separating gel. A 10 well comb was inserted into the gel such that the bottom of the wells were approximately 1 cm above the separating gel. Polymerization was allowed for at least 30 minutes. The apparatus was assembled and the upper and lower chambers were filled with 1 X running buffer. Electrophoresis was conducted at 100 to 200V (constant voltage), and was terminated immediately after the bromophenol blue dye migrated out of the bottom of the gel.

2.1.6.2 Transfer to nitrocellulose

The gel was soaked in western transfer buffer for 20 minutes at room temperature with gentle agitation. A piece of nitrocellulose was cut to the size of the gel, and the gel was then assembled in a BioRad Mini Trans-Blot Cell apparatus between a double layer of gel blotting paper. Transfer was done for 2 hours at 100 V and at 4°C. After transfer, the blot was treated as described in 2.1.6.3.

2.1.6.3 Immunodetection

The membrane was incubated in 50 mL of skim milk solution with gentle shaking for 1 to 2 hours at room temperature or at 4°C overnight; otherwise, it was stored at -20 °C in skim milk solution. The membrane was briefly rinsed with 20 to 50 mL of TBS-T followed by four-ten minute incubations at room temperature in 50 to 100 mL of TBS-T. The anti-Hex A antibody was diluted 5000-fold in 5 to 10 mL of TBS-T and incubated with the membrane for two hours at room temperature with constant shaking in a suitable

container.

The membrane was rinsed and washed as before, and incubated with a 1:15,000 dilution of anti-rabbit antibody conjugated to horse-radish peroxidase in 15 or 30 mL of TBS-T (dilutions were made immediately prior to use). The membrane was rinsed and washed as before.

The membrane was then placed on a piece of plastic wrap. Amersham's enhanced chemiluminescence kit was used to detect the bound secondary antibody. The two solutions provided in the kit were mixed (1:1), and a total of 2 mL was used for every 5.5 cm x 8.5 cm membrane. The membrane was patted once with paper towels to remove excess TBS-T and the ECL solutions were drawn over the membrane and incubated for 60 to 90 seconds at room temperature. The membrane was patted once with paper towels to remove the ECL solutions. The membrane was covered with plastic wrap and immediately exposed to REFLECTION™ film for various times in the presence of a REFLECTION™ chemiluminescence enhancing screen.

2.1.7 Northern blot analysis of *HEXA* mRNA in fibroblasts

2.1.7.1 Total RNA extraction

Materials

Homogenization solution:

5.0 mL 4M guanidinium isothiocyanate (Gibco/BRL), buffered by 25 mM sodium citrate (pH 7.0)
5.0 mL buffer-saturated phenol (Gibco/BRL), containing 0.4% hydroxyquinoline
0.5 mL 2 M sodium acetate (pH 4.0)
72 μL 2-mercaptoethanol

Chloroform

2-propanol

Total RNA was isolated (Sambrook *et al.*, 1989) from one 150 mm x 20 mm culture dish of confluent fibroblasts. The medium was aspirated and 750 μL of homogenization solution (Sathyamoorthy *et al.*, 1994) was added directly to the plate. The cells were immediately scraped off and collected into a microcentrifuge tube. The homogenate was passed through a pipette tip or 22-gauge syringe needle 10 to 15 times and incubated at room temperature for 5 minutes. Chloroform was added (200 μL), and the tube was shaken rapidly by hand for 15 seconds and allowed to stand at room temperature for 10 minutes. The sample was centrifuged at 12, 000 x g for 15 minutes at 4°C, and the aqueous phase was transferred to a sterile microcentrifuge tube. The RNA was precipitated by adding 0.5 mL of 2-propanol, followed by an incubation at room temperature for 10 minutes. The RNA was pelleted by centrifugation at 12, 000 x g for 10 minutes at 4°C. The supernatant was removed and the pellet was washed by mixing in 1 mL of 75% ethanol. The sample was centrifuged at 7,500 x g for 5 minutes at 4°C. The ethanol was removed, the pellet was air dried, resuspended in 50 μL of sterile distilled water, and stored at -80 °C. An aliquot of RNA was diluted in 1 mL of autoclaved distilled water and the concentration of RNA was determined spectrophotometrically at OD_{260}:

RNA conentration $=(OD_{260\ [sample]})$ x (dilution of sample) x (40 μg RNA/OD_{260})

2.1.7.2 Formaldehyde gel electrophoresis

Materials

Agarose (Genetic Technology Grade; ICN Pharmaceuticals, Inc)

10 X MOPS buffer (1 L):	41.8 g MOPS (3-[*N*-Morpholino] propanesulfonic acid) (Sigma) 4.1 g sodium acetate 20 mL EDTA (0.5 M) pH 7.0
37% formaldehyde (v/v)	
Formamide (Gibco/BRL)	
Gel loading buffer:	50 % glycerol 1 mM EDTA, pH 8.0 0.25 % bromophenol blue 0.25 % xylene cyanol FF
Ethidium bromide (5 mg/mL)	

A formaldehyde gel was prepared essentially as described in Ausubel *et al.*, 1987. Distilled water (121.5 mL) was boiled with 1.5 g agarose. After cooling, 15 mL of 10 X MOPS and 4.5 mL of formaldehyde was added, and the solution was mixed thoroughly. The gel was poured on a Gibco/BRL HORIZON™ 11-14 apparatus casting tray and allowed to cool. The gel was placed in 1 X MOPS as the running buffer, and the samples were prepared with the following components:

10 μg	RNA (up to 11 μL)
4.0 μL	10 X MOPS
5.3 μL	formamide
15 μL	formaldehyde (37% v/v)

The samples were heated at 65°C for 15 minutes, briefly centrifuged, and then quickly cooled on ice. The following components were added, and the sample was loaded on the gel.

4 μL	agarose gel loading buffer
1 μL	ethidium bromide

The RNA was fractionated at 100 V for 3 hours, visualized over an ultraviolet

lamp box, and photographed (see 2.5.3.1).

2.1.7.3 Transfer to nitrocellulose

Materials

20 X SSC (1 L): 175.3 g NaCl
88.2 g sodium citrate
pH 7.0 with HCl
autoclaved

Gel blot paper

NitroPlus nitrocellulose transfer membrane, 0.45 micron (Micron Separations Inc.)

Fractionated RNA was transferred directly to nitrocellulose (Sambrook *et al.*, 1989, Ausubel *et al.*, 1987). A glass plate was wrapped with Whatmann paper and placed over a glass tray such that the ends of the paper were touching the bottom of the tray. The tray was filled with 500 mL of 20 X SSC and the gel blotting paper was soaked with the same buffer. The gel was inverted and placed on the gel blotting paper. A piece of nitrocellulose transfer membrane was cut to the exact size of the gel, briefly soaked in boiling water, and placed over the inverted gel. Air bubbles were removed and three pieces of gel blotting paper of the same size were placed over the nitrocellulose. The apparatus was covered with plastic wrap and the section covering the gel/blot sandwich was removed with a razor blade. The gel was then covered with a small stack of paper towels held down by a glass plate, and allowed to transfer for 20 hours.

The nitrocellulose was air dried and baked between two pieces of gel blotting paper in a vacuum oven at 80°C for 2 hours.

2.1.7.4 Probing of mRNA using the *HEXA* cDNA

The 2 kb α-subunit cDNA was removed from αpSVL (see 2.5.2) with *Xho*I/*Bam*HI and purified as described in 2.5.4.2. The entire purified DNA sample was separated by agarose electrophoresis and subjected to a second purification to ensure that no contaminating vector DNA was present. The DNA fragment was used as a probe (see 2.1.7.4.2).

2.1.7.4.1 Prehybridization of transferred RNA

Materials

Pre-hybridization solution:

50% deionized formamide (Gibco/BRL)
5 X SSC (see 2.1.7.3)
10 X Denhardt's: 1% bovine serum albumin (Fraction V)
1% Ficoll^R 400 (Pharmacia)
1% polyvinylpyrrolidone
stored at -20°C
50 mM NaH_2PO_4, pH 6.5
250 μg/mL sheared salmon sperm DNA

Prehybridization was performed essentially as described by Williams & Mason (1985). Deionized formamide was prepared by stirring 5 g Dowex AG501 (BioRad) per 100 mL formamide for 1.3 hours at room temperature. The formamide was filtered through a Whatmann #2 filter without vacuum, and stored at -20°C.

The blot was placed in a plastic bag with 15 to 20 mL of prehybridization solution and incubated at 42°C overnight with gentle shaking.

2.1.7.4.2 Random primer labelling of probe

cDNA probes were prepared according to the method of Feinberg & Vogelstein, 1983. The *HEXA* cDNA was purified as described in 2.5.4, and approximately 75 ng was incubated with approximately 5 μg of random hexanucleotides (Pharmacia) in a volume

of 14 μL. The mixture was boiled for 3 minutes, briefly centrifuged, and immediately placed on ice. The following was added and incubated at room temperature overnight:

2.5 μL	0.5 mM dCTP, dGTP, dTTP (Pharmacia)
2.5 μL	10X Klenow fragment buffer (Promega)
5.0 μL	α-^{32}P-dATP (10 μCi/μL) (ICN Pharmaceuticals, Inc)
1.0 μL	5 u/μL Klenow fragment (Promega)

The labelled components were separated using a NICK™ Column (Sephadex^{R} G-50 DNA Grade) (Pharmacia). The labelled DNA was collected in 400 μL of equilibration buffer (10 mM Tris-HCl pH 7.5, 1 mM EDTA). The level of radioactivity associated with an aliquot of the eluted DNA was measured by scintillation counting. The probe generally had a specific activity of $>10^{8}$ cpm/μg DNA.

2.1.7.4.3 Hybridization

Materials

Hybridization solution:

10 mL	prehybridization solution (see 2.1.7.4.1)
2.5 mL	50% dextran sulphate (Pharmacia)

The probe was heated in a boiling water bath for 5 minutes and then placed in the hybridization solution with the blot and incubated with rocking overnight at 42°C in a sealed plastic bag as described by Williams & Mason, 1985. The inclusion of dextran sulphate increases the rate of hybridization approximately 10-fold and can increase the sensitivity approximately 100-fold (Wahl & Stark, 1979).

2.1.7.4.4 Washing and exposure

The blot was washed under three different conditions:

1. 1 hour at 60°C in 2 X SSC/0.1% SDS, with a buffer change every 15 minutes

2. 30 minutes at 65°C in 0.2 X SSC/0.1% SDS

3. 30 minutes at 65°C in 0.1 X SSC/0.1% SDS

The nitrocellulose was briefly air-dried, wrapped in plastic, and exposed to X-OMAT AR film (Kodak) at -80°C in the presence of a CRONEX™ intensifying screen for one to three days.

2.2 Mutation identification from fibroblast DNA

2.2.1 SSCP analysis

SSCP analysis was used to screen for mutations in DNA sequences. Radiolabelled PCR products harbouring the exons of interest were separated on a non-denaturing gel, and alterations in their mobility predicted that a mutation was present in that DNA fragment.

2.2.1.1 PCR reaction

The PCR reaction was essentially done as previously described by Orita *et al.*, 1989, except that the DNA was labelled during the PCR reaction rather than by end-labelling (Triggs-Raine *et al.*, 1991). The PCR reaction was set up with the mixture below; the genomic DNA was added last. The reaction was then overlaid with approximately 50 μL paraffin oil to prevent evaporation of the sample:

0.5 μg	genomic DNA
1.0 μL	oligonucleotide primer A (0.5 μg/μL)
1.0 μL	oligonucleotide primer B (0.5 μg/μL)
5.0 μL	10 X PCR buffer: 500 mM KCl 100 mM Tris-HCl (pH 8.3) 15 mM $MgCl_2$ 0.1% gelatin
1.0 μL	each of 10 mM dCTP, dGTP, dTTP (Pharmacia)

0.5 μL 10 mM dATP (Pharmacia)
1.0 μL α^{32}P-dATP (>3000 Ci/mmol) (ICN Pharmaceuticals, Inc.)
distilled water was added to give a final volume of 50 μL
0.3-0.5 μL Taq polymerase

PCR reactions were done using a Perkin Elmer Cetus Thermocycler. Reactions were routinely incubated at 94°C for 10 minutes prior to the start of the thermocycling program. The amplification was carried out for 30 to 35 cycles using the following cycling conditions:

30 seconds	94°C (denaturation)
30 seconds	60°C (annealing)
90 seconds	72°C (extension)

2.2.1.2 Gel electrophoresis

The gel mixture was prepared in 60 mL with the following components:

6 mL	glycerol (99.5% stock; Gibco/BRL)
10 mL	30% acrylamide:bisacrylamide (29:1) (Gibco/BRL)
6 mL	10X TBE buffer
38 mL	water
0.2 mL	15% ammonium persulfate

The gel mixture was degassed and 30 μL TEMED was added followed by brief mixing. The gel was poured through a 60 cc syringe between two 31.0 cm x 38.5 cm glass separated by a 0.4 mm spacer, and a well maker was inserted. The plates were held together with bulldog clamps at the sides adjacent to the well maker. The samples were separated on a BioRad Model S2 gel electrophoresis apparatus

The PCR reactions were diluted in the following manner:

2 μL PCR reaction (1/10 diluted)
2 μL sequencing stop solution: 95% formamide
0.1% bromophenol blue
0.1% xylene cyanol

The mixture was heated at 95°C for 3 to 5 minutes and loaded onto a gel. In addition, an extra sample was prepared from the normal control reaction in sequencing stop solution. This reaction was not heated and it represented the non-denatured control.

The samples were separated at 12 mA overnight at room temperature, and a duplicate gel was prepared at 4°C because the electrophoretic mobility of mutant DNA fragments can be influenced by temperature. When the bromophenol blue reached the bottom of the gel, the apparatus was disassembled and the gel was transferred to gel blotting paper. The gel was covered with plastic wrap and dried on a BioRad Model M583 gel dryer at 80°C. The gel was exposed for 18 hours at room temperature to XOMAT™-AR film (Kodak).

2.2.1.3 Analysis of results

The mobility of the radioactive DNA bands was analyzed. Differences in the banding pattern, compared to the normal control, indicated the presence of a mutation.

2.2.2 Restriction enzyme digest analysis of PCR products

2.2.2.1 Analysis of amplified genomic DNA

DNA was amplified as described in section 2.2.1.1 except that the ^{32}P-labelled dATP was not included and the concentration of dATP was increased accordingly. A 10 μL aliquot of the reaction was incubated with 1 μL of the desired restriction enzyme at the appropriate temperature for 2 hours. The restriction enzyme digests were analyzed by gel electrophoresis as described in 2.5.3.

2.2.2.2 Analysis of amplified cloned DNA

For the amplification of cloned DNA, 1 ng of DNA was routinely used as a

template for the PCR reaction. The reaction mixture was set up as follows:

80 μL sterile distilled water
10 μL PCR buffer (see 2.2.1.1)
2 μL each of 10 mM dATP, dCTP, dGTP, dTTP
1 μL sense primer (0.1 μg/μL)
1 μL antisense primer (0.1 μg/μL)
1 μL plasmid (1 ng)
0.3-0.5 unit Taq polymerase

Amplification was done under the conditions described in 2.2.1.1. Restriction enzyme digestion was conducted as described in 2.2.2.1, and analyzed by gel electrophoresis as described in 2.5.3.

2.3 Metabolic labelling analysis of β-hexosaminidase in human fibroblasts

2.3.1 Antibodies used

2.3.1.1 Anti-α-subunit

A polyclonal antiserum was raised in goat against the α-subunit after SDS denaturation of the human placental Hex A isoenzyme (Hasilik & Neufeld, 1980). It was used to immunoprecipitate monomeric α-subunits of Hex A as precursors from non-denatured cell lysates. Both precursor and mature α-subunit could be detected using immunoprecipitation from SDS-treated cell lysates.

2.3.1.2 Anti-Hex B

A polyclonal antiserum raised in goat against purified human placental Hex B (Hasilik & Neufeld, 1980) was used to immunoprecipitate both β-subunit-containing dimers, Hex B ($\beta\beta$) and Hex A ($\alpha\beta$).

2.3.1.3 Anti-Hex A

Rabbit antisera against human Hex A were raised in the Hybridoma Core Facility

of the Canadian Genetic Diseases Network at The University of British Columbia (UBC). A purified human placental Hex A protein, provided by Dr. Don Mahuran (University of Toronto) was used to immunize New Zealand white rabbits according to established protocols at UBC. The antiserum was used to detect α- and β-subunits as monomers or dimers using immunoprecipitation or western blot analysis. On immunoblots, it cross-reacted with an additional polypeptide which was likely a contaminating protein in the original Hex A preparation.

2.3.2 Pulse-chase analysis of metabolically labelled fibroblasts

Materials

TRAN^{35}S-LABEL (ICN Pharmaceuticals, Inc) $>$1000 Ci/mmol

[^{32}P] Orthophosphate (H_3PO_4 in H_2O, HCl free) 400-500 mCi/mL (ICN Pharmaceuticals, Inc)

1 M ammonium chloride (Gibco/BRL) (see 2.3.2.5)

Depletion medium:
D-MEM (ICN Pharmaceuticals, Inc):
without methionine
without cysteine
supplemented with glutamine (Gibco/BRL)

or without sodium phosphate (Gibco/BRL)

Penicillin/Streptomycin (see 2.1.1)

Labelling Medium:

3.8 mL	depletion medium (see above)
200 μL	dialyzed FBS (Gibco/BRL)
$\geq$ 250 μCi	TRAN^{35}S-LABEL *or* [^{32}P] Orthophosphate

Chase Medium

4.5 mL	α-MEM (10% FBS) (Gibco/BRL)
0.5 mL	10 X amino acid chase mix: L-methionine (0.75 mg/mL) L-cysteine (5.0 mg/mL)

2.3.2.3 Pulse

Fibroblasts were grown to confluence on one 100 mm x 20 mm culture dish in α-MEM supplemented with 10% fetal bovine serum. The medium was aspirated and the cells were rinsed once with 5 mL of PBS. The cells were then incubated with 3 mL of depletion medium for 1 hour to deplete intracellular methionine and cysteine. The medium was removed and replaced with 3 mL of labelling medium supplemented with 5% dialyzed fetal bovine serum and 20 μL of TRAN^{35}S-LABEL (approximately 250 μCi). Incubations were routinely done for 3 hours.

2.3.2.4 Chase

The labelling medium was replaced with 5 mL of chase medium that contained a five-fold excess of methionine and cysteine, with respect to the original concentrations in α-MEM. The cells were harvested at various time points thereafter.

2.3.2.5 Pulse-chase in the presence of 10 mM NH_4Cl

The secretion of hexosaminidase isoenzymes was studied in the presence of 10 mM ammonium chloride essentially as described by Proia *et al.* (1984), with some modifications. This was done by an overnight incubation in chase medium without FBS and in the presence of 10 mM NH_4Cl (see 2.3.2).

2.3.3 Immunoprecipitation of metabolically labelled hexosaminidase isoenzymes

Materials

PBS (see 2.1.1)

Lysis buffer:
10 mM Tris-HCl
150 mM NaCl
1% NP40 (BioRad)
1 mM Pefabloc^{R}SC (AEBSF) (Boehringer Mannheim)

0.02 % NaN_3

10 X BSA: 100 mg BSA/mL (in lysis buffer)

N-ethylmaleimide, 4 mM in lysis buffer containing BSA (10 mg/mL)

Denaturation buffer: 20 mM Tris-HCl, pH 7.4
1% SDS
20 mM DTT

Anti-human fibronectin rabbit polyclonal antiserum (Gibco/BRL)

Dialysis tubing (1 mL/cm) (Spectra/Por^R MWCO 3, 500)

Protein A-bearing *S.aureus* fixed cells (Pansorbin) (Calbiochem)

Wash buffer: 10 mM Tris-HCl, pH 8.6
600 mM NaCl
0.1% SDS
0.1% NP40

Resuspension/dialysis buffer: 10 mM Tris-HCl, pH 7.4
150 mM NaCl

SDS-PAGE loading buffer: 125 mM Tris-HCl, pH 6.8
1% SDS
10 % glycerol

100 mM dithiothreitol (DTT)

Bromophenol blue, 1% (w/v)

2.3.3.1 Preparation of cell extracts

Cell extracts were prepared based on a modified protocol from Proia *et al.* (1984). Labelled fibroblasts were rinsed twice with PBS and scraped off dishes in 500 μL of lysis buffer containing Pefabloc (1 mM). The lysates were transferred to 1.5 mL microcentrifuge tubes and incubated at 4°C with rocking for 10 minutes. The lysates were cleared by centrifugation at $>10,000$ x g for 10 minutes at 4°C. A 30 μL aliquot was

removed to determine the protein concentration (see 2.1.4) and 50 μL of 10 X BSA was added to the remaining sample. The lysates were stored at -80°C. Equal amounts of protein were placed in separate tubes and brought to equal concentrations with lysis buffer containing 1 X BSA.

Fibronectin was removed from lysates by incubating with 5 μL of anti-human fibronectin with rocking for 30 minutes to 1 hour at 4 °C. The antiserum was removed by incubating, with rocking, with 60 μL of Pansorbin for 15 minutes. The Pansorbin was removed by centrifugation at $>10,000$ x g, and the sample was treated with Pansorbin two additional times. The final cleared lysate was separated into three equal volumes. Each volume was incubated, with rocking, with 2 μL of the desired antiserum (see 3.3.1) overnight at 4 °C.

2.3.3.2 Preparation of medium extracts

The medium was collected into a 50 ml centrifuge tube and cleared by centrifugation for 10 minutes at 5, 000 x g in a Sorvall SS-34 rotor. Ammonium sulfate was added to the supernatant at a final concentration of 70% saturation in a 50 mL screw-capped tube. The ammonium sulfate was allowed to dissolve by rocking at 4 °C. The samples were cleared by centrifugation 20 minutes at 10, 000 x g in the same rotor. The supernatant was discarded and the pellet was dissolved in 1 mL of resuspension buffer containing 1.5% BSA. The sample was transferred to dialysis tubing and dialyzed overnight against the same buffer with one change of buffer after 8 hours. The sample was pre-cleared with anti-human fibronectin and Pansorbin followed by an overnight incubation with the desired antiserum (see 2.3.3.1).

2.3.4 Isolation of immune complexes

Immunoprecipitations were done essentially as described by Proia *et al.* (1984), with some modifications. The samples from above (see 2.3.3), were incubated with 60 μL of Pansorbin for 60 minutes. The cells were pelleted by centrifugation (> 10, 000 x g), and the supernatant was discarded. The pellet was resuspended in 600 μL of wash buffer (see 2.3.3). The cells were pelleted again and resuspended in 1 mL of resuspension buffer (see 2.3.3). The cells were pelleted again, resuspended in 50 μL of SDS-PAGE loading buffer, and heated in a boiling water bath for 5 minutes. The supernatant was cleared by centrifugation (> 10, 000 x g), and transferred to a tube containing 10 μL of DTT and 1 μL of bromophenol blue (1 % w/v). This was heated in boiling water for 5 minutes, and 15 μL was subjected to SDS-PAGE (see in 2.3.5).

2.3.4.1 Immunoprecipitation of precursor and mature α-subunits using the anti-α antiserum

Under non-denaturing conditions, only precursor α-subunits could be immunoprecipitated with the anti-α antiserum (Hasilik & Neufeld, 1980). To expose the epitope that would make the mature α-subunit immunoprecipitable with the anti-α antiserum, anti-Hex A immunoprecipitates that would be expected to contain mature α-subunits were isolated with Pansorbin. The immunocomplexes were collected by centrifugation at >10, 000 x g for 2 minutes, resuspended in 50 μL of denaturation buffer and heated at 100°C for 10 minutes. The solution was then cleared by centrifugation at >10, 000 x g for 2 minutes and the supernatant was diluted 10-fold with 4 mM N-ethylmaleimide in lysis buffer containing BSA (10 mg/mL). Of the anti-α

antiserum, 4 μL was added to the diluted solution, incubated overnight with rocking at 4°C, and immunoprecipitation was conducted as described in 2.3.4.

2.3.5 Analysis by SDS-PAGE and fluorography

Materials

5 or 12% separating gels:

distilled water	4.77 or 2.45 mL
30% acrylamide:bisacrylamide (100:1)	1.67 or 4.0 mL
10% SDS	0.4 mL
50% glycerol	1.0 mL
5X separating buffer:	2.0 mL
(0.5 M Tris, 1.5 M glycine, pH 8.8 without adjustment)	
10% ammonium persulfate	150 μL
TEMED	5 μL

4% stacking gel:

distilled water	5.9 mL
30% acrylamide:bisacrylamide (100:1)	1.34 mL
10% SDS	0.4 mL
0.1 M EDTA, pH 7.6	0.4 mL
50% glycerol	1.0 mL
1.0 M Tris-HCl, pH 6.8	0.7 mL
10% ammonium persulfate	250 μL
TEMED	5 μL

Gel fixing solution: 10% acetic acid
20% methanol

ENTENSIFY (Part A and B) (NEN Research Products)

10 X running buffer: 1.0 M Tris
1.5 M Glycine
1% SDS

The protocol that provided the best separation of all components of the β-hexosaminidase isoenzyme precursors was a modified protocol from Doucet *et al.*, 1990 and Doucet & Trifaro, 1988. The samples were separated on a discontinuous polyacrylamide gel containing 1% SDS, 5% glycerol, 50 mM Tris-HCl with an

acrylamide:bisacrylamide ratio of 100:1. The acrylamide percentage was in a gradient from 5 to 12 percent and was made using a gradient maker. The 4% stacking gel was degassed before pouring. Electrophoresis was conducted on a BioRad Protean™ II apparatus at 350 V (constant voltage). The thickness of the gels ranged from 0.75 mm to 1.5 mm. The upper buffer chamber contained 1 X running buffer, and the lower buffer chamber contained 0.5 X running buffer. When the bromophenol blue dye reached the bottom of the gel, the apparatus was disassembled and the gels were fixed in an excess of gel fixing solution for at least 1 hour with one change of solution after every 20 or 30 minutes. The gels were treated with ENTENSIFY solutions A and B according to manufacturer's instructions, dried (see 2.2.1.2), and fluorography was done using Kodak X-OMAT™ AR film at -80°C for an overnight to a 7 day period, depending on the desired exposure.

2.4 Introduction of vectors into bacterial cells

2.4.1 Strains

DH5α: *supE44 ΔlacU169* (Φ80 *lacZΔM15*) *hsdR17 recA1 endA1 gyrA96 thi-1 relA1*

JM109: *recA1 supE44 endA1 hsdR17 gyrA96 relA1 thi Δ(lac-proAB)* F'[*traD36 proAB*$^+$ *lacI*^{q} *lacZΔM15*]

JM101: supE thi-1 *Δ(lac-proAB)* F'[*traD36 proAB+ laqI*^{q} *lacZΔM15*]

TOP10: F' *mcrA Δ(mrr-hsdRMS-mcrBC) Φ80ΔlacZM15 ΔlacX74 deoR recA1 araD139(ura,leu)7697 galU galK* λ-*rpsL(streptomycin*^{r}*) endA1 nupG* F'[*proAB, laqI*^{q}*, lacZΔM15, Tn10 (tet*^{r}*)*]

2.4.2 Bacterial growth media

Several types of bacterial growth medium were used (Sambrook *et al.*, 1989). All medium components were autoclaved together, unless specified otherwise. Their components are described in this section, and they are referred to in the sections where they are used.

LB medium (for 1 L):	Bacto tryptone, 10 g Bacto Yeast Extract, 5 g NaCl, 10 g
LB (low salt)(for 1 L):	Bacto tryptone, 10 g Bacto Yeast Extract, 5 g NaCl, 5 g
SOC medium (for 1 L):	Bacto Tryptone, 20 g Bacto yeast extract, 5 g NaCl, 0.5 g 2.5 mM KCl 20 mM glucose (added after autoclaving) pH 7.0
M9 minimal salts agar:	M9 minimal salts (Gibco/BRL) 10 g in 969 mL H_20 Bacto agar 15 g After autoclaving: 1 mL 1M $MgSO_4$ 10 mL 0.1M $CaCl_2$ 10 mL 5% NaCl 10 mL 20% glucose 1 mL 1M thiamine

2.4.3 Preparation of electrocompetent cells

Materials

500 mL LB (low salt) (see 2.4.2)

1.5 L ice cold distilled water (autoclaved)

A single colony was picked and grown overnight in 5 to 10 mL of LB. A 100-fold dilution of the culture was made in 500 mL of LB (low salt) and grown for 4 to 5 hours or until mid-log phase. The culture was cooled on ice, poured into centrifuge bottles, and

centrifuged at 4000 x g for 15 minutes in a Sorvall GSA rotor. The cell pellets were gently resuspended in 1 volume of ice cold distilled water. The cells were centrifuged again and gently resuspended in one half volume of ice-cold distilled water. This was repeated again with one-half volume, 1 quarter volume, and finally with one-twentieth volume of water. The cells were gently resuspended in 0.002 of the original volume in 10% glycerol and immediately frozen using dry ice. The cells were stored at -45°C or -80°C in aliquots of 40 μL in microcentrifuge tubes.

2.4.4 Electroporation

Materials

Electrocompetent cells (see 2.4.3)

SOC (see 2.4.2)

Plasmids were introduced into bacterial strains by electroporation using the protocol that was recommended by BTX, Inc. One 40 μL aliquot of electrocompetent cells (see 2.4.3), was thawed entirely on ice and 1 to 1.5 μL of plasmid DNA containing solution was gently pipetted into the cell suspension. The cell suspension was pipetted once and transferred to a pre-chilled BTX disposable electroporation cuvette. The cuvette was tapped on the table surface 3 times, the exterior was patted dry, and inserted into the electroporation chamber. Electroporation was done at the suggested settings: 2.5 kV resistance, 29 Ω, and 1.3 charging volts. Immediately after electroporation, 960 μL of LB or SOC was added. The transformation mixture was incubated at 37°C for 30 to 60 minutes. Up to 200 μL of the transformation mixture was plated onto LB agar containing ampicillin (100 μg/mL). Smaller volumes were also routinely plated. As a positive

control for transformation efficiency, 1 ng of any plasmid construct was transformed separately. Efficiency of transformation was calculated as the number of transformants per μg of transformed plasmid DNA.

2.5 Construction of cDNA expression constructs

2.5.1 Vectors used

2.5.1.1 pBluescript

pBluescript (pBS) was purchased from Stratagene. Both pBS- and pBS+ versions were utilized. This vector allowed for the production of single-stranded DNA in *E.coli* JM109 or JM101 (see 2.4.1) and for sequencing of cloned DNA from the T3 and T7 promoters.

2.5.1.2 pSVL

pSVL was purchased from Pharmacia. It harbours the late SV40 promoter *(+ori)* and allows expression of cloned DNA in mammalian cells, but is highest in Cos-7 cells that express the T-antigen.

2.5.1.3 pCD

The expression vector, pCD, was used to express the *HEXB* cDNA in the cDNA construct, pCD43 (see 2.5.2.2). pCD was removed from pCD43 using *Xho*I and it was used as a cloning vector. pCD harbours the SV40 early promoter, allowing for expression of cloned DNA as described for pSVL.

2.5.1.4 pRc/CMV

pRc/CMV, (Invitrogen), is a 5.5 kb vector designed for a high-level of stable and

transient expression in eukaryotic hosts. The vector replicates episomally in cell lines that are latently infected with SV40 or which express the SV40 large T-antigen.

2.5.2 Sources of cloned cDNA constructs

2.5.2.1 *HEXA* cDNA

The normal α-subunit cDNA was removed from the pTK18 construct (Myerowitz *et al.*, 1985), with *Nar*I/*Pst*I and subcloned into the *Acc*1/*Pst*1 cloning site of pBS(-). This construct was named pHHEXA2 and was used for mutagenesis (see 2.8). The cDNA was removed with *Xho*I/*Bam*HI and subcloned into the *Xho*I/*Bam*HI cloning site of pSVL. This construct was named αpSVL. The pTK18 construct was kindly provided by Dr. Roy Gravel (McGill University).

2.5.2.2 *HEXB* cDNA

A full length *HEXB* cDNA (pCD43) was isolated by O'Dowd *et al.* (1985), and was kindly provided by Dr. Roy Gravel. The 2 kb *Xho*I fragment harbouring the cDNA was removed from pCD43 and subcloned into the *Xho*I cloning site of pBS(+). This construct was named pHEXBBS(+) and was used for site-directed mutagenesis (see 2.8).

2.5.2.3 β-galactosidase cDNA

The β-galactosidase cDNA was removed from the pRSV-β-gal construct by *Hind*III/*Sca*I and ligated into pBluescript to give the pBS-lacZ construct which was digested with *Hind*III/*Apa*I to release the lacZ fragment. The lacZ fragment was subcloned into the *Hind*III/*Apa*I sites of pRc/CMV to give the pRc/CMV-β-gal construct. This was kindly provided by Dr. David Litchfield from the Manitoba Cancer and Treatment Foundation, Winnipeg.

2.5.3 Separation of DNA using TBE-gel electrophoresis

2.5.3.1 Agarose TBE-gel electrophoresis

Materials

5 X TBE: 446 mM Tris
445 mM Boric acid
10 mM EDTA, pH 8.0

Agarose, Genetic Technology Grade (ICN Pharmaceuticals, Inc)

Ethidium Bromide (10 mg/mL in distilled water)

Agarose gel loading buffer: 0.25% bromophenol blue
0.25% xylene cyanol
30% glycerol

1 kb DNA ladder (Gibco/BRL) (100 ng/μl in agarose gel loading buffer)

DNA fragments were routinely separated and visualized by agarose gel electrophoresis in 1 X TBE (Sambrook *et al.*, 1989). DNA fragment sizes were determined by comparison to the 1 kb DNA ladder. For the separation of native plasmids or DNA fragments that were 500 bp or larger, 0.8 to 1.0% agarose gels were used. For DNA fragments smaller than 500 bp, 1.5% and 2% agarose gels were used. For the visualization of a 20 bp fragment, a 2.5% gel was sufficient. For high resolution separation of more than two fragments smaller than 500 bp, acrylamide TBE-gels were used (see 2.5.3.2).

The agarose was placed in a 250 mL Erlenmeyer flask containing 100 mL 1 X TBE. The solution was boiled in a microwave oven, gently mixed, and 5 μL of ethidium bromide was added. Upon cooling to approximately 55°C, the gel was was poured onto an agarose gel casting tray for a Gibco/BRL HORIZON™ 11-14 apparatus. The desired

well maker was inserted, and the gel was allowed to solidify. The gel was placed in a buffer tank containing 1 X TBE such that the buffer was approximately 1 cm above the top of the gel. The DNA sample of interest was diluted in 1 or 2 X agarose gel loading buffer and in a final volume between 10 and 25 μL which was loaded into the wells of the gel. Electrophoresis was done at a constant voltage between 100 and 200 V until the bromophenol blue migrated two-thirds of the length of the gel. The DNA in the gel was visualized with an ultraviolet transilluminator and photographed with Polaroid type 667 ISO 3600/36° film using a Polaroid MP-4 land camera.

2.5.3.2 Acrylamide TBE-gel electrophoresis

DNA samples were prepared as described in 2.5.3.2 and separated on a 1 mm 10% acrylamide:bisacrylamide (29.2:0.8) gel made with 1 X TBE. The samples were separated on a Gibco/BRL Vertical Gel Electrophoresis System Model V16, or on the BioRad Mini-PROTEAN™ II cell apparatus (see 2.1.6.1). The gels were run in 1 X TBE at 100 to 200 V until the bromophenol blue migrated approximately two-thirds of the length of the gel. The gel was stained in 0.1% ethidium bromide for 10 minutes and then destained using distilled water. The DNA fragments were visualized and photographed (see 2.5.3.1).

2.5.4 Subcloning procedures

DNA subcloning was done essentially as described in Sambrook *et al.*, 1989. Specific details and modifications are described in 2.5.4.1-3.

2.5.4.1 Preparation of cloning vector

Materials

Restriction enzyme buffer (enzyme specific)

Buffer-saturated phenol (Gibco/BRL)

Chloroform

3 M Sodium acetate, pH 4.8

95% ethanol

70% ethanol

sterile distilled water

Plasmids that were used as cloning vectors were purified as described in 2.6.2. The cloning vector of interest was routinely prepared by restriction enzyme digestion in a volume of 100 μL at a concentration of 0.1 μg plasmid/μL. Generally, 10 or 20 U of the desired resitrction endonuclease was added to the reaction mixture. In the case of a restriction enzyme digest using two enzymes, each enzyme digest was conducted independently and complete digestion was confirmed by agarose gel electrophoresis (see 2.5.3.1), before the second enzyme was added.

The digested plasmid DNA was extracted using phenol and chloroform. The final volume was increased to 600 μL with distilled water and the DNA was extracted with an equal volume of phenol. This was done by mixing at maximum speed for 30 seconds using a vortex followed by centrifugation for 10 minutes at maximum speed. The upper aqueous layer was then extracted with an equal volume of chloroform in the same manner. The plasmid DNA in the aqueous layer was precipitated in the presence of 10% of 3 M sodium acetate (pH 4.8), and approximately 2.5 volumes of 95% ethanol.

2.5.4.2 Preparation of cloning insert

Of the plasmid containing the insert of interest, approximately 5 μg was digested in a 50 μL volume. The extent of digestion was determined by examining a 3 to 5 μL aliquot by agarose gel electrophoresis (see 2.5.3.1). Upon complete digestion, the restriction enzyme digest was separated by agarose gel electrophoresis and the DNA fragment of interest was removed from the gel using a sterilized razor blade. The DNA was purified using a GENECLEAN II kit (BIO101), or the GlassMax purification system (Gibco/BRL). All purified DNA products were resuspended in sterile distilled water.

2.5.4.3 Ligation Reaction

Materials

5X Ligation buffer(Gibco/BRL):	250 mM Tris-HCl, pH 7.6 50 mM $MgCl_2$ 5 mM ATP 5 mM DTT 25% (w/v) polyethylene-glycol 8000

T4 DNA ligase ($\geq$400 U/μL) (New England Biolabs)

To estimate the relative amount of cloning vector and insert used in a ligation reaction, one-tenth of the prepared samples were subjected to agarose gel electrophoresis and the quantity of DNA was estimated visually (see 2.5.3.1). Approximately 100 ng of vector and insert were included in a ligation in a volume of 15 μL in the presence of 1 X ligation buffer and 0.5-1.0 μL of T4 DNA ligase. Ligation reactions were carried out at 14°C for at least 8 hours, and a ligation reaction where the insert was excluded was used as a negative control for vector re-ligation. The ligations were transformed as described in 2.4.4, and the ligation products were analyzed by gel electrophoresis as described in 2.6.1.

2.6 Plasmid DNA purification

Materials

LB broth (ampicillin 100 μg/mL) (see 2.4.2)

S1 (Resuspension buffer): 50 mM Tris-HCl
10 mM EDTA, pH 8.0

S2 (Cell disruption buffer): 0.2 N NaOH
1% SDS

S3 (Neutralizing Buffer): 2.8 M potassium acetate, pH 5.2

RNAse A (Boehringer Mannheim)

2.6.1 Mini-scale

Single colonies from transformations (see 2.4.4) were picked with a sterile toothpick and inoculated into 5 mL tubes containing 2 mL of LB broth supplemented with 100 μg/mL ampicillin. The cultures were grown at 37°C for 8 hours, or up to an overnight period with constant shaking at 250 to 350 rpm.

To extract plasmid DNA, 1.5 mL of the bacterial culture was centrifuged for 1 minute at 14,000 x g using a microcentrifuge. It was ensured that the LB medium was completely removed. The bacterial pellet was resuspended in 200 μL of S1 by pipetting. The cell suspension was lysed with 200 μL of S2 for five minutes with no agitation. The solution was neutralized with 200 μL of S3 by inverting several times until there was a white precipitate in a clear background solution. This was incubated on ice for 5 to 10 minutes. The supernatant was cleared by centrifugation at $>$10,000 x g for 5 to 10 minutes, mixed with 1 mL of ethanol (95%), and incubated on ice for 20 minutes or at -80°C for 10 minutes. Nucleic acids were pelleted by centrifugation for 10 minutes at

$>$10,000 x g. The supernatant was discarded and the nucleic acid pellet was rinsed with 70% ethanol, and centrifuged again. The ethanol was completely removed. The nucleic acid pellet was air dried for 10 to 15 minutes, and was resuspended in 50 μL of double-distilled water containing RNase A (1 to 5 μg). After a 30 minute incubation at room temperature, 10 μL was used for digestion in a final volume of 20 μL.

2.6.2 Large-scale purification of plasmids

Of an overnight mini-culture (see 2.6.1), 500 μL was inoculated into a volume of 200 to 500 mL of LB containing ampicillin (100 μg/mL). The culture was grown at 37°C for 12 to 18 hours with constant shaking at 250 to 300 rpm.

The culture was poured into centrifuge bottles and centrifuged at 4,500 x g for 15 minutes at 4°C. The LB was poured off and any remaining LB was removed with a Pasteur pipette. The bacterial pellet was resuspended in 50 mL of S1 containing 100 μg/mL RNase A. The resuspended cells were separated into four-12 mL aliquots. The cells in each 12 mL aliquot were lysed with 12 mL of S2 buffer and repeatedly inverted, gently, until the solution became clear. Of the S3, 12 mL was added and the tube was inverted several times until the solution was clear with a white precipitate. This was followed by an incubation on ice for 15 minutes. The solution was cleared by centrifugation at 12, 000 g for 30 to 45 minutes.

The plasmid DNA in the supernatant was separated by chromatography using a pre-equilibrated Nucleobond AX500 column and the manufacturer's protocol (The Nest Group, Inc., Southbora,MA). For plasmid preparations using this method, the columns were re-equilibrated and re-used after plasmid DNA isolation.

2.6.3 Spectrophotometric determination of DNA concentration

Purified plasmid DNA concentrations were usually estimated by measuring the optical density of the sample at 260 nm ($O.D._{260}$) through a one cm light path (Warburg and Christian, 1942). The following calculation was used to determine DNA concentration:

DNA concentration ($\mu g/\mu L$)=($O.D._{260[sample]}$) x (dilution factor) x (50 μg DNA/$O.D._{260}$)

2.7 Sequencing of cloned DNA

Materials

1 M NaOH

5 M ammonium acetate, pH 4.8

α-^{35}S-dATP (NEN)

Pharmacia T7 sequencing kit

10 X TBE (modified) (1 L): 162 g Tris
27.5 g Boric acid
9.59 g EDTA

Gel mix (70 mL): 29.4 g urea (Gibco/BRL, Ultrapure)
10.5 mL 40% acrylamide:bisacrylamide (19:1)
7 mL 10X TBE (modified)
distilled water

2.7.1 Alkali denaturation of sequencing template and sequencing reactions

Sequencing of cloned DNA was conducted using the method of Sanger *et al.* (1977). Of the column purified plasmid DNA (see 2.6.2), 2 to 4 μg was subjected to alkali denaturation. A mini-plasmid preparation that had been extracted with phenol:chloroform (see 2.5.4.1) was sufficient for this procedure. Plasmid DNA was brought to a volume of 16 μL with water and 4.0 μL of 1 M NaOH was added. After

a 5 to 10 minute incubation at room temperature, 2.0 μL of 5 M ammonium acetate was added, then mixed, and 50 μL of 95% ethanol was added to precipitate the DNA from the solution. The mixture was kept on ice for at least 15 minutes and the plasmid DNA was pelleted in a microcentrifuge at $>10,000$ x g. The pellet was washed with 750 μL of 70% ethanol, air dried, and resuspended in 10 μL of distilled water. When several sequencing reactions were desired using the same template, the amount of plasmid and the volume of the reaction were increased accordingly.

The resuspended denatured plasmid was then sequenced using Pharmacia's T7 Sequencing™ kit. The annealing mixture is described below:

Denatured template DNA	10 μL
Primer (10 ng/μL)	2 μL
Annealing Buffer (kit)	2 μL
	14 μL

The mixture was incubated at 65°C for 5 minutes, followed by a 10 minute incubation at 37°C, and a final incubation at room temperature for 10 minutes.

The labelling reaction (described below) was incubated at room temperature for 5 minutes:

Annealing reaction	14 μL
Labelling Mix "A"(kit)	3 μL
α-^{35}S dATP	1 μL
T7 DNA polymerase (1:5)	2 μL
	21 μL

A 4.5 μL aliquot of the labelling reaction was added to 2.5 μL of A,C,G,T Mix-Short (kit), and incubated at 37°C for 5 minutes. Each of the four reactions was stopped with 5 μL of stop solution (kit).

Of the reactions, 3 μL was separated by sequencing gel electrophoresis (see

2.7.2).

2.7.2 Sequencing gel electrophoresis

The sequencing gel (see 2.7) was poured as described in 2.2.1.2, and a sharkstooth comb was used as a well maker. The gel was pre-warmed at approximately 55 W (1200 volts) for 30 minutes. The sequencing reactions were heated in a boiling water bath for 3 to 5 minutes, and a 3 μl aliquot was loaded onto the sequencing gel. The samples were separated at 55 W (1200 volts) until the bromophenol blue dye migrated to the bottom of the gel. The gel was dried and exposed to film (see 2.2.1.2).

2.8 Site-directed mutagenesis

2.8.1 Single-stranded DNA preparation

Materials

M9 minimal salts agar (see 2.4.2)

E.coli JM109

M13KO7 helper phage, $>10^{11}$ pfu (New England Biolabs)

Kanamycin sulfate (100 mg/mL) (Gibco/BRL)

30% PEG 3350 (1.5 M NaCl)

Buffer-saturated phenol

Chloroform

3 M Sodium acetate, pH 4.8

Single-stranded template DNA was prepared (Ausubel *et al.*, 1987) in the

pBLUESCRIPT vector. The plasmid DNA construct was introduced (see 2.44) into *E.coli* JM109 (see 2.4.1) that was previously selected from M9 minimal agar supplemented with thiamine, and a single transformant was grown overnight in 5 mL of LB (100 μg/mL ampicillin). The following day, 200 μL was subcultured into 20 mL of LB with no antibiotics and grown for 2 hours or until very early log phase. M13K07 helper phage was then added to a final concentration of 10^{-8} pfu, and incubated for 90 minutes. Kanamycin sulfate was then added at a final concentration of 70 μg/mL. The culture was grown for 14 hours at 37°C under constant shaking (300 rpm).

The culture was centrifuged for 10 minutes at 8, 000 rpm in a Sorvall SS-34 centrifuge, and the bacterial pellet was discarded. The medium was cleared by centrifugation two additional times. The cleared medium was incubated with 0.2 volumes of 30% PEG 3500 at room temperature for 15 minutes. The mixture was centrifuged for 5 minutes, and the supernatant was discarded. Centrifugation was repeated three additional times until there was a compact visible pellet and all supernatant was removed.

The pellet was resuspended in 600 μL of distilled water and mixed, using a vortex at maximun speed, for 60 seconds in the presence of 600 μL of phenol/chloroform (1:1). The mixture was incubated at room temperature for 5 minutes and mixed again for 1 minute, then centrifuged for 5 minutes. The aqueous layer was extracted once more with phenol/chloroform and then finally with chloroform. One tenth the volume of 3 M sodium acetate and two volumes of 95% ethanol were added to the aqueous phase and incubated on dry ice for ten minutes to precipitate the ssDNA. The ssDNA was pelleted by centrifugation at >10, 000 x g for 10 minutes, followed by a wash with 1 mL of

70% ethanol to remove excess salts. The ssDNA was finally resuspended in 100 μL of sterile distilled water.

2.8.2 Annealing of oligonucleotide to the ssDNA

The single-stranded DNA was mixed with the following components and incubated in a 500 mL beaker containing 250 to 300 mL of water heated to exactly 70°C. As a negative control, a separate reaction containing no oligonucleotide was used.

15 μL ssDNA (approximately 200 ng)
2 μL 5'-phosphorylated oligonucleotide (approximately 20 ng) (University of Calgary)
2 μL 10 X annealing buffer: 200 mM Tris, pH 7.4
20 mM $MgCl_2$
500 mM NaCl
1 μL distilled water

The beaker was placed on ice such that only the bottom surface of the beaker touched the ice. The temperature of the water surrounding the sample in the tube was monitored.

2.8.3 Second strand synthesis

When the temperature reached 30°C (60 to 75 minutes later), the sample was briefly centrifuged and the following components were added in the following order:

2.5 μL 10 X synthesis buffer: 0.4 mM dATP, dCTP, dGTP, dTTP (Pharmacia)
0.75 mM ATP (Pharmacia)
17.5 mM Tris-HCl, pH 7.5
3.75 mM $MgCl_2$
21.5 mM DTT
0.5 μL H_20
1.0 μL diluted T7 polymerase (2 u/μL) (New England Biolabs)
1.0 μL T4 DNA ligase (>400 u/μL) (New England Biolabs)

The mixture was briefly pipetted and incubated on ice for 5 minutes. This was followed by an incubation at room temperature for 5 minutes, and a final incubation in

a 37°C water bath for 30 minutes.

2.8.4 Isolation of mutagenesis reaction products

The reactions were subjected to electrophoresis on a 0.8% agarose gel. As a positive control, 200 ng of plasmid DNA and ss DNA was also separated. The reactions were then analyzed. If the reaction was successful, a change in the migration pattern of the ss DNA was observed. The reaction samples migrated at the same rate as the plasmid control, and there was no single-stranded DNA detectable in comparison to the negative control.

If the reaction was successful, the newly-synthesized DNA was isolated as described in 3.1.1. Of the final product, 30 to 50% was introduced into DH5α cells by electroporation as described in 2.4.4.

2.8.5 Identification of mutant cDNA clones

The transformants of the mutagenesis reaction were isolated by streaking onto a separate LB agar plate or into 2 mL of LB broth (ampicillin 100 μg/mL) and grown overnight at 37°C. If the mutation that was incorporated destroyed or created a restriction enzyme site, then the surrounding region of DNA was amplified by PCR (see 2.2.2.2). The streaked out colonies were picked with a sterile toothpick, or 1 μL of the liquid culture was used as a template for the PCR reaction. Mutant clones were sequenced (see 2.7) and subcloned into the expression vector (see 2.5.4).

2.8.5.1 αG1422C

The phosphorylated oligonucleotide 5'-CCAGGCTCTGCCCCAGAGCAG was used to incorporate the G1422C transversion in the *HEXA* cDNA. The αG1422C mutants

were identified as described in 2.8.3 using the oligonucleotides A (5'-TGAGCAGAAGGCTCTGGTGA), and B (5'-AACTCACAGCGGAAGTGTGA), in the PCR reaction. The mutants were identified by the absence of a *Hae*III restriction enzyme site in the PCR product only in the presence of the mutation.

2.8.5.2 αG805A

The phosphorylated oligonucleotide 5'-TCCAGGGATACTTGGTCCCCAGGA was used to incorporate the G805A point mutation that is associated with adult-onset TSD. Mutant clones were identified from *ScrF*I restriction enzyme digest of PCR products (see 2.8.3), that were produced with an upstream oligonucleotide (primer A), and the oligonucleotide, 5'-CAAGGAGTCAGTAATCCAGAGTAC (primer B), that created an *ScrF*I restriction enzyme site in the presence of the G805A mutations.

2.8.5.3 αC508T

The phosphorylated oligonucleotide 5'-GCTTTCCTCACTGGGGCTTGCTG was used to incorporate a C508T transition that is associated with infantile TSD (Fernandes *et al.*, 1992b). The presence of the mutation was detected by testing for the absence of an *ScrF*I restriction enzyme site.

2.8.5.4 β-subunit mutant identification

The construct pHEXBBS(+) (see 2.5.2.2), harbouring the *HEXB* cDNA in the 5'-3' orientation was used for site-directed mutagenesis (see 2.8.2). The oligonucleotide 5'-CCAAGATTATGCCCTCGGGCAAG was used to incorporate a G1473C mutation (nucleotide sequence based on Proia, 1988), in the β-subunit cDNA construct. Mutants were identified by the absence of a *Hae*III restriction enzyme site in PCR products of

clones (see 2.8.3). The sequence from a unique *Aoc*I restriction enzyme site in the coding sequence to the stop codon was sequenced to verify the sequence. The *Aoc*I/*Kpn*I was removed and subcloned to the native pHEXBBS(+) cDNA construct. The *Xho*I fragment was subsequently subcloned to the *Xho*I site of pCD to give the final mutant expression construct.

2.9 Expression of *HEXA* and *HEXB* cDNA constructs in Cos-7 cells

2.9.1 Growth and storage of Cos-7 cells

Cos-7 cells (American Type Culture Collection) were grown, subcultured and stored as described in 3.1.1, with the exception that confluent cultures were never used.

2.9.2 cDNA transfection

Materials

Growth medium (see 2.1.1)

Phosphate buffered saline (PBS): 2.7 mM KCl
1.1 mM KH_2PO_4
138 mM NaCl
8.1 mM Na_2HPO_4

Cos-7 cells grown on one 150 mm x 20 mm culture dish at approximately 85% of confluence were subcultured among 10 dishes in α-MEM (see 2.1.1), and were allowed to proliferate to 70-80% of confleunce. At that time, the medium was aspirated and the plates were briefly rinsed with 5 mL of trypsin-EDTA. Each dish was incubated with 3 mL of trypsin-EDTA for 5 to 10 minutes while tapping the plates and pooling all of the cells into a 50 mL centrifuge tube. Any remaining cells were collected in PBS, and the final volume was brought to 50 mL with PBS. The cell suspension was gently mixed,

and a 500 μL aliquot was used to determine the cell number with a Coulter counter at the recommended settings: current (I)=100; full scale (mA)=1; polarity=auto; lower threshold (T_L)=3.0; upper threshold (T_U)=99.9; alarm threshold=25; attenuation (A)=32; preset gain=4. The cells were pelleted in a clinical centrifuge at 2, 000 rpm for 10 minutes, resuspended again in 50 mL of PBS, and centrifuged again. The cells were finally resuspended in PBS at a concentration of 3 x 10^6 cells/360 μL PBS. Generally, there were enough cells for 10 to 15 transfections.

The desired amount of each vector for transfection was transferred to microcentrifuge tubes, and the volume was brought to 40 μL with PBS. Routinely, 6.5 μg of αpSVL was used for Hex S expression and 2.0 μg of pRc/CMV-β-gal was used as the reporter gene. When the β-subunit cDNA (pCD43) was co-expressed, 2.5 μg of plasmid DNA was used. However, the amount of pCD43 DNA used was later increased (see 2.9.6).

Of the cell suspension, 360 μL was added to each tube of plasmid, pipetted once, and the final 400 μL volume was transferred to a BTX electroporation cuvette (2 mm gap), that was pre-chilled on ice. The cuvette containing the cell/plasmid mixture was tapped 10 times from each side to ensure mixing, then tapped on the table 3 times, and subjected to electroporation using a BTX Electro Cell Manipulator^R 600 (150 charging volts, 48 Ω, 1200 μF), and then placed on ice for 5 to 10 minutes. Transfected cells were plated onto a 150 mm x 20 mm cell culture dish containing approximately 20 mL of α-MEM supplemented with antibiotics and FBS (see 2.1.1.1). After 24 hours, the medium was replaced. After 72 hours, post-transfection, the cells were harvested and lysates were

prepared as described in 2.1.3.

2.9.3 Analysis of hexosaminidase transiently expressed in Cos-7 cells

2.9.3.1 Hexosaminidase assay

Of the transfection lysates, 3 μL was incubated with 7 μL of citrate phosphate buffer and 20 μL of 3 mM 4-MUGS. The reaction was carried out as described in 2.1.5.2. The samples were measured as described in 2.1.5.3.

2.9.3.2 β-galactosidase assay

Materials

Z-buffer: 60 mM Na_2HPO_4
40 mM NaH_2PO_4
10 mM KCl
1 mM Mg_2SO_4
pH 7.0 adjusted with NaOH/HCl

3 mM 4-MUG-β-galactoside, in Z-Buffer (Sigma)

Glycine carbonate (see 2.1.5)

The amount of coexpressed β-galactosidase was determined (MacGregor *et al.*, 1991) with the use of the substrate 4-MUG-β-galactoside. Of the transfection lysate, 3 μL was resuspended with 97 μL of Z-buffer. The 4-MUG-β-galactoside (3 mM) was heated at 100°C for 1 minute to dissolve the substrate, and 30 μL was added to the lysate. The reaction occurred at 37 °C for 30 minutes. The reaction was stopped with 870 μL of glycine carbonate and measured as described in 2.1.5.3.

2.9.3.3 Correction of Hex A activity based on transfection efficiency

The extent of β-galactosidase co-expression was used as a measurement of transfection efficiency. The specific β-galactosidase activity in Cos-7 cell extracts was

determined as described for determining specific Hex A activity in 2.1.5.4.

The relative efficiency was determined using the following calculation:

Relative efficiency=

$$\frac{\text{s.a. of sample (nmol 4-MUG-}\beta\text{-gal hydrolyzed/mg protein/hr)}}{\text{average s.a. in experiment (nmol 4-MUG-}\beta\text{-gal hydrolyzed/mg protein/hr)}}$$

The endogenous levels of β-galactosidase in Cos-7 cells was determined but not included in the calculation because the values were negligible in comparison to the transfected cells.

The observed Hex A activity in transiently expressing Cos-7 cells was then corrected based on β-galactosidase activity using the following calculation:

Hex A and S activity in transfected cells=

$$\frac{\text{Hex activity (transfected cells) - Hex activity (mock transfected cells)}}{\text{Relative efficiency}}$$

2.9.3.4 Western blot analysis

Of the Cos-7 cell extracts, 20 μg was subjected to Western blot analysis (see 2.1.6).

2.9.3.5 Metabolic labelling analysis in transiently transfected cells

The transfection protocol was modified for pulse-chase analysis of transfected α- and β- subunits. The protocol in 2.9.2 was used with the following modifications:

1) The amount of pCD43 used in Hex A expression was increased to 10 μg.

2) The cell number per transfection was increased to 3.5×10^6.

3) Two electroporations were done for every cDNA expression of interest. They were pooled together, and plated equally among three 100 mm x 20 mm culture dishes.

4) Pulse-chase analysis was conducted such that all cultures were labelled at the same time (pulse), and the final chase time was completed at 72 hours post transfection.

5) Cells were collected as described in 3.9.2. Cell extracts were made in microcentrifuge tubes by pipetting in 100 μL of lysis buffer (see 2.3.3), followed by an incubation on ice for 15 minutes. The lysates were cleared by centrifugation.

6) Lysates were precleared with 3-10 minute incubations of 30 μL of Pansorbin.

7) Only 1 μL of antiserum was used in each immunoprecipitation.

8) Immunoprecipitations were carried out as described in 2.3.3.1.

2.9.4 Analysis by DEAE cellulose chromatography

Materials

10 mM Sodium phosphate buffer (NaP_i), pH 6.0

0.215 M NaCl in NaP_i

0.3 M NaCl in NaP_i

0.5 M NaCl in NaP_i

The separation of β-hexosaminidase isoenzymes was achieved based on protocols modified from Mahuran *et al.* (1985) and Emiliani *et al.* (1990). DEAE cellulose columns were prepared in 3 mL syringes. The column material was heated in 10 mM NaP_i at 100 °C for 20 minutes and allowed to cool. Approximately 1 mL of DEAE-cellulose was packed onto the column and washed with 10 mL of NaP_i. Up to 2 mg of cell extract was loaded onto the column and allowed to incubate at 4°C for 20 minutes.

The lysate was fractionated into 40-1 mL fractions. The first 5 fractions were

collected in NaP_i buffer to elute Hex B. The next 20 fractions were collected from a 0 to 250 mM NaCl linear gradient in the same buffer to fractionate Hex A. This was followed by a step-gradient fractionation with 215, 300, 500 mM NaCl where 5 fractions were collected at each step. Hex S eluted at 215 mM and unknown hexosaminidase isoforms eluted at 300 mM and 500 mM NaCl.

Of each fraction, 10 μL was assayed using the substrate 4-MUG. The peak fractions were then assayed using 4-MUGS, an α-subunit specific substrate. The identity of each peak was characterized by Dr. Zhimin Cao using western blot analysis (data not shown).

3 RESULTS

3.1 Clinical diagnosis of the proband

A proband, designated as HSC3236, was diagnosed with a juvenile-onset form of TSD by Dr. Joe T.R. Clarke at the Hospital for Sick Children, Toronto, Canada. The case history described below, was provided by Dr. Clarke.

The proband presented at age 16 with an acute psychotic episode characterized by marked social and emotional withdrawal, paranoia, obsessional thinking, and compulsiveness associated with marked agitation. He had a history of increasing clumsiness, ataxia, and dysarthria dating back to age 10, though only becoming clinically obvious at age 14. Hex A activity in the serum with the use of 4-MUGS as a substrate was 13 nmol/ml/hr (controls: 126-173 nmol/ml/hr). The proband, and subsequently his younger brother, were diagnosed with a subacute encephalopathic form of G_{M2} gangliosidosis, Type I. At age 19, chronic psychosis with intermittent acute exacerbations remained the most disabling symptom in both the proband and his affected brother, although both exhibited some ataxia and moderately severe dysarthria. The father was of German and Dutch descent and his mother was of Portuguese and English descent. There was no family history of neurodegenerative disease.

3.2 Identification of mutations in the *HEXA* gene of HSC3236 fibroblast DNA

The mutations in the *HEXA* genes of HSC3236 fibroblasts were identified by Dr. Barbara Triggs-Raine and Timothy Salo at the University of Manitoba, Winnipeg,

Canada. The results of their analyses are presented below.

Each of the fourteen exons of the *HEXA* gene of HSC3236 fibroblast DNA was analyzed for mutations using SSCP (single-stranded conformational polymorphism) analysis. Gel mobility shifts, indicating nucleotide changes, were observed in SSCP analysis of exon 11 (not shown) and exon 13 (figure 7a). Heteroduplex analysis confirmed the presence of a 4-bp insertion (+TATC 1278) in exon 11 of one allele (Myerowitz & Costigan, 1988) (not shown). Sequencing of exon 13 revealed a G1422C transversion (figure 7b). This would be expected to result in a cysteine for tryptophan substitution at amino acid 474 (W474C), in the α-subunit of Hex A.

The presence of the G1422C transversion was confirmed by restriction endonuclease digestion using *ScrF*I and *Hae*III. The G1422C transversion was predicted to destroy these two restriction enzyme sites. *ScrF*I digestion of a normal 235 bp PCR product that harboured exon 13 and the surrounding sequences, produced 152, 50, and 33 bp DNA fragments (figure 8a). The loss of the *ScrF*I site resulted in an additional 202 bp DNA fragment, and a corresponding reduction in the levels of both 152 and 50 bp DNA fragments in the digests of the proband, his affected brother, and father. *Hae*III digestion of the same 235 bp PCR product produced 121, 41, 32, 20, and 21 bp DNA fragments; the 20 and 21 bp fragments are not shown (figure 8b). The loss of the *Hae*III site resulted in an additional 153 bp fragment, and a corresponding reduction in the levels of the 121 bp and 32 bp fragments. Restriction endonuclease analysis confirmed their heterozygosity for the G1422C transversion.

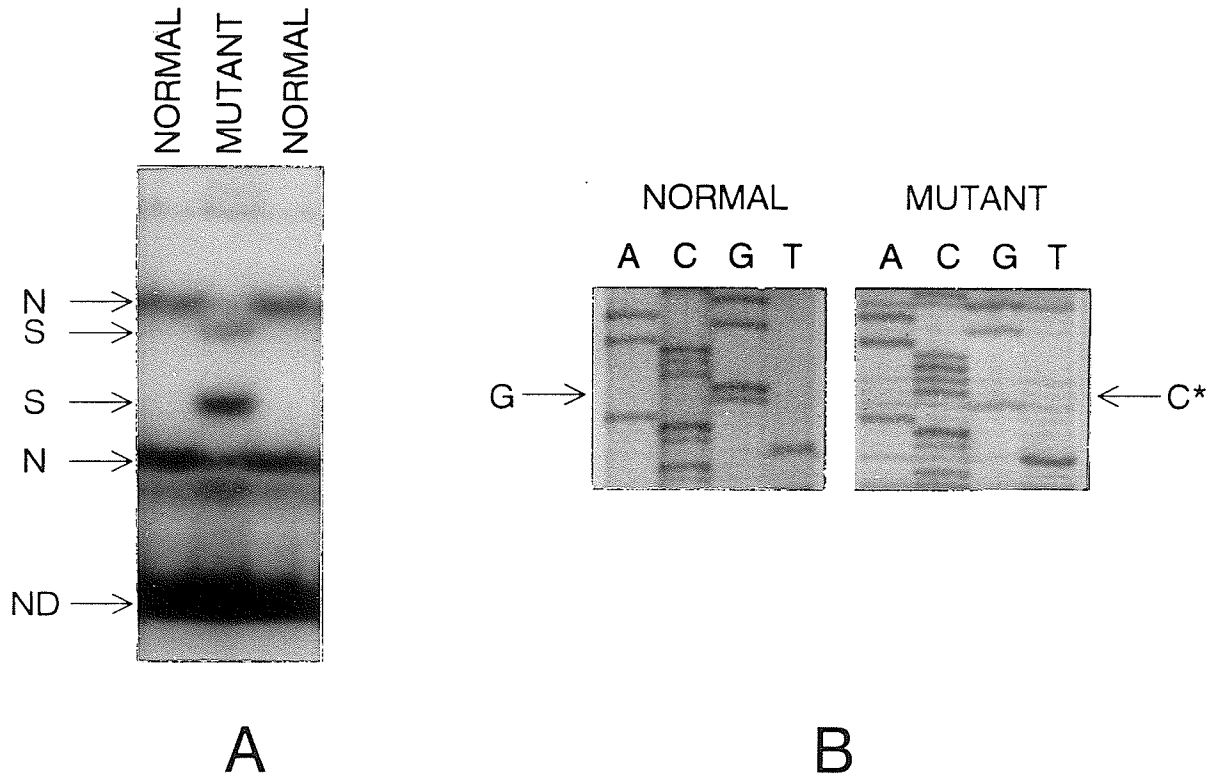

Figure 7 ***Detection of a mutation in exon 13.*** (A) SSCP analysis of exon 13 PCR products. Band shifts (S), in the denatured PCR product from HSC3236 fibroblasts were demonstrated in comparison to bands from two denatured normal *(N)*, exon 13 products. The non-denatured DNA is indicated, *(ND)*. (B) Sequence analysis of exon 13. A G to C base pair substitution is indicated on the autoradiograph. The normal DNA sequence is shown on the left. The DNA sequence found in HSC3236 fibroblasts is indicated on the right as "mutant".

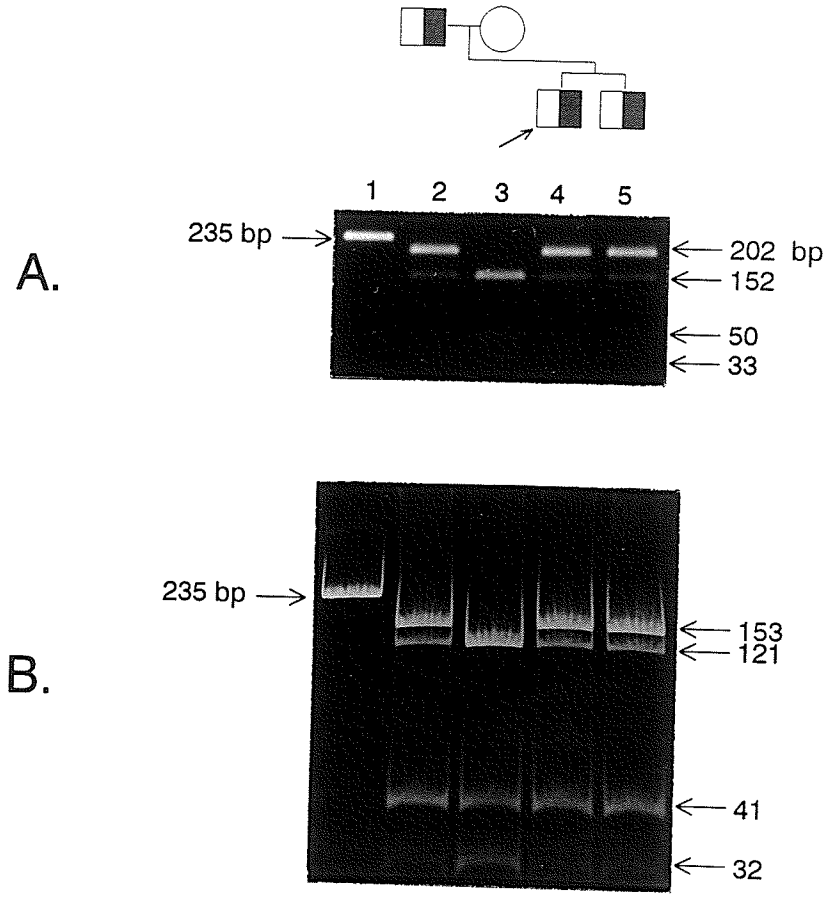

Figure 8 ***Scr*FI** ***and Hae*III** ***restriction enzyme digests.*** A 235 bp DNA fragment (1) harbouring exon 13 and surrounding sequences was amplified by PCR from genomic DNA of the patient (4), the patient's father (2), mother (3), and brother (5). The DNA fragment was incubated with *Scr*FI in A, or *Hae*III in B, restriction endonucleases to test for the presence of the G1422C transversion. The fragment sizes produced from restriction enzyme digestion are shown.

3.3 Hex A activity and α-subunit levels in HSC3236 fibroblasts

Hex A activity in HSC3236 fibroblasts and controls was determined using 4-MUG and 4-MUGS. The level of Hex A activity in HSC3236 fibroblast lysates was in the TSD range, although slightly higher than that found in fibroblast lysates from a proband with infantile TSD (table 1).

Western blot analysis using the anti-Hex A antiserum was done to look for α-subunit expression in HSC3236 fibroblast lysates. No mature α-subunit was detected in HSC3236 fibroblasts (figure 9). Although there were precursor α- and β-subunits detected, these were not well separated, and they were less abundant than in normal fibroblasts. Hence, it was difficult to compare the α-subunit precursor levels to those of the control lysates. Normal and TSD fibroblast lysates were used as positive and negative controls, respectively, for mature α-subunit expression. SD fibroblast lysates were used as a negative control for β-subunit expression and had a decreased level of mature α-subunit, probably because α-containing dimers are less likely to be formed if the β-subunit is absent (d'Azzo *et al.*, 1984). The level of the β-subunit in HSC3236 fibroblasts appeared similar to the normal and TSD fibroblast lysates. The identity of the cross-reacting protein that was present in TSD and SD lysates was unknown (labelled x in figure 9).

3.4 Analysis of αW474C expression in transiently transfected Cos-7 cells

3.4.1 Hexosaminidase activities and western blot analysis of overexpressed αW474C

To demonstrate that the G1422C (W474C) mutation could result in a deficiency in Hex A activity, the mutation was incorporated into the normal α-subunit cDNA

Table 1. Hexosaminidase activity in HSC3236 fibroblasts and controls

Fibroblasts	Total Hex (nmol 4-MUG hydrolyzed/mg protein/hr)	% Hex A (as determined after heating at 52°C for 2 hours) Observed Range	Hex A and S (nmol 4-MUGS hydrolyzed/mg protein/hr)
Normal	5291±511	54-61	473/482
HSC3236	5445±149	3.5-13	60/71
TSD	4680±169	0.7-10	18/37
SD	26.5±4.4	96-99	4.8/15.1

Total β-hexosaminidase activity was determined in HSC3236, normal (MCH065), TSD (WG1881), and SD (GM00294) fibroblast lysates using 4-MUG. The values are based on an average (±sample standard devitation) of six assays. The proportion of Hex A activity was also determined by 4-MUG after heat treatment of lysates at 52°C for 2 hours. The observed range of Hex A activity, with the use of 4-MUGS; two values are given, and each value is an average of duplicate assays.

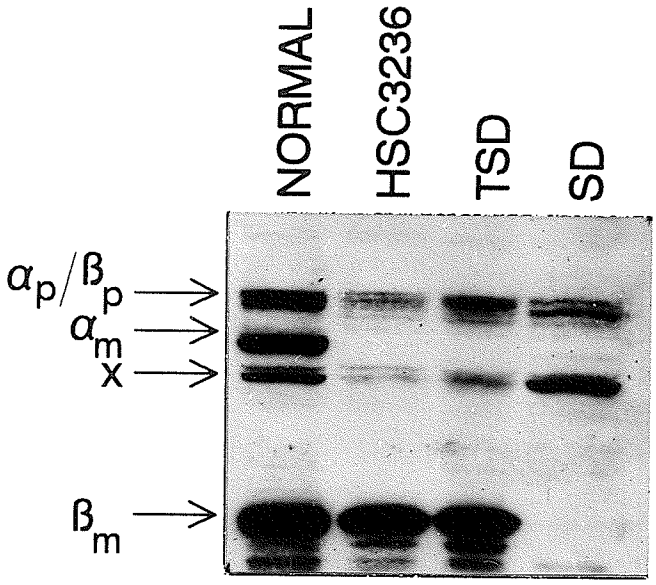

Figure 9 ***Western blot analysis of HSC3236 fibroblast lysates.*** Hex A expression in HSC3236 fibroblast lysates was analyzed by western blot using the anti-Hex A antiserum. Normal (WP09), TSD (WG1881), and SD (GM00294) fibroblast lysates were used as controls. The detection of precursor α-subunits (α_p), precursor β-subunits (β_p), mature α-subunits (α_m), and mature β-subunits (β_m), are indicated. A cross reacting protein is designated as "x".

(αpSVL) by site-directed mutagenesis. This produced the αW474C mutant cDNA construct that was capable of producing the mutant α-subunit in Cos-7 cells. The αW474C construct was transiently expressed to form αα homodimers (Hex S), or it was co-expressed with the β-subunit cDNA construct (pCD43) to make the more stable heterodimer, Hex A (αβ).

The level of expressed Hex S activity produced when the αW474C construct was transiently expressed in Cos-7 cells was measured using 4-MUGS. In three independent experiments (table 2), the αW474C construct produced a higher level of expressed activity in comparison to that of the αR170W and mock expression lysates. However, this increase was not statistically significant. The αR170W mutation is associated with infantile TSD and therefore, no activity was expected, making it a useful negative control for mature α-subunit expression (Fernandes *et al.*, 1992b). In comparison, normal α-subunit cDNA (αpSVL) expression produced specific activities approximately 9 to 10 times greater than that of mock transfected Cos-7 lysates, indicating that a sufficient level of expression was attained to make observable differences between overexpressed Hex S and endogenous Hex A levels. Although pRc/CMV-β-gal was always co-transfected to express β-galactosidase as a measure of transfection efficiency, it was observed that total Hex A and Hex S activities in duplicate transfections were more consistent than β-galactosidase activities. Therefore, both non-normalized and normalized values are shown in tables 2 and 3.

Western blot analysis using the anti-Hex A antiserum was conducted to ensure that the αW474C mutant polypeptide was being expressed and that the reduced level of

Table 2. Hex S activities in αW474C Cos-7 expression lysates.

Experiment	Wild Type	αW474C	αR170W	Mock
1	736 (958)	91 (12)	68 (ND)	80
2	752 (1064)	160 (98)	71 (ND)	78
3	841 (726)	129 (29)	68 (ND)	93
average ± $S.D_{sample}$	776 ± 56 (916±173)	127 ±35 (46±46)	69 ± 2 (ND)	84 ± 8
%wild type	100% (100%)	16% (5%)	9% (ND)	11%

The expressed Hex S activity in αW474C, normal, αR170W, and mock transfection lysates from duplicate transfections of three independent experiments was determined using 4-MUGS. Total activity, and corrected activity based on β-galactosidase co-expression is shown. Hexosaminidase activity is expressed as nmol 4-MUGS hydrolyzed/mg protein/hr, and normalized activities based on relative β-galactosidase co-expression is shown in parentheses. Normalized enzyme activity = (Enzyme activity - Mock) x (Efficiency of Transfection). ND indicates that activity could not be detected. The proportion of expression for each mutant is also expressed as a percentage of wild type Hex S activity.

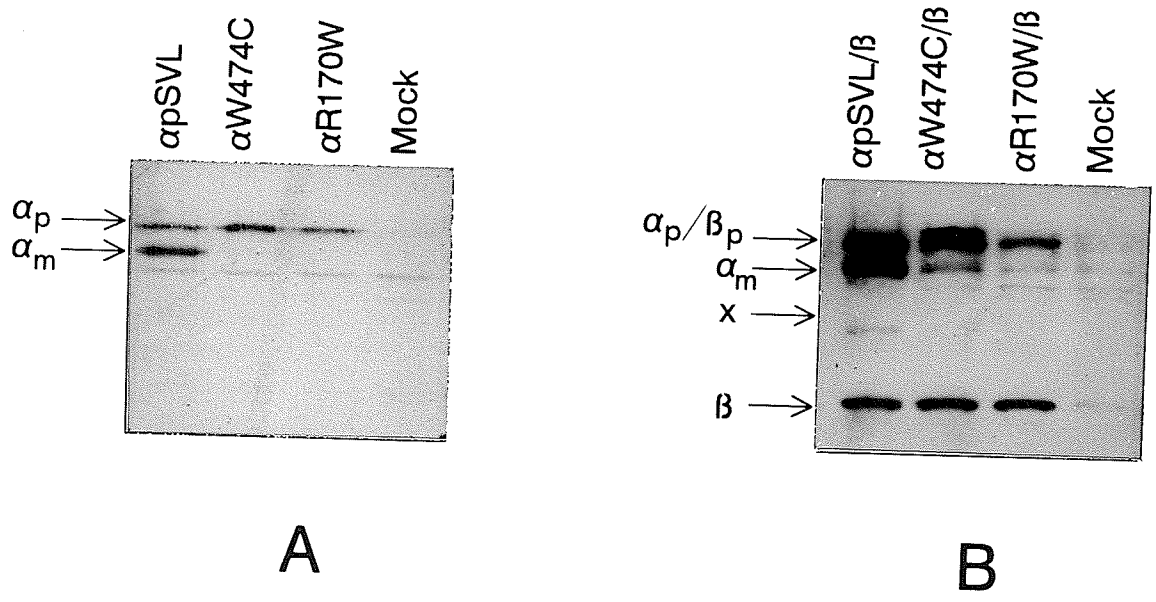

Figure 10 ***Western blot analysis of αW474C expression as Hex S (αα) or co-expression with the β-subunit to make Hex A (αβ).*** (A) αW474C transfection lysates were analyzed by western blot using the anti-Hex A antiserum. αpSVL, αR170W, and mock expression levels are shown as controls. (B) The αW474C mutant, αpSVL, and αR170W were co-expressed with the β-subunit. The expression levels were analyzed with the anti-Hex A antiserum by western blot analysis. Precursor α-subunits (α_p), precursor β-subunits (β_p), mature α-subunit (α_m), and mature β-subunit (β_m) are indicated for A and B.

Hex S activity in αW474C transfection lysates was due to a reduced level of mature Hex S protein (figure 10a). The levels of αW474C subunit detected were consistent with the measured enzyme activities. Although all of the expressed α-subunits were present in their precursor form, neither of the mutant α-subunits, αW474C or αR170W, were detectable in their mature lysosomal for. The level of mature α-subunit produced by the wild-type cDNA (αpSVL) was well above the level in mock transfected controls. These observations were consistent in repeated experiment.

To see if the αW474C α-subunit could produce αβ heterodimers (Hex A), the β-subunit cDNA (pCD43) was co-transfected. Total Hex A (αβ) and S (αα) activity produced in transiently expressing Cos-7 cells was determined using 4-MUGS (table 3). Hexosaminidase activities in αW474C/β transfection lysates were always higher than those of αR170W/β and mock co-transfection lysates. The normal α- and β-subunits produced specific activities toward 4-MUGS 12 to 19 fold higher than mock transfected Cos-7 cells. However, the proportion of activity contributed only by Hex A (αβ heterodimers), could not be determined from crude cell lysates using this method because the substrate, 4-MUGS, is cleaved by both enzymes, Hex S and Hex A, which were present in wild-type co-transfection lysates (not shown). Although Hex B was formed in α/β co-transfections, it could not have been detected using 4-MUGS, an α-subunit specific substrate (Bayleran *et al.*, 1984).

Western blot analysis using the anti-Hex A antiserum was used to determine if a mature αW474C subunit was produced in αW474C/β co-transfection lysates (figure 10b). A peptide corresponding to the molecular mass of the normal mature α-subunit was

Table 3. Hex A and S activities in αW474C/β Cos-7 expression lysates.

Experiment	Wild Type	αW474C/β	αR170W/β	Mock
1	968 (807)	113 (100)	67 (4)	61
2	1535 (1466)	287 (190)	165 (87)	78
3	1354 (1297)	147 (52)	108 (12)	95
average ± $S.D_{sample}$	1286± 290 (1190±342)	182±92 (114±70)	113±49 (34±46)	78±17
%WildType	100% (100%)	14% (9%)	9% (3%)	6%

Total expressed Hex A and S activity in αW474C, normal, αR170W, and mock transfection lysates from duplicate transfections of three independent experiments was determined using 4-MUGS. Total activity, and corrected activity based on β-galactosidase co-expression is shown. Hexosaminidase activity is expressed as nmol 4-MUGS hydrolyzed/mg protein/hr, and normalized activities based on relative β-galactosidase co-expression is shown in parentheses. Normalized enzyme activity = (Enzyme activity - Mock) x (Efficiency of Transfection). ND indicates that activity could not be detected. The proportion of expression for each mutant is also expressed as a percentage of wild type activity.

detected in αW474C/β expression lysates. Although a similar peptide was detected in αR170W/β expression lysates, it was less abundant and found at a similar level in the mock expression lysates. This indicated that the endogenous Cos-7 proteins were immunoreactive toward the anti-Hex A antiserum. The precursor α- and β-subunits were readily detectable in αW474C/β expression lysates and controls, and the mock levels were nearly undetectable, as expected. These observations demonstrated that the αW474C mutant was synthesized, although very little mature α-subunit was produced when it was co-expressed with the β-subunit. Because the anti-Hex A antiserum could detect both α- and β-subunits, we could not rule out the possibility that the apparent mature α-subunit peptide in αW474C/β transfection lysates was an intermediately processed form of the β-subunit. However, this peptide was not present in the negative control (αR170W/β) lysates, indicating that a mature α-subunit was present in αW474C/β lysates.

3.4.2 Analysis of αW474C and β-subunit association in Cos-7 cells using DEAE-cellulose chromatography

To confirm that the low level of mature α-subunit observed by western blot analysis was produced because αW474C and β-subunits associated to make αβ heterodimers (Hex A), Hex A and other overexpressed isoenzymes from αβ co-transfection lysates were separated using ion-exchange chromatography. The hexosaminidase activity in each fraction was detected using 4-MUG. Each of αW474C and αR170W mutant cDNA constructs was co-transfected with the β-subunit cDNA, and transfection lysates (2 mg) with similar levels of co-expressed β-galactosidase activity

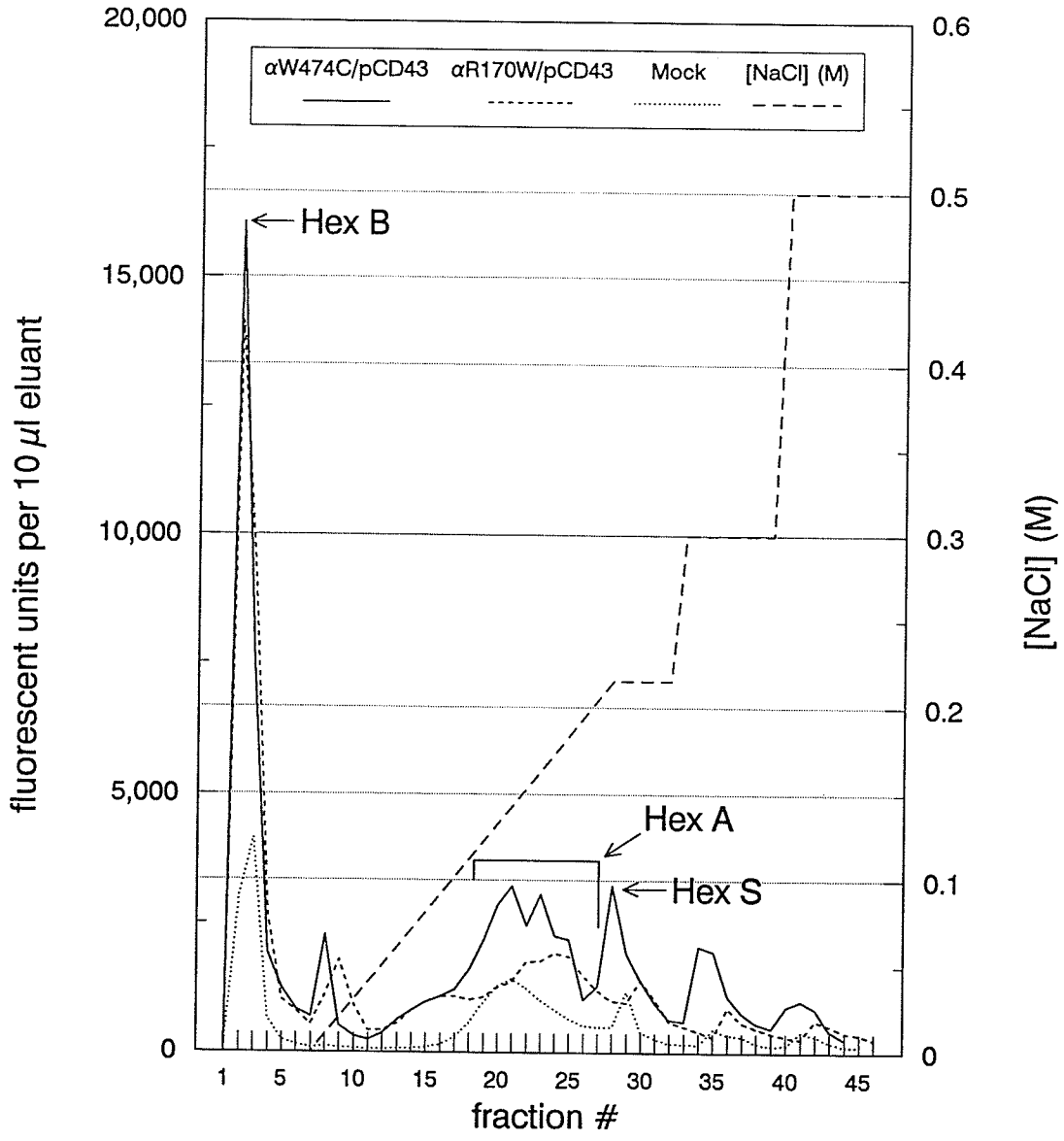

Figure 11 ***Separation of transiently expressed isoenzymes by ion-exchange chromatography using DEAE cellulose.*** αW474C/β, αR170W/β, and mock transfection lysates were fractionated in sodium phosphate (NaPi), pH 6.0, using a 1.0 mL DEAE cellulose column. Fractions were collected (1.0 mL), and the hexosaminidase activity in 10 μL of each fraction was assayed using 4-MUG. Fractions 1-7 were collected in NaPi. Fractions 8 through 28 were collected from a linear NaCl gradient (0-0.215 M). Fractions 29-34 were collected in 0.215 M NaCl. Fractions 34-40 were collected in 0.3 M NaCl, and fractions 41-45 were collected in 0.5 M NaCl. The peaks observed in the 0.3 M and 0.5 M NaCl fractions were unknown hexosaminidase species that were observed in repeated experiments. The peaks (Cao *et al.*, unpublished data) corresponding to Hex B, Hex A, and Hex S are indicated.

were selected for each mutant and analyzed. There was a higher level of β-hexosaminidase activity in the Hex A fractions (fractions 18-25 of the 0-0.215 M NaCl linear gradient) of αW474C/β transfection lysates than in αR170W/β and mock transfection lysates (figure 11). The Hex S activity in (fractions 29-34) in αW474C/β transfection lysates was also higher than that of both negative control lysates.

Hex B eluted in fractions 1-7; a four-fold increase above background was obtained in both αW474C/β and αR170W/β expression lysates when compared to mock levels, although Hex B levels were slightly higher in αW474C/β lysates. The peak that followed Hex B was likely Hex B remaining on the column when the NaCl gradient was started. If the increased level of Hex B was because a higher level of protein than estimated was loaded, then this could have accounted for the higher Hex A levels. This difference could also be the result of variability in transfection efficiency since we have previously observed that β-galactosidase expression can be more variable than β-hexosasminidase expression. Because of the potential variability between transfections and therefore the elution profiles, these small differences in β-hexosaminidase activity observed in αW474C/β and αR170W/β transfections were not considered to be significant. We used a more sensitive approach, pulse-chase analysis, to determine if αβ heterodimers could be detected in transiently transfected Cos-7 cells (see below).

3.5 Pulse-chase analysis of transiently expressed α- and β-subunits in Cos-7 cells

3.5.1 Detection of overexpressed human α- and β-subunits in transiently transfected Cos-7 cells using immunoprecipitation

We wanted to demonstrate that the Cos-7 transfection previously used to analyze overexpressed enzyme activity could produce a sufficient level of overexpressed α- and β-subunits for detection by immunoprecipitation. The normal α-subunit was expressed alone to make Hex S, or it was co-transfected with the β-subunit to make $\alpha\beta$-heterodimers, as before. In addition, the β-subunit was transfected alone to produce Hex B ($\beta\beta$) as a positive control for β-subunit expression. However, it was expected that the β-subunit levels in $\alpha\beta$ co-transfections would be low because only 2.5 μg of β-subunit plasmid DNA was used in transfections. This was much lower than the amount of α-subunit plasmid DNA (6.5 μg) that was used for Hex S expression. Therefore, the amount of β-subunit cDNA that was transfected for the Hex B control was increased to ensure that β-subunits were abundant. No plasmid DNA was used in the mock transfected cells.

After an 8 hour incubation with [^{35}S]-methionine and cysteine, the overexpressed proteins were immunoprecipitated with the anti-α, anti-Hex B, and anti-Hex A antisera (figure 12). The α-subunit was readily detected when it was expressed as $\alpha\alpha$ homodimers (Hex S) or as $\alpha\beta$ heterodimers (Hex A). However, the β-subunit was very low in $\alpha\beta$ co-transfections, suggesting that the amount of β-subunit cDNA that was transfected needed to be higher to enhance β-subunit expression.

The α- and β-subunit levels detected in the mock transfected lysates were apparently high, suggesting that these proteins may mask the detection of mutant proteins. However, the mock levels shown were immunoprecipitated from a much higher level of protein; a negligible amount was detected from an equivalent level of protein

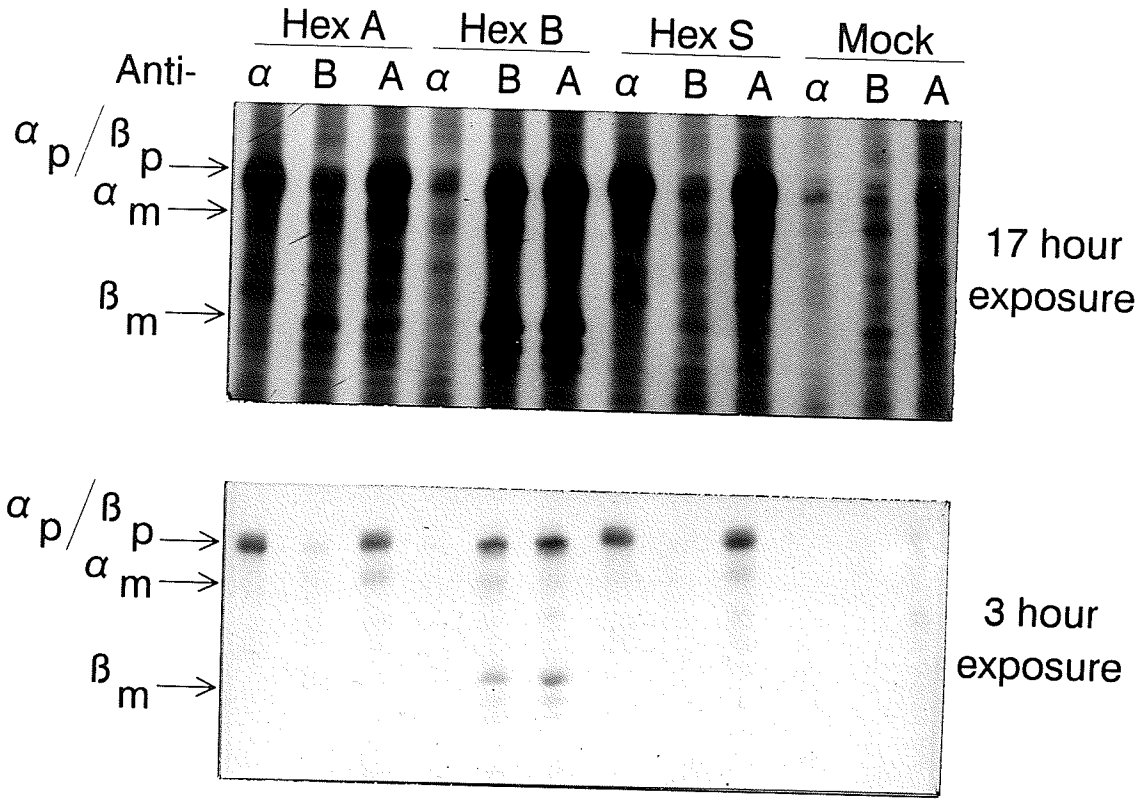

Figure 12 ***Metabolic labelling of transiently expressed normal α- and β-subunits.*** Cos-7 cells were transfected with both α- and β- subunit cDNA to express Hex A ($\alpha\beta$), or the β-subunit cDNA alone to express Hex B ($\beta\beta$), or the α-subunit cDNA alone to express Hex S ($\alpha\alpha$). The cells were metabolically labelled for 8 hours with 0.15 mCi [^{35}S]-methionine and cysteine at 64 hours post-transfection. Cell lysates were prepared at 72 hours post-transfection, and immunoreactive peptides from one-third of each lysate were immunoprecipitated using anti-α (α), anti-Hex B (B), or anti-Hex A (A) antisera. To demonstrate the potential effect of the Cos-7 endogenous immunoprecipitable proteins in mock transfected lysates, the autoradiograph is shown after a 17 hour and a 3 hour exposure at -80°C. Precursor α-subunits (α_p), precursor β-subunits (β_p), mature α-subunits (α_m), and mature β-subunits (β_m) are indicated.

(not shown). A 17 and a 3 hour exposure of the immunoprecipitated peptides are shown to demonstrate that the effect of the endogenous levels could be a reflection of exposure time. Further, β-subunit levels were nearly undetectable when compared to α-subunit levels after a 3 hour exposure. This preliminary experiment indicated that labelled α- and β-subunits from transiently transfected cells were readily detectable, the mock levels could have been reduced if protein levels were normalized, and that β-subunit expression needed to be increased for easier detection of $\alpha\beta$ association in Cos-7 cells.

3.5.2 Analysis of mature α-subunit expression with increasing amounts of transfected β-subunit cDNA

To increase the probability that α-subunits would associate with β-subunits to make Hex A ($\alpha\beta$ heterodimers), the level of β-subunit expression was increased by using more β-subunit cDNA construct (pCD43) in co-transfections. As the amount of co-transfected pCD43 was increased from 2.5 to 10 μg, gradual increases of mature α-subunit appeared in α/β co-immunoprecipitations using anti-Hex B or anti-Hex A (figure 13). These observations suggested that Hex A was being produced. However, experiments to confirm the identity of the mature α-subunit with the use of an α-subunit-specific antiserum or by measuring increases in Hex A enzyme activity were not conducted. When 10 μg of pCD43 was transfected, the levels of mature α-subunit were highest. The amount of pCD43 that was transfected in previous studies (2.5 μg), resulted in very low levels of immunoprecipitated α-subunit protein, as expected from the preliminary analysis (figure 12). If 12 μg or more of pCD43 was transfected, very few cells survived the electroporation, suggesting that a higher cell number or a smaller

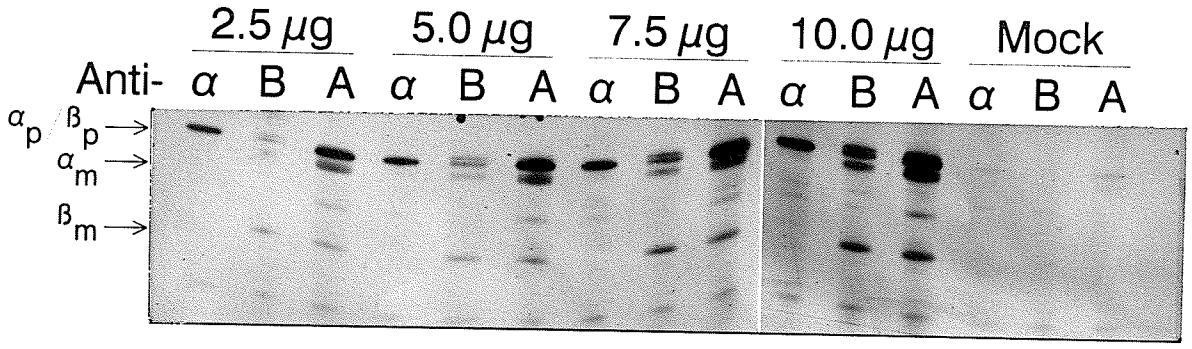

Figure 13 ***Increased mature α-subunit expression with an increased amount of transfected pCD43.*** Cos-7 cells were transfected with 2.5, 5, 7.5, or 10 μg of pCD43 and 6.5 μg of αpSVL. Transfected cells were incubated for 8 hours in the presence of 0.1 mCi [^{35}S]-methionine and cysteine. Cell lysates were made and immunoprecipitations were conducted with anti-α, anti-Hex B and anti-Hex A antisera. Precursor α-subunits (α_p), precursor β-subunits (β_p), mature α-subunits (α_m), and mature β-subunits (β_m) are indicated.

quantity of total plasmid DNA would have been needed to compensate for the apparent toxicity of the plasmid DNA. In subsequent $\alpha\beta$ co-expressions, 10 μg of pCD43 was used, and the α-subunit cDNA construct (αpSVL) was reduced, although insignificantly, from 6.5 to 6.0 μg in order to compensate for some cell survival.

3.5.3 Analysis of newly-synthesized α- and β-subunits in Cos-7 cells co-transfected with αpSVL and pCD43

To achieve a high level of [^{35}S]-methionine and cysteine-labelled unprocessed α- and β-subunit precursors for pulse-chase analysis in transiently transfected Cos-7 cells, we looked for the time point where the α- and β-subunits were most abundant, yet still in their precursor form. These could then be subjected to pulse-chase analysis. Because the mature α-subunit was not detectable after a 2 hour pulse-labelling, and at very low levels after 4 hours, an intermediate time of 3 hours was chosen as the standard pulse-labelling time for pulse-chase analysis of mutant α-subunit proteins (figure 14).

The subunit levels were also examined after 6 hours and 8 hours. Only small increases in α- and β-subunit levels were evident at these times, suggesting that [^{35}S]-methionine and cysteine levels were limiting the level of protein synthesis, or that an insufficient amount of antiserum was used to immunoprecipitate the increased levels of labelled peptides.

3.5.4 Pulse-chase analysis of the W474C mutant α-subunit in transiently transfected Cos-7 cells

Pulse-chase analysis of the αW474C mutant was conducted in transiently transfected Cos-7 cells to determine if the αW474C mutant could be detected in its

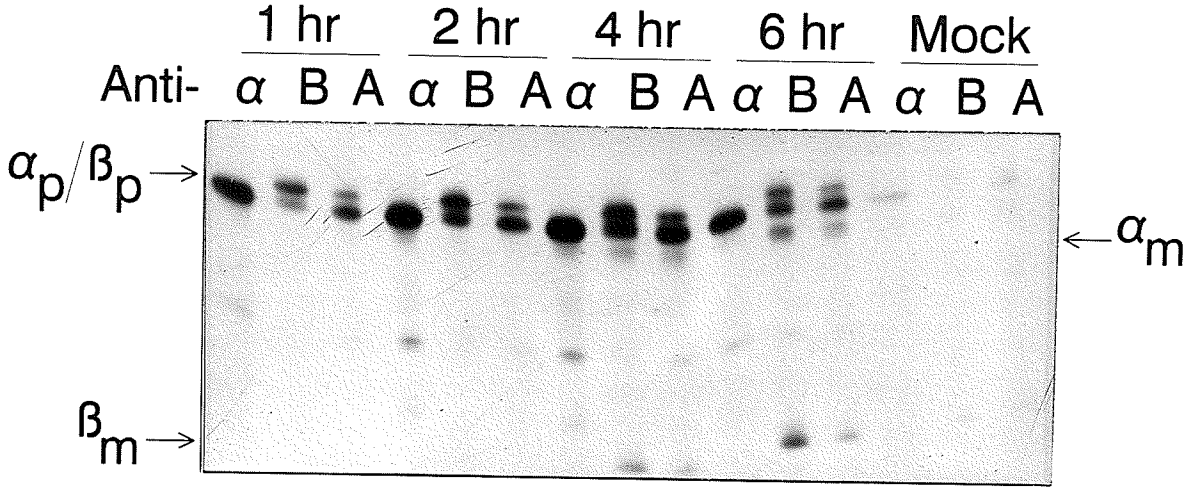

Figure 14 ***Metabolic labelling of Cos-7 cells transiently co-expressing α- and β-subunits.*** Cos-7 cells were co-transfected with 6.5 μg of αpSVL and 10 μg of pCD43. The cells were incubated with 0.1 mCi [^{35}S]-methionine and cysteine at 64 hours post-transfection. Labelling was done for 1, 2, 4, and 6 hours. Cell lysates were then prepared and the over-expressed proteins were immunoprecipitated with anti-α, anti-Hex B, or anti-Hex A. Precursor α-subunits (α_p), precursor β-subunits (β_p), mature α-subunits (α_m), and mature β-subunits are indicated (β_m). The mock levels are also shown.

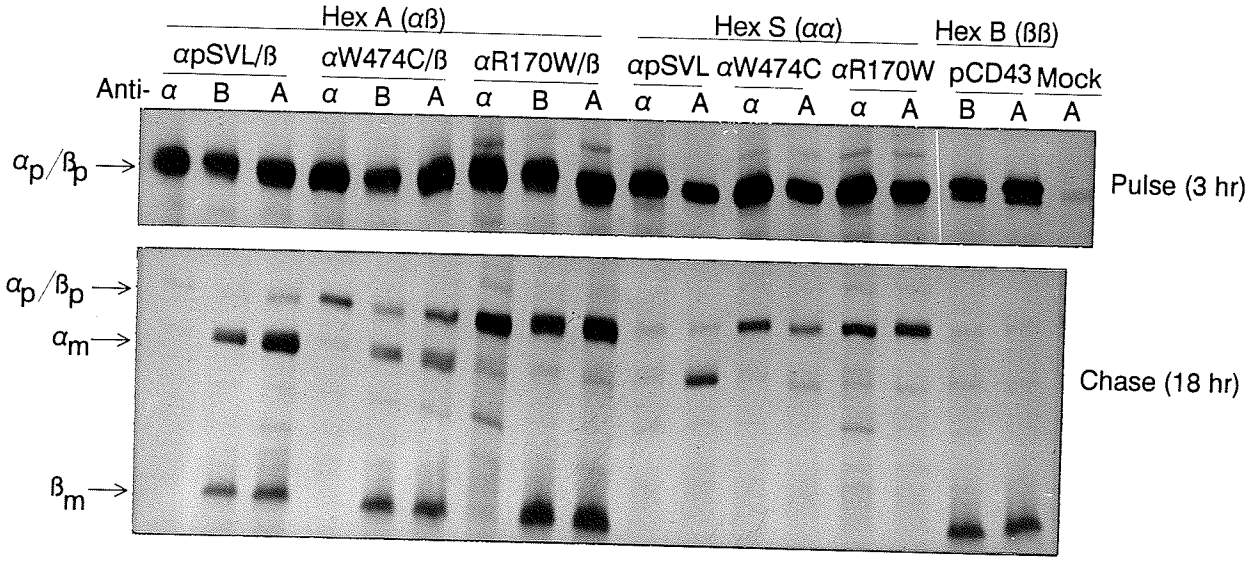

Figure 15 ***Pulse-chase analysis of the αW474C mutant in transiently expressing Cos-7 cells.*** The αW474C mutant was co-expressed with the β-subunit in transiently transfected Cos-7 cells. Transfected cells were labelled with 0.1 mCi [^{35}S]-methionine and cysteine for 3 hours followed by an 18 hour chase in complete medium containing an excess of unlabelled methionine and cysteine. Immunoprecipitations were conducted on normalized levels of lysates using the anti-α, anti-Hex B, or anti-Hex A antiserum. Wild-type and αR170W were used as positive and negative controls, respectively, for α-subunit processing. In addition, the αW474C mutant and controls were expressed alone to make Hex S as a negative control for Hex A formation. Hex B was expressed as a negative control for Hex A formation, and a positive control for Hex B expression. The mock levels are shown only after a 3 hour pulse. Precursor α-subunits (α_p), precursor β-subunits (β_p), mature α-subunits (α_m), and mature β-subunits (β_m) are indicated.

mature form when it was transfected alone to make Hex S, or when it was co-transfected with the β-subunit cDNA to make Hex A. After an 18 hour chase, an apparent mature αW474C subunit co-immunoprecipitated with the β-subunit in anti-Hex B immunoprecipitations of αW474C/β co-expression lysates (figure 15). This peptide was not present when the αW474C mutant was expressed alone to make Hex S, suggesting that the mutant αα homodimers are less stable. The expression of the α- or β-subunits alone to produce Hex S or Hex B, served as internal controls for α- or β-subunit processing, respectively. Although the level of immunoprecipitated peptides were normalized on the basis of transfection efficiency (equal levels of β-galactosidase activity per microgram of total protein used in the immunoprecipitation), a high level of β-subunit in αR170W/β co-transfection lysates may have been attributed to undetectable variability between transfections.

It was necessary to confirm that the peptide corresponding to a mature α-subunit in αW474C/β transfection lysates was an α-subunit, and not an intermediately processed β-subunit. Overexpressed subunits from αW474C/β and control transfection lysates were immunoprecipitated using the anti-Hex A antiserum, the immunoprecipiated products were denatured to make the mature α-subunit immunoprecipitable with the anti-α antiserum that was finally used to immunoprecipitate precursor and mature α-subunits. There was a significant amount of mature α-subunit detected in αW474C/β transfection lysates, although lower than in normal αpSVL/β transfection lysates (figure 16). There was no mature α-subunit detected in the αR170W/β negative control transfection lysates, as expected. This result confirmed that the αW474C subunit

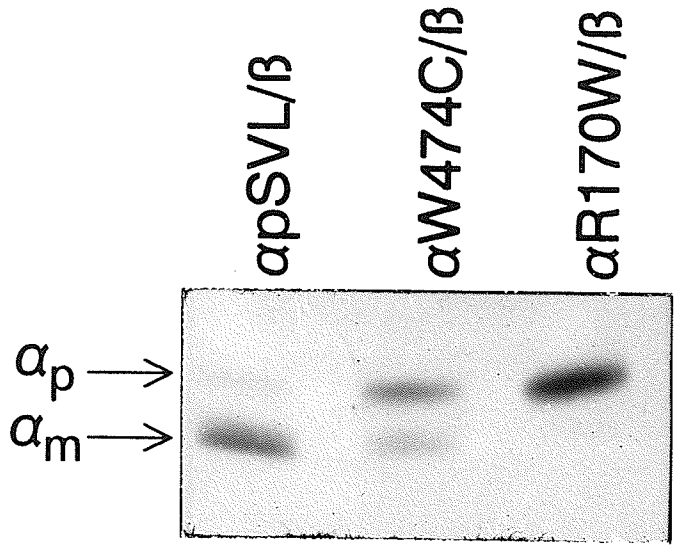

Figure 16 ***Immunoprecipitation of precursor and mature α-subunits from αW474C/β transfection lysates.*** Equal amounts of protein from αpSVL/β, αW474C/β, and αR170W/β co-transfection lysates were presorbed with the anti-Hex A antiserum. The immunoprecipitates were subjected to denaturation, and precursor (α_p) and mature (α_m) α-subunits were immunoprecipitated using the anti-α antiserum.

could be processed to its mature form when it was co-expressed with the normal β-subunit. Furthermore, these observations were consistent with western blot analysis of αW474C/β transfection lysates (figure 10b).

3.6 Analysis of *HEXA* mRNA levels in HSC3236 fibroblasts

Northern blot analysis was used to determine if the G1422C transversion allowed for normal *HEXA* mRNA expression and processing. An abundant abnormal mRNA species in total RNA of HSC3236 fibroblasts was detected (band c; figure 17). A partial deficiency of a major 2 kb *HEXA* mRNA (band a), and an absence of a naturally occurring alternatively polyadenylated mRNA (band b) (Myerowitz *et al.*, 1985; Proia & Soravia, 1987) was also detected. The major 2 kb and the alternatively polyadenylated transcript were present in the normal and SD controls. No mRNA was detected in the TSD control, as expected. These observations suggested that the G1422C transversion at the first nucleotide of exon 13 affects normal splicing of *HEXA* mRNA in HSC3236 fibroblasts. In addition, the reduced levels of the major 2 kb transcript was consistent with expression from only one allele since the second allele was predicted to harbour the 4-bp insertion that results in an absence of *HEXA* mRNA (Boles & Proia, 1995).

3.7 Metabolic labelling of normal human fibroblasts

3.7.1 Optimization of pulse-time for pulse-chase analysis in human fibroblasts

A preliminary study was conducted to determine the pulse time that would allow for a high level of radioactive precursor α-subunit and very little mature α-subunit. A

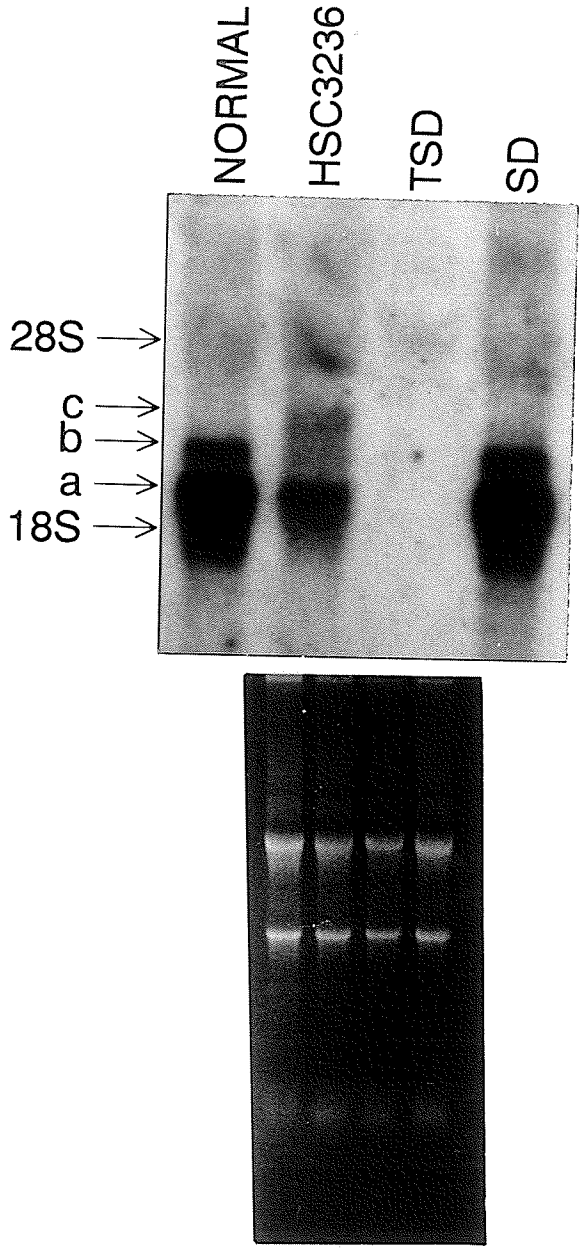

Figure 17 ***Northern blot analysis of total RNA of HSC3236 fibroblasts.*** Total RNA (15 μg) of HSC3236 fibroblasts was probed with the *Xho*I/*Bam*HI fragment of αpSVL that harbours the *HEXA* cDNA. An abnormal mRNA transcript that appeared only in HSC3236 fibroblasts is indicated by "c". Normal (MCH065), TSD (WG1881), and SD (GM00294) total fibroblast RNA were used as controls. Normal mRNA is indicated by "a" and "b" that correspond to a major mRNA transcript and a naturally occurring alternatively polyadenylated *HEXA* mRNA, respectively. The 28S and 18S rRNA bands are indicated. The integrity and relative levels of RNA that were analyzed are shown below after formaldehyde gel electrophoresis and prior to transfer to nitrocellulose.

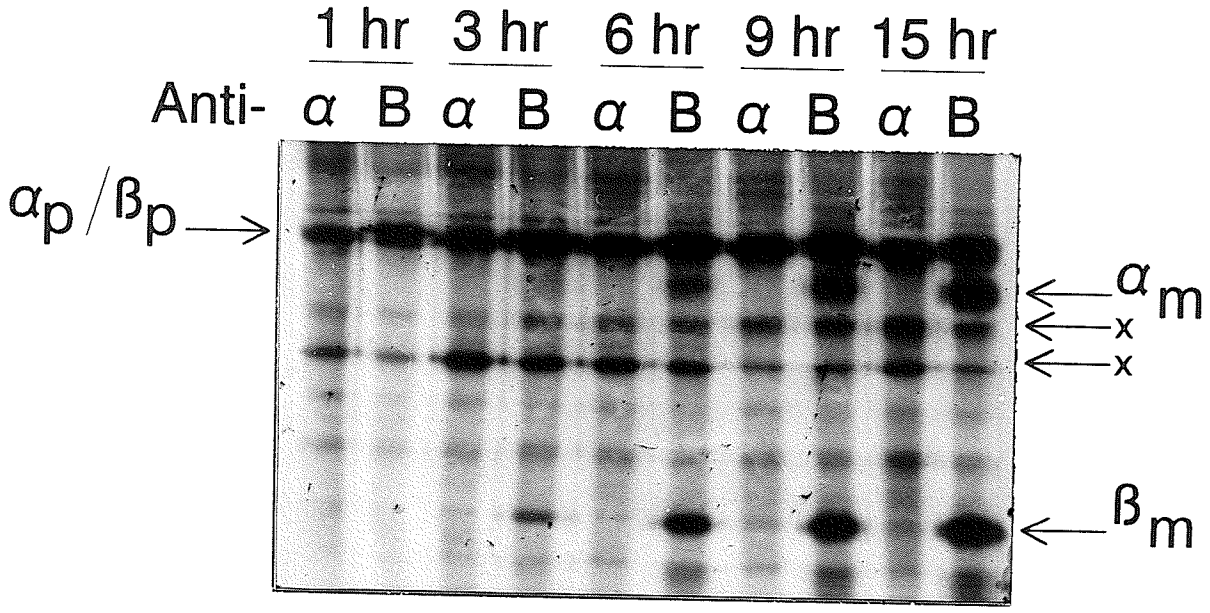

Figure 18 ***Metabolic labelling of normal fibroblasts.*** Normal fibroblasts (MCH065), were incubated with 0.4 mCi of [^{35}S]-methionine and cysteine for 1, 3, 6, 9, and 15 hours. Cell lysates were prepared and the anti-α and anti-Hex B antisera were used to immunoprecipitate radioactive α- and β-subunits. Immunoprecipitated precursor α-subunits (α_p), precursor β-subunits (β_p), mature α-subunits (α_m), and mature β-subunits (β_m), are indicated. Cross-reacting proteins were present (indicated by "x"); their identity was unknown.

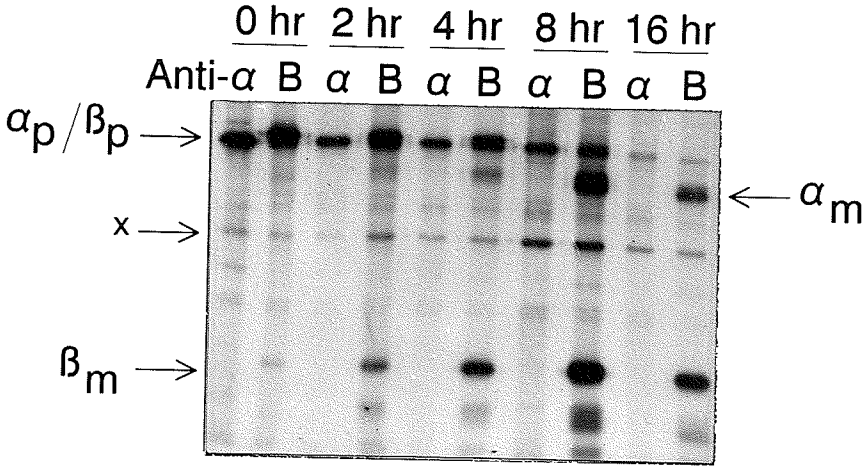

Figure 19 ***Pulse-chase analysis of α- and β-subunits in normal fibroblasts.*** Normal fibroblasts (MCH065), were incubated with 0.4 mCi of [^{35}S]-methionine and cysteine for 3 hours. This was followed by a chase for 2, 4, 8 and 16 hours. Cell lysates were made, and immunoprecipitations were conducted with the anti-α and anti-Hex B antisera. Precursor α-subunits (α_p), precursor β-subunits (β_p), mature α-subunits (α_m), and mature β-subunits (β_m) are indicated. A cross-reacting protein was present (indicated by "x"); its identity was unknown.

steady increase of newly-synthesized α- and β-subunits and their mature forms were detected as the pulse time was increased from 1 to 15 hours (figure 18). A three-hour pulse resulted in a high level of precursor α- and β-subunits, with some processing of only the β-subunit to its mature form. The presence of the mature β-subunit, and a small level of mature α-subunit, after a three hour pulse, was consistent with a faster dimerization rate of the β-subunit (Proia *et al.*, 1984). Because the mature α-subunit co-immunoprecipitated with the β-subunit in anti-Hex B immunoprecipitations after longer incubation times, a three-hour pulse time was used in subsequent experiments.

3.7.2 Pulse-chase analysis of newly-synthesized α- and β-subunits in normal fibroblasts

Normal fibroblasts were used to predict the appropriate chase times for pulse-chase analysis of HSC3236 and other Hex A-deficient cell lines (figure 19). Both precursor α- and β-subunit levels decreased with increasing chase time, and there was a corresponding increase of both mature α- and β-subunits. Following a three hour pulse with [^{35}S]-methionine and cysteine, 8 and 16 hour chase times in complete medium resulted in an abundant mature α-subunit protein that was predicted to be sufficient for the analysis of α-subunit processing in HSC3236 and other Hex A-deficient fibroblasts. The decreased level of the mature α- and β-subunits between 8 and 16 hours may reflect a variation in cell number during labelling, or a degradation or secretion of newly-synthesized radioactive α and β-subunits.

3.8 Metabolic labelling of α- and β- subunits in HSC3236 fibroblasts

3.8.1 Pulse-chase analysis of α- and β- subunits in HSC3236 fibroblasts

To examine the size and abundance of the mutant α-subunit in HSC3236 fibroblasts during its transit to the lysosome, pulse-chase analysis was used. Labelled α- and β-subunit proteins were isolated after various times of chase and compared to those of normal, TSD, and SD fibroblasts (figures 20 and 21). The HSC3236 α-subunit was synthesized to its expected molecular mass. However, the level of synthesis of the mutant α-subunit was low, and apparently half of that of normal or SD α-subunit levels. This observation was made initially in an experiment using non-normalized levels of protein in the immunoprecipitations (figure 20), and in subsequent experiments using normalized protein levels (figure 21). A reduced level of α-subunit synthesis was expected because it was predicted that protein could be produced only from the *HEXA* allele harbouring the G1422C mutation and not from the allele harbouring the 4-bp insertion.

Pulse-chase analysis also suggested that the mutant α-subunit in HSC3236 fibroblasts can dimerize with the β-subunit. The presence of the α-subunit precursor in immunoprecipitations using anti-Hex B suggested that the α- and β-subunit of HSC3236 fibroblasts associate after three hours. However, similar results were observed in TSD fibroblasts, suggesting that the apparent α-precursor is actually an intermediate form of the precursor β-subunit. These findings made it impossible to determine if there was a low level of α-subunit precursor that co-immunoprecipitated with the β-subunit using the anti-Hex B antiserum.

The effect of the W474C amino acid substitution on the stability of newly

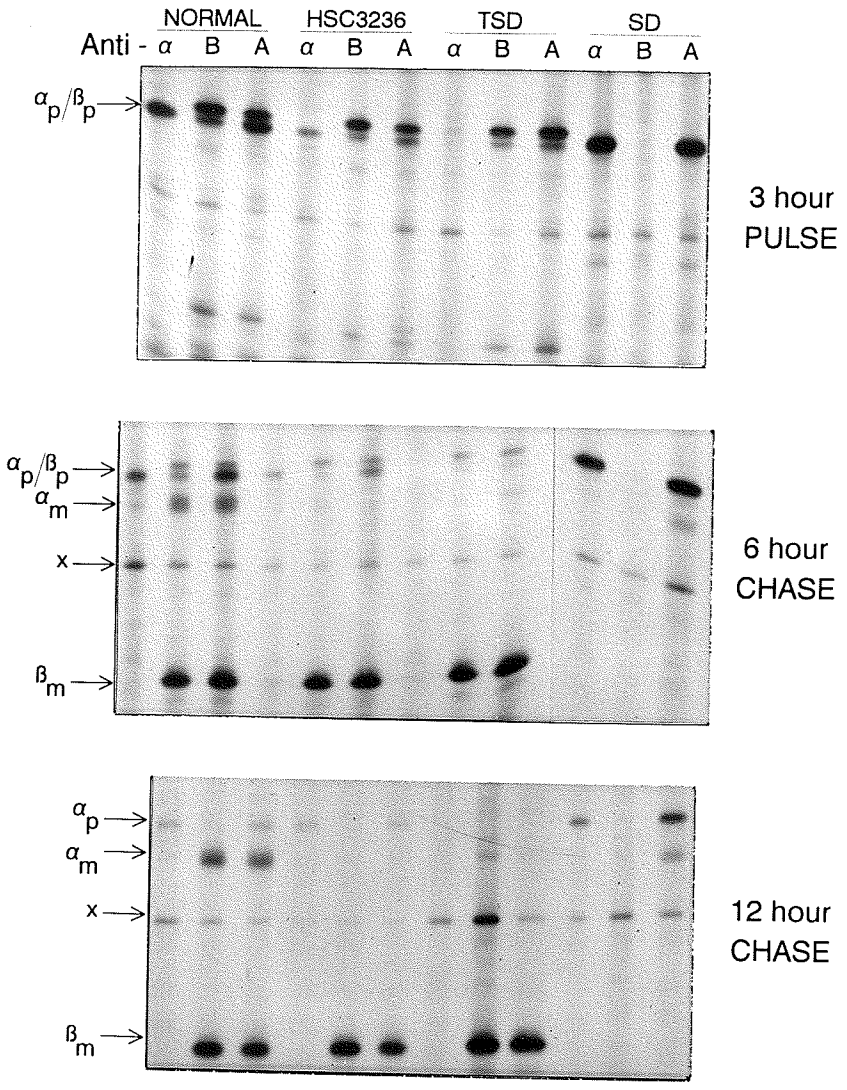

Figure 20 ***Pulse-chase analysis (I) of α- and β-subunits in HSC3236 fibroblasts.*** HSC3236, normal (MCH065), TSD (WG1881), and SD (GM00294) fibroblasts were incubated for 3 hours in the presence of 0.25 mCi [^{35}S]-methionine and cysteine. This was followed by chase times of 6 and 12 hours in complete medium containing a 5-fold excess of unlabelled methionine and cysteine. Immunoprecipitations from cell lysates were conducted using anti-α, anti-Hex B, and anti-Hex A antisera. Precursor α-subunits (α_p), precursor β-subunits (β_p), mature α-subunits (α_m), and mature β-subunits (β_m) are indicated. A cross reacting protein (indicated as "x"), was present; its identity was unknown.

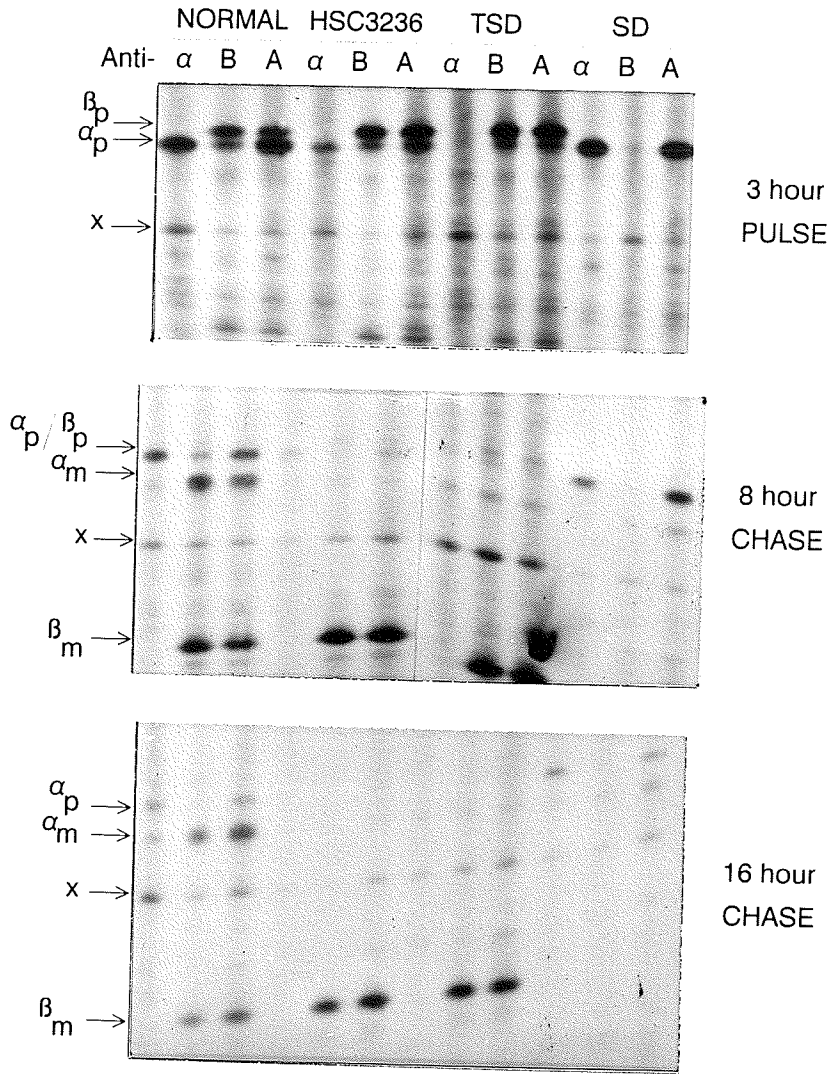

Figure 21 ***Pulse-chase analysis (II) of α- and β-subunits in HSC3236 fibroblasts.*** HSC3236, normal (MCH065), TSD (WG1881), and SD (GM00294) fibroblasts were incubated for 3 hours in the presence of 0.25 mCi [^{35}S]-methionine and cysteine. This was followed by chase times of 8 and 16 hours in complete medium containing a 5-fold excess of unlabelled methionine and cysteine. Equalized levels of protein from each cell lysate were used in immunoprecipitations with anti-α, anti-Hex B, and anti-Hex A antisera. Precursor α-subunits (α_p), precursor β-subunits (β_p), mature α-subunits (α_m), and mature β-subunits (β_m) are indicated. A cross reacting protein (indicated as "x"), was present; its identity was unknown.

synthesized α-subunits during processing to the lysosome in HSC3236 fibroblasts could not be predicted. Therefore, the processing of the HSC3236 α-subunit to its mature lysosomal form was analyzed after two time points to ensure that a mature α-subunit would be detected if it was processed to its lysosomal form. A mature α-subunit in HSC3236 fibroblasts was never detected after a 6 hour chase time (figure 20), or 8 hours (figure 21). Similarly, no mature α-subunit was detected after the longer chase time of 12 hours, or 16 hours. We felt that analyses after two chase times were important because the mature α-subunit may have been unstable and only detectable after a short time. On the other hand, the α-subunit might have been detectable after a longer chase time if the W474C amino acid substitution caused aggregation, delaying α-subunit maturation.

3.8.2 Treatment of [^{35}S]-labelled HSC3236 fibroblasts with 10 mM ammonium chloride

To determine if newly-synthesized HSC3236 α-subunits were properly folded and processed to the late-endosomal compartments, we tested to see if the protein could be secreted from these compartments. HSC3236 fibroblasts and controls were incubated in the presence of 10 mM NH_4Cl to increase the pH of the lysosomal environment and subsequently induce the missorting of newly-synthesized α-subunits to the medium where they could be recovered by immunoprecipitation. Newly-synthesized [^{35}S]-methionine and cysteine-labelled α-subunits of HSC3236 fibroblasts treated with 10 mM NH_4Cl could not be detected in the medium using the anti-α or anti-Hex A antisera (figure 22). A

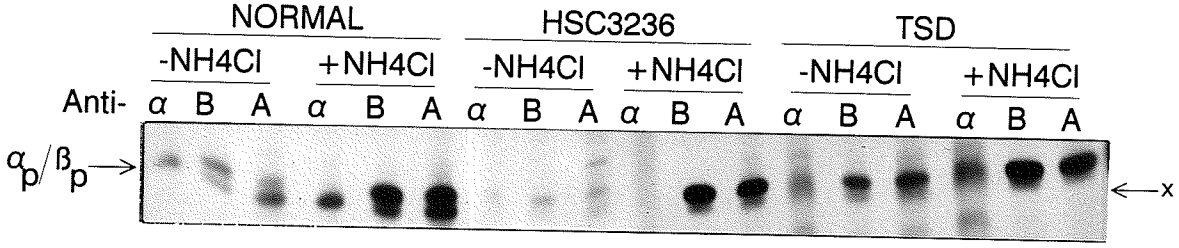

Figure 22 ***Immunoprecipitation of α- and β-subunits from the medium of HSC3236 fibroblasts treated with 10 mM NH_4Cl.*** Proteins in HSC3236 fibroblasts were labelled with 0.25 mCi of [^{35}S]-methionine and cysteine for three hours and were chased for 21 hours in the presence of 10 mM NH_4Cl to induce the missorting of newly-synthesized proteins to the culture medium. Untreated HSC3236 fibroblasts, and treated and untreated normal (MCH065), and TSD (WG1881) fibroblasts were used as controls. Medium extracts were prepared and anti-α, anti-Hex B, and anti-Hex A, were used to immunoprecipitate their respective polypeptides. Precursor α-subunits (α_p), and precursor β-subunits (β_p), are indicated. A cross-reacting protein that was detected in anti-α immunoprecipitations of TSD lysates is indicated as "x".

protein in TSD fibroblasts cross-reacted with the anti-α subunit antiserum (figure 22).

3.8.3 Phosphorylation of high-mannose oligosaccharide side-chains

To determine if the HSC3236 α-subunit is properly folded and that high mannose chains are phosphorylated, HSC3236 and control fibroblasts were incubated with [^{32}P]-phosphate. The presence of phosphate on α-subunit monomers was assessed after immunoprecipitation with the anti-α antiserum. The immunoprecipitated peptides of HSC3236 fibroblasts were similar to those in the TSD control, suggesting that the α-subunit was not phosphorylated or that phosphorylated α-subunit levels were below the level of detection (figure 23). Precursor α-subunits in the normal and SD controls were detected using the anti-α and anti-Hex A antisera. The α-subunit levels were higher in the SD control, demonstrating the stability of normal α-subunits as monomers. Higher levels were consistently observed in SD fibroblasts (figures 20, 21, and 22). This suggested that the defect in the α-subunit of HSC3236 fibroblasts may prevent the vast majority of newly-synthesized α-subunits from accumulating in the salvage compartments and subsequent transport to the Golgi. Precursor β-subunits were present in anti-Hex B and anti-Hex A immunoprecipitates of normal, HSC3236, and TSD cell lysates, but undetectable in SD fibroblasts, as expected. Since phosphorylated α-subunit precursors in HSC3236 fibroblasts were not detected, it was possible that the vast majority of newly-synthesized α-subunits were retained in the early processing compartments where they were degraded.

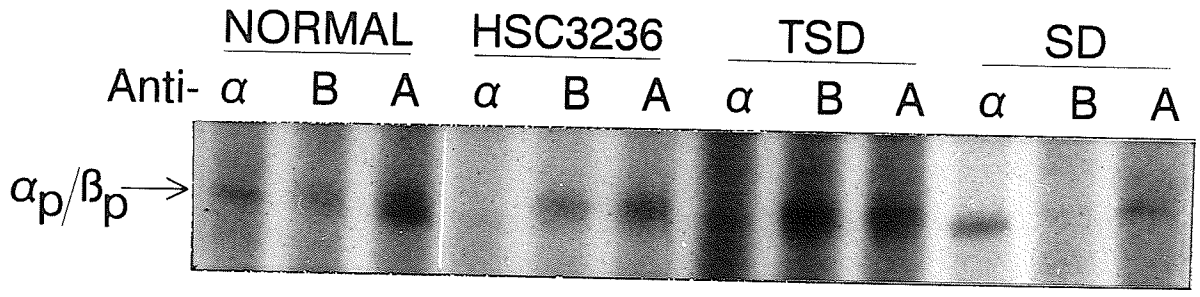

Figure 23 ***Analysis of α-subunit phosphorylation in HSC3236 fibroblasts.*** HSC3236 fibroblasts were incubated in the presence of 0.5 mCi carrier-free [^{32}P] for 3 hours. Normal (MCH065), TSD (WG1881), and SD (GM00294) fibroblasts were used as controls. Anti-α, anti-Hex B, and anti-Hex A antisera were used to immunoprecipitate their respective peptides from cell lysates. Precursor α-subunits (α_p), and precursor β-subunits (β_p), are indicated.

3.9 Transient expression of Hex B in Cos-7 cells

3.9.1 Maximizing expression of human Hex B in Cos-7 cells

Expression of human Hex B in Cos-7 cells was maximized to ensure that the small amounts of Hex B activity that might be associated with mutant β-subunits could be detected over the high endogenous level of Cos-7 β-hexosaminidase. When the amount of pCD43 used in transfections was increased to 10 or 12 μg, an 8 to 10-fold increase of human Hex B activity, as measured using 4-MUG, was attained in comparison to mock transfection lysates in duplicate experiments (figure 24). In comparison, Hex B activity was approximately 5 to 6-fold above background when only 2.0 μg of pCD43 was transfected, and only a 25% increase was observed when the amount of pCD43 transfected was doubled to 4 μg. However, Hex B activity was almost doubled when 12 μg of pCD43 was transfected. In subsequent experiments, 10 μg of pCD43 was routinely transfected.

3.9.2 Expression of the βW503C mutant to produce Hex B

The association of αW474C with residual levels of Hex activity and its conservation among several known hexosaminidases, including the human β-subunit, led to the hypothesis that a mutant β-subunit cDNA construct (βW503C), harbouring the amino acid substitution equivalent to the αW474C mutation, could produce residual Hex B activity in transiently transfected Cos-7 cells. Although the βW503C mutant resulted in a small increase above the mock levels in three independent experiments (table 4), similar levels of activity were observed in transfection lysates of a control β-subunit construct (βNegative). Therefore, the residual activity observed in βW503C lysates might

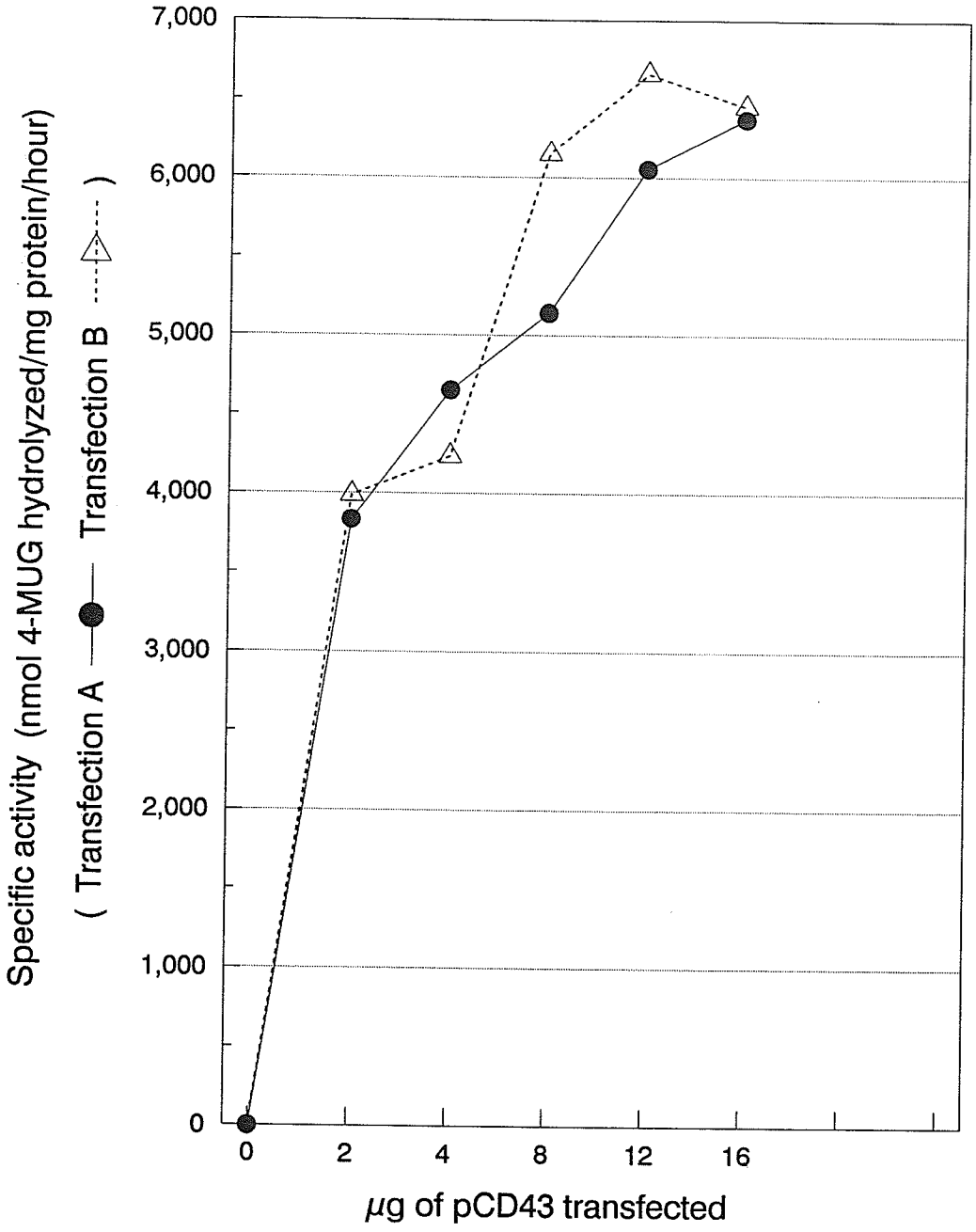

Figure 24 ***Maximum Hex B expression in Cos-7 cells.*** Increasing amounts of β-subunit cDNA, pCD43, were transiently expressed in Cos-7 cells. Hex B activity was measured using 4-MUG. The values corrected for transfection efficiency and with the endogenous Hex activity subtracted are shown.

Table 4. Hex B activity in βW503C Cos-7 expression lysates.

Experiment	Wild Type pCD43	βW503W	βNegative	Mock
1 (n=2)	4377 (3297)	722 (241)	673 (154)	621
2 (n=3)	5374 (4723)	738 (89)	804 (138)	666
3 (n=3)	5560 (6277)	751 (180)	662 (114)	642
average$\pm$S.D$_{sample}$	5195$\pm$731 (4949$\pm$1343)	739$\pm$59 (161$\pm$72)	718$\pm$78 (133$\pm$33)	585$\pm$78
% wild type	100% (100%)	14% (3%)	14% (3%)	11%

Hex B activity in Cos-7 cells overexpressing pCD43, βW503C, βNegative, and mock transfection lysates was measured using 4-MUG and expressed as nmol 4-MUG hydrolyzed/mg protein/hr. The raw values are given and the corrected values based on transfection efficiency, with the mock values substracted, are shown in parentheses.

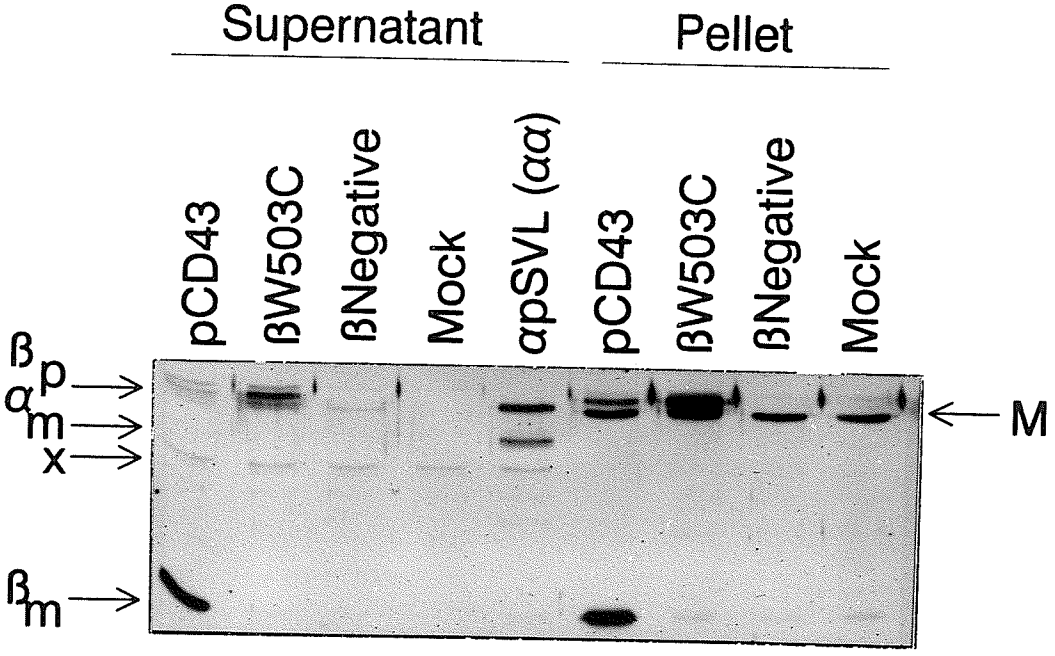

Figure 25 ***Western blot analysis of βW503C Cos-7 expression lysates.*** βW503C, βNegative, pCD43, and mock transfection lysates were analyzed by western blot using the anti-Hex A antiserum. The supernatant and pellet fractions of the lysate were analyzed. The precursor β-subunit (β_p), and mature β-subunit (β_m), are indicated. A peptide present in the mock transfected lysate is indicated as "M".

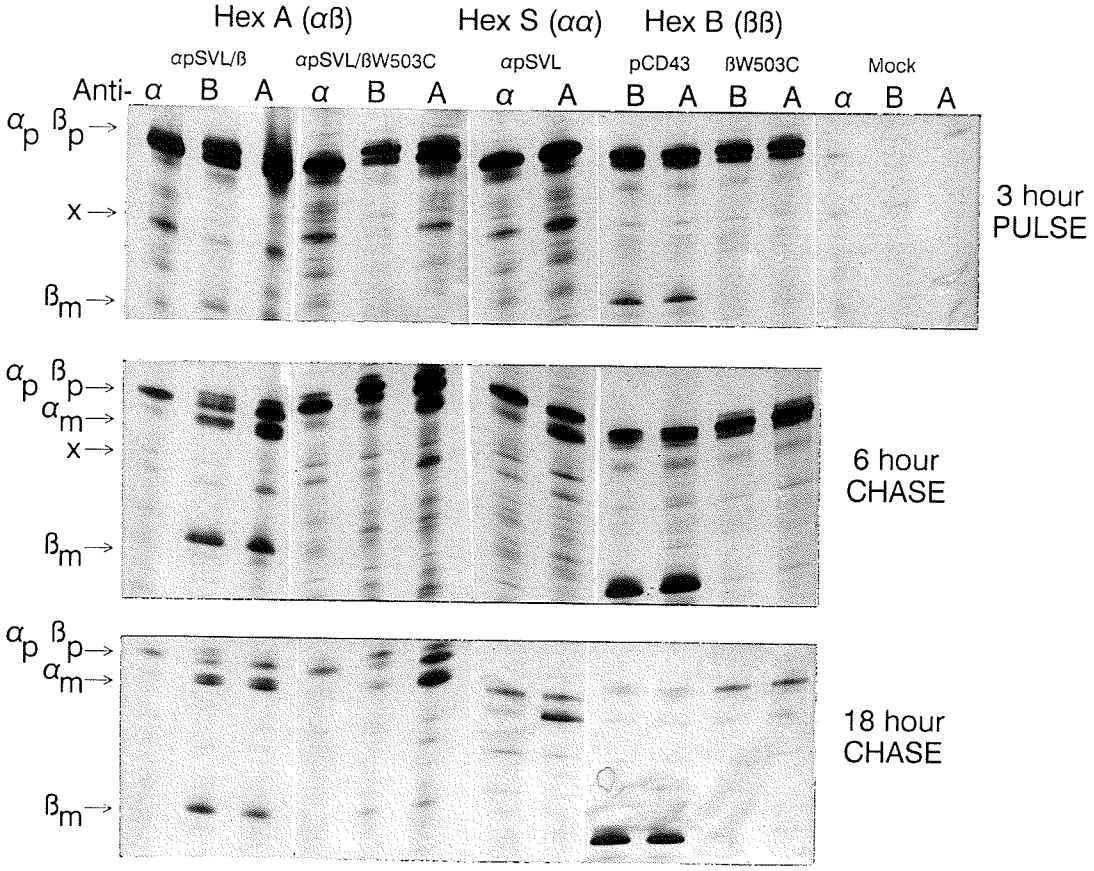

Figure 26 ***Pulse-chase analysis of the βW503C mutant in transiently expressing Cos-7 cells.*** The βW503C mutant was expressed alone, or co-expressed with the normal α-subunit in transiently expressing Cos-7 cells. Transfected cells were labelled with 0.1 mCi [^{35}S]-methionine and cysteine for 3 hours followed by an 18 hour chase in complete medium containing an excess of unlabelled methionine and cysteine. Immunoprecipitations were conducted from transfection lysates using the anti-Hex B and anti-Hex A antisera. Hex B and Hex S expression lysates were used as controls. The mock levels are shown only after a 3 hour pulse. Precursor α-subunits (α_p), precursor β-subunits (β_p), mature α-subunits (α_m), and mature β-subunits (β_m) are indicated.

be an artifact of the Cos-7 transfection system. The βNegative construct was initially made to express a β-subunit with a W503F amino acid substitution. Since β-subunits could not be produced from this construct, it was given the name βNegative. Expression of the normal β-subunit cDNA, pCD43, resulted in an 8 to 10 fold increase in Hex B above the mock levels, demonstrating the consistency in wild-type Hex B activity levels among these experiments and those described above. The raw values are listed in table 4. In addition, the endogenous hexosaminidase activity was subtracted from the raw values and the final values were corrected according to transfection efficiency as measured by the relative levels of co-expressed β-galactosidase.

Western blot analysis using the anti-Hex A antiserum was used to detect β-subunit expression in βW503C Cos-7 expression lysates. To ensure that all overexpressed peptides were detected, the supernatant (20 μg) and the pellet (one-fourth) that resulted from freeze-thaw extractions were analyzed (figure 25). A mature β-subunit was not detected in the supernatant or pellet of βW503C transfections. The precursor levels were readily detectable in the pellet, and lower levels were present in the supernatant. A peptide that was smaller than the β-subunit precursor that was detected only in the pellets, was related to an endogenous Cos-7 protein. In the pCD43 positive control supernatant there was a significant amount of mature β-subunit, however the precursor was less prominent. The precursor was detected more readily in the cell pellet, although the actual amount of protein analyzed was not determined.

Pulse-chase analysis was used to study the processing of the βW503C mutant to its mature form when it was expressed alone to produce Hex B, or when it was co-

expressed with the normal α-subunit cDNA to produce mature $\alpha\beta$ heterodimers, which would be expected to be more stable. After a 6 or 18 hour chase, the level of precursor declined significantly in βW503C expression lysates. Very low levels of mature β-subunit were observed using the anti-Hex B or anti-Hex A antisera in both Hex B and Hex A expression systems (figure 26). This suggests that, like the mutant α-subunit, it was retained in the early biosynthetic compartments where it was likely degraded. The newly-synthesized levels of β-subunit were easily detected after a three hour incubation with [^{35}S]-methionine and cysteine. However, the stabilizing effect of the normal α-subunit could not be clearly demonstrated, and therefore, the results of αW474C/β co-tranfections were not reciprocated by the presence of an abundant β-subunit. The phosphorylation status and secretion of the transfected mutant β-subunit mutant were not analyzed in Cos-7 cells.

4 DISCUSSION

4.1 Molecular and clinical diagnosis of late-onset TSD

The molecular and clinical heterogeneity of subacute and chronic G_{M2} gangliosidosis (late-onset TSD) is portrayed by a broad range of clinical characteristics and variability in the age of onset. Although the subacute form is usually indistinguishable from its chronic counterpart, the early age of onset in the proband (HSC3236) at 10 years-old, psychosis, and the development of debilitating ataxia and dysarthria over the clinical course were consistent with a subacute form of the disease. However, the diagnosis of the proband was difficult. This was likely compounded by a pan-ethnic background with no indication of Jewish ancestry, and naivety that psychosis has a strong correlation with metabolic disorders, particularly late-onset TSD (Rosebush *et al*, 1995). Nevertheless, profound Hex A deficiency was found in the proband, and a similar clinical course was found in the brother of the proband, strongly supporting the diagnosis as a subacute form of TSD. This led to the identification of a heteroallelic genotype in the patient.

4.2 Compound heterozygous genotype and diagnosis

A G1422C transversion (W474C) in the *HEXA* gene was found to segregate through the father to both affected sons (figure 8). Segregation of the 4-bp insertion (not shown), which is associated with infantile TSD, from the mother to both siblings strongly suggested that the G1422C mutation (W474C) was responsible for residual Hex A

activity (table 1), resulting in a subacute TSD phenotype. Compound heterozygosity at the *HEXA* locus for one frequent and one less frequent mutation, is common in late-onset TSD probands. The presence of the 4-bp insertion, the most prevalent TSD-causing mutation in the Ashkenazi Jewish population, on the maternal allele suggests a non-Jewish origin for this mutation. The segregation of the newly-identified G1422C mutation through the father suggests that it has a Dutch or German origin. TSD alleles have also been identified in those ethnic groups. The reader is referred to Gravel *et al.* (1995) for a summary of mutations in the *HEXA* gene and their ethnic origin.

To demonstrate that the G1422C mutation (W474C) was not a polymorphism and that it could result in a reduced level of β-hexosaminidase activity, the mutant α-subunit was transiently transfected into Cos-7 cells (tables 2 and 3). This was necessary because our study did not rule out the possibility that Hex A deficiency was due to a second mutation on the same allele that was not sensitive to detection using SSCP analysis. However, the Cos-7 expression studies clearly showed that the G1422C mutation could result in Hex A deficiency (tables 2 and 3), making it unlikely that a second mutation was present on the same allele.

Carrier screening for the 4-bp insertion or the G1422C mutation using DNA-based methodology is the most accurate method of detecting carriers. Unlike the insertional mutation, the G1422C transversion is presumed to be a very rare mutation since it has not been previously described, and therefore, DNA-based screening for the mutation could not be justified. The possibility that the mutation exists in TSD carriers that have been previously ascertained by biochemical methods could not be ruled out. If the

G1422C mutation was identified in more patients and shown to be associated with a less severe phenotype, DNA-screening might be justifiable for this mutation.

4.3 Correlation of enzyme activity with phenotype

Small differences in Hex A activity levels are believed to determine the onset of the various forms (infantile, subacute, and chronic) of TSD. Although precise differences in Hex A activity between the subacute and chronic forms have not been demonstrated *in vivo* or *in vitro*, Hex A activity in fibroblasts of chronic TSD patients using the natural substrate of Hex A, [^{3}H]-G_{M2} ganglioside, was shown to be higher than that of subacute patients (Conzelmann & Sandhoff, 1983). Recent studies have extended this correlation in fibroblasts and in white blood cells using a fluorescent substrate sulforhodamine-G_{M1} (Agmon *et al.*, 1996). Most significantly, the latter study was able to demonstrate differences in the Hex A activity in tissues of patients with chronic TSD and Hex A pseudodeficiency.

In our subacute TSD proband, HSC3236, we were able to detect low levels of Hex A activity in fibroblasts (table 1), indicating that some mature Hex A was present. However, the mature α-subunit of Hex A could not be detected in fibroblast extracts using western blot analysis (figure 9). The subacute phenotype in our proband indicated that at least one *HEXA* allele in the proband was responsible for producing residual Hex A activity. Because the 4-bp insertion in exon 11 has previously been shown to result in no stable mRNA, the residual activity must result from the allele harbouring the G1422C mutation (W474C). To verify that this mutation allowed for low levels of mature Hex

A activity, we transiently overexpressed the mutant enzyme in Cos-7 cells.

The transient expression of the W474C mutant α-subunit in Cos-7 cells clearly demonstrated that the W474C substitution resulted in a higher level of enzyme activity than in the negative controls (tables 2 and 3). The level of enzyme activity was consistent with the level of mature α-subunit protein observed using western blot analysis (figure 10). Our observations were consistent with the late-onset phenotype found in the patient and the low levels of Hex A activity detected using 4-MUGS in HSC3236 fibroblasts (table 1). This study was done in coordination with a study of the pseudodeficiency-causing mutations, C739T (R247W) and C745T (R249W), that result in a decreased level of hexosaminidase activity, but a normal clinical phenotype (Triggs-Raine *et al.*, 1992 and Cao *et al.*, 1993). As expected, the level of Hex A enzyme activity in the presence of the R247W or R249W mutations was substantially higher (Cao *et al.*, unpublished results) than the level associated with the G1422C mutation (W474C) which results in a subacute form of Tay-Sachs disease.

Initially we expressed only the W474C mutant α-subunit in Cos-7 cells to produce Hex S ($\alpha\alpha$). As described above, this resulted in a level of activity that was consistently above that of the negative control, but the difference was not statistically significant. This result probably reflected the instability of the $\alpha\alpha$ homodimer in comparison to the major α-subunit-containing heterodimer, Hex A ($\alpha\beta$). Trop *et al.* (1992) had initiated the use of an $\alpha\beta$ co-transfection system to produce Hex A in Cos-7 cells rather than Hex S. The co-expression system takes advantage of the more stable properties of Hex A to analyze and differentiate between α-subunit mutations that are associated with late-onset and

infantile TSD.

To determine if the W474C mutation resulted in a level of activity that was clearly greater than that of the negative control, we expressed the mutant α-subunit with the β-subunit to produce Hex A (table 3). In our studies, hexosaminidase activity in αW474C/β co-transfection lysates was consistently higher than in the negative control (αR170W/β) co-transfection lysates. This was expected because the R170W mutation is associated with infantile TSD (Fernandes *et al.*, 1992b) that occurs due to a complete deficiency of Hex A. This study extends those that expressed the G250D juvenile-onset (Trop *et al.*, 1992), and the G269S adult-onset mutations that allowed for higher levels of Hex A expression in $\alpha\beta$ co-transfections (Brown & Mahuran, 1993) in comparison to the E482K mutation that is associated with infantile disease (Paw *et al.*, 1991).

Although a mature W474C mutant α-subunit could not be detected in HSC3236 fibroblasts using western blot analysis (figure 9), we demonstrated that a mature W474C α-subunit could be processed to its mature heterodimeric size when it was co-expressed with the β-subunit in transiently transfected Cos-7 cells (figures 10b and 15). Our subsequent studies were aimed at understanding at what point in the pathway that the W474C mutation alters the processing of the α-subunit.

4.4 Analysis of the processing of the W474C mutant α-subunit

The Cos-7 expression analysis provided evidence that the W474C mutant α-subunit could be processed to its mature lysosomal form as an $\alpha\beta$ heterodimer. We wanted to confirm that a residual level of mature α-subunit could be produced at

physiological concentrations of α- and β-subunits in HSC3236 fibroblasts and determine where the defect in its processing occurred. We incorporated [^{35}S]-methionine and [^{32}P] into HSC3236 fibroblasts, and followed the processing of the W474C α-subunit by immunoprecipitation after various pulse-chase intervals. HSC3236 fibroblasts were a useful system to identify the processing defect because the α-subunit was produced only from the allele harbouring the G1422C mutation (W474C). The second allele harboured the 4-bp insertion which does not result in protein synthesis, and therefore, it could not "mask" the expression of the W474C α-subunit. This was beneficial for identifying the W474C-containing α-subunit and the defect associated with its lysosomal targetting.

To analyze the size and abundance of the mutant precursor α-subunit in HSC3236 fibroblasts, the conditions for the separation of the α- and β-subunit precursors had to be optimized because it was difficult to distinguish these precursors. Separation of these precursors was attained using the SDS-PAGE system of Doucet and colleagues (Doucet & Trifaro, 1988; Doucet *et al.*, 1990). This system had several advantages over the protocol of Laemmli (1970) (used in the analysis of figure 9), that may explain why the separation of the α- and β-subunits was attainable. First, the high acrylamide:bisacrylamide ratio (100:1) results in a high porous matrix for separating proteins of similar molecular mass. Second, the presence of 0.4% SDS was significantly higher than traditional protocols, and was expected to decrease protein aggregation and protein complex formation. Third, the anode buffer had a lower ionic strength in comparison to the cathode buffer, and was predicted to prevent the broadening of proteins smaller than 150 kDa. In addition, the buffer was free of strong electrolytes that

have been predicted to cause artifacts in the electrophoretic migration of some proteins. Moreover, the presence of 5% glycerol may have influenced the electrophoretic mobility of the subunits. The use of this electrophoresis system to separate the α- and β-subunit precursor peptides made it easier to assess the relative levels of α- and β-subunit precursors in HSC3236 fibroblasts.

The first property of the mutant α-subunit that we examined by metabolic labelling was the synthesis of the precursor α-subunit. It was not surprising to observe that the level of precursor α-subunit in HSC3236 fibroblasts was about 50% of that in normal cells (figures 20 and 21). This was consistent with α-subunit expression from only one allele. The α-subunit precursor that was synthesized from the W474C allele was abundant and had a normal molecular mass, suggesting that the majority of α-subunit mRNA from the allele harbouring the G1422C transversion was stable. Further, the normal electrophoretic mobility of the HSC3236 α-subunit suggested that the protein was normally glycosylated (figures 20 and 21).

Given that a substantial level of α-subunit protein was synthesized, but very little mature α-subunit was found (figures 20 and 21), this suggested that there was a defect in the α-subunit processing pathway leading to the lysosome. We used pulse-chase analysis to see if the precursor α-subunit was exiting the endoplasmic reticulum and entering the salvage compartments, and subsequently the Golgi where phosphorylation of high-mannose chains was expected to occur. To do so, we tested for the ability of the mutant to be secreted from the pre-lysosomal compartments; a process that is dependent on the presence of mannose 6-phosphate on N-linked oligosaccharide side chains. We

could not detect the secretion of the W474C α-subunit (figure 22), and we explained this observation by verifying that the α-subunit was not phosphorylated (figure 23). Since we had predicted that glycosylation of the α-subunit was normal, the lack of phosphorylation on high mannose chains of the HSC3236 α-subunit was likely due to the inaccessibility to the sites of phosphorylation in the late ER/salvage and Golgi compartment, rather than the absence of a recognizable substrate. Taken together, we predicted that the W474C mutation caused the vast majority of newly-synthesized α-subunits to be retained in the endoplasmic reticulum of HSC3236 fibroblasts.

Next we examined the α-subunit in HSC3236 fibroblasts to determine if the W474C mutation altered subunit association. Although the association of α- and β-subunit precursors was possible after three hours in normal fibroblasts (figures 20 and 21), the various forms of the β-subunit precursor that resulted from differences in glycosylation levels made it difficult to assess the level of precursor α-subunit. At least two forms of precursor β-subunits that differed in carbohydrate content were detected in TSD fibroblasts using both anti-Hex B and anti-Hex A antisera (figures 20 and 21). Because the smaller β-subunit precursor had an electrophoretic mobility identical to that of the precursor α-subunit, it was impossible to determine the extent of αβ association by using the anti-Hex B antiserum to co-immunoprecipite the α- and β-subunits from HSC3236 fibroblasts. Because of there was a low level of A activity detected in HSC3236 fibroblasts, we anticipitated that we would detect αβ co-immunoprecipitation using the anti-Hex B antiserum. However, the levels of immunoprecipitated protein from HSC3236 lysates was similar to those observed in TSD lysates (figures 20 and 21).

Given the subacute phenotype, the low levels of Hex A activity in fibroblasts of the proband (table 1), and evidence that mature $\alpha\beta$ co-immunoprecipitation was possible in transiently transfected Cos-7 cells (figure 15), we predicted that the level of precursor $\alpha\beta$ association in HSC3236 fibroblasts was below the level of detection.

The subacute phenotype that is associated with the G1422C (W474C) mutation, and low levels of mature W474C α-subunit that could be produced in transiently transfected Cos-7 cells (figures 10b, 15 and 16), suggested that there must be low levels of mature α-subunit in fibroblasts. However, the low levels of mature α-subunit must be below the level of detection. The absence of mature Hex A was surprising given that Hex A is an abundant enzyme in normal fibroblasts, and that confluent cell cultures were used to ensure a high level of lysosomal enzyme activity (Williams *et al.*, 1973). However, the absence of detectable mature α-subunit could be explained by a much lower level of α-subunit expression in fibroblasts in comparison to transiently transfected Cos-7 cells. Another major difference between α-subunit levels in overexpressing Cos-7 cells and human fibroblasts is that splicing of *HEXA* mRNA was not a factor in Cos-7 cells because expression was conducted using the *HEXA* cDNA. Therefore, we could not rule out the possibility that the G1422C mutation (W474C) resulted in abnormal splicing and contributed to a further decrease in α-subunit protein expression in HSC3236 fibroblasts.

4.5 Aberrant mRNA splicing and late-onset disease

The position of the G1422C transversion in the *HEXA* gene of HSC3236 fibroblasts, at the first nucleotide of exon 13, suggested that the mutation may affect

normal splicing at the 3' acceptor splice-site of intron 12. The transversion has no effect on the "GT-AG" rule that suggests the 5' and 3' splice sites require the presence of the conserved sequences of GT and AG, respectively (Breathnach & Chambon, 1981). However, Northern blot analysis of total RNA from HSC3236 fibroblasts identified an abnormal *HEXA* mRNA species that was predicted to be due to the G1422C transversion (band c, figure 17). Although the levels of the abnormal mRNA were very low, they may contribute to a decreased level of α-subunit synthesis, giving rise to an additional decrease in the level of Hex A activity. Interestingly, mutations at this position have been shown to affect normal splicing in other genes (see Krawczak *et al.*, 1992). Therefore, we could not rule out the possibility that the abnormal mRNA detected by Northern blot analysis (figure 17) was an abnormal *HEXA* mRNA splice product in HSC3236 fibroblasts. A survey of the splice sites of 100 genes (Krawczak *et al.*, 1992) demonstrated that a G is most likely to occur at the first nucleotide of an exon. A G at the first nucleotide of exon 13 in the normal *HEXA* gene is consistent with these findings.

The abnormally large mRNA detected by Northern blot analysis of HSC3236 RNA (figure 17) is believed to harbour intron 12 and/or intron 13. Since some studies have shown that normal splicing in contingent upon the formation of a 3'- splice-site complex prior to 5'-splice-site complex formation (Robberson *et al.*, 1990; Talerico and Berget, 1990), it would be reasonable to conclude that intron 12 is retained. However, the possibility that the 3' splice site of intron 13 is being utilized in place of the 3' splice-site of intron 12, suggests that both introns 12 and 13 may be contained in the abnormal mRNA species. In addition, the possibility that an alternative cryptic 3' splice site is

being utilized to give rise to the abnormal mRNA could not be ruled out. Using RT-PCR with primers that flank the suspect region to amplify the abnormal message if it is stable, or using intron sequence-specific probes to detect the presence of either intron, would verify the sequences associated with abnormal mRNA species.

Mutations in the *HEXA* gene that affect normal splicing rarely occur in late-onset TSD disease patients; most have often been associated with "classical" infantile TSD (reviewed in Gravel *et al.*, 1995). A G to A silent mutation in the last nucleotide of exon 5 is one exception that is associated with late-infantile TSD (Akli *et al.*, 1990). One additional mutation that affects normal splicing, that was found in compound heterozygosity with the B1 variant mutation in exon 5, has been described as the underlying cause of late-infantile TSD (Richard *et al.*, 1995). Interestingly, the G805A late-onset disease-causing mutation (G269S) occurs at the last nucleotide of exon 7, and therefore, it may affect normal splicing in addition to Hex A activity. The most common example of a splice-site mutation, +1 IVS-12 G→C, is associated with infantile disease; it accounts for 15 to 20 percent of all TSD alleles in the Ashkenazi Jewish population (Arpaia *et al.*, 1988; Myerowitz, 1988; Ohno & Suzuki, 1988; Triggs-Raine *et al.*, 1990; Yoo *et al.*, 1993).

Mutations that affect normal splicing of the *HEXB* gene have also been identified (reviewed in Gravel *et al.*, 1995). In some cases, these mutations are associated with late-onset Sandhoff disease, suggesting that these mutations allow for some normal splicing, and therefore residual Hex B expression. Understanding the effects of mutations in the β-subunit are important because a normal β-subunit is necessary for Hex A ($\alpha\beta$)

formation.

4.6 Evolutionary conservation of W474

CLUSTAL V multiple alignment (Higgins *et al.*, 1992) of several β-hexosaminidase-related genes demonstrated that W474 of the human *HEXA* gene falls in an evolutionarily conserved region. W474 itself is conserved in both the human *HEXA* and *HEXB* (O'Dowd *et al.*, 1985) genes, the murine *HEXA* (Beccari *et al.*, 1992) and *HEXB* (Bapat *et al.*, 1988; Triggs-Raine *et al.*, 1994) genes, and the more distantly related *Dictyostelium discoideum* hexosaminidase (Graham *et al.*, 1988) and *Candida albicans* (*HEX1*) (Cannon *et al.*, 1994) genes (figure 27). In the more distantly related chitobiase (Soto-Gil & Zyskind, 1989), structural homology to the human α-subunit is likely retained by the aromatic side chain of the phenylalanine residue. The neighbouring P475 and R476 residues are also conserved, including those in the hexosaminidase gene of *Vibrio vulnificus* (Somerville & Colwell, 1993). Moreover, a second W residue at codon 485 is completely conserved, suggesting an important tertiary structure surrounding W474 that is likely disrupted by the cysteine substitution. In addition, the first 13 amino acids in exon 13, including W474, are completely conserved in the murine *HEXA* and to a lesser extent in both the human and murine *HEXB* genes.

Because of the high similarity between the α- and β-subunits, we decided to see if a W to C substitution at the conserved W residue in the human β-subunit at amino acid position 503 would result in low levels of mature Hex B expression when it was transiently expressed in Cos-7 cells. Pulse-chase analysis of the βW503C mutant subunit

W474

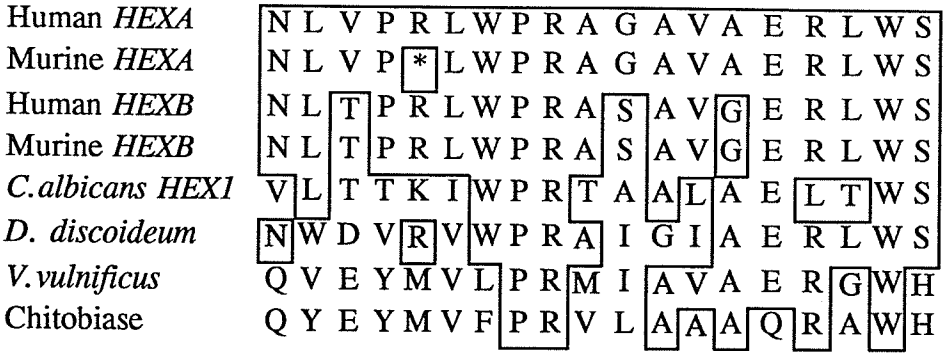

Figure 27 ***Evolutionary conservation of W474 in the human HEXA gene and other related genes.***

in Cos-7 cells suggested that the mutation caused retention of the newly-synthesized β-subunits in the early processing compartments where it was degraded (figure 26). Phosphorylation and secretion of precursor βW503C subunits was not analyzed in Cos-7 cells.

4.7 Future directions

There is no treatment or cure for Hex A deficiency at the present time. Cases of late-onset TSD have more potential for successful treatment in comparison to infantile TSD because there is a residual level of Hex A. Therapies that could enhance the small levels of G_{M2} ganglioside hydrolysis would be useful in delaying the clinical manifestations associated with the disease. The mutation in the HSC3236 proband is one associated with late-onset TSD and it could prove to be useful in future studies aimed at developing therapies to increase levels of residual enzyme activity.

The effect of the G1422C mutation on normal *HEXA* mRNA splicing is likely the most important molecular mechanism that should be examined in the HSC3236 proband. Since small differences in Hex A levels are believed to differentiate the subacute and chronic forms of G_{M2} gangliosidosis, then a defect in mRNA splicing is contributing to α-subunit deficiency and is likely predisposing the proband to a more rapid clinical course. Identifying the sequences associated with the abnormal mRNA observed in HSC3236 fibroblasts (figure 17) using RT-PCR, or Northern blot analysis with sequence-specific probes, should be sufficient to demonstrate if the G1422C mutation affects α-subunit expression at the RNA level. In addition, mini-gene constructs, harbouring

introns 12 and 13 and the G1422C mutation, that could be expressed in Cos-7 cells would be useful in determining if the mutation could affect splicing and the level of mature α-subunit protein. The G805A mutation that is also associated with late-onset TSD and is believed to affect normal *HEXA* mRNA splicing at the 5' splice site of exon 8 of the *HEXA* gene. It would be useful to see if the G805A and G1422C mutations affect *HEXA* mRNA splicing *in vitro*, and to what extent that α-subunit protein levels are affected. Together, both mutations could provide valuable information about other mutations that are believed to affect mRNA processing and protein structure.

There is no direct relationship between the clinical phenotype and the effect that a mutation has on α-subunit protein targeting. Whether a mutation causes an early or late protein processing defect, small amounts of mutant α-subunit must be processed to a mature Hex A ($\alpha\beta$) enzyme in late-onset TSD patients. Since some HSC3236 α-subunits must escape retention in the ER, they may have a weaker affinity for proteins involved in retaining misfolded mutant polypeptides. The HSC3236 α-subunit would be useful in understanding early protein processing modifications and the proteins involved with folding or retention of mutant α-subunits in the RER. The retention of the HSC3236 α-subunit may be the result of a particular secondary structure that is created or destroyed by the cysteine for tryptophan substitution.

The $\alpha\beta$ co-transfection system in Cos-7 cells has been used to analyze three mutations, E482K, G269S, and now the W474C substitution in this study, that are associated with processing defects. Although these mutations could be assayed for their association with late-onset TSD by producing mature α-subunit, this type of assay system

still needs to be applied to the remaining mutations associated with late-onset TSD. With the same token, these studies would be useful in developing a stronger correlation between genotypes and biochemical or clinical phenotypes.

The structure of the α-subunit and those surrounding the W474 amino acid are believed to be predictable because of a high degree of sequence similarity with hexosaminidases from lower organisms. An on-going effort (Triggs-Raine, unpublished) to solve the crystal structure of hexosaminidase from *Streptomyces plicatus* would be useful in understanding how the region surrounding W474 could be affected by an amino acid substitution. Although the prokaryotic-related hexosaminidases are easiest to study, the effect of mutations on lysosomal targeting could not be analyzed in a prokaryotic system. However, the structural effects on subunit association and stability could be predicted from other related hexosaminidases.

An understanding of Hex A structure might be useful for designing gene-delivery systems for gene therapy of TSD. With no available cure at the current time, gene-delivery systems appear to be a mainstream method of treatment. However, the problems associated with overcoming the blood-brain barrier and targeting affected neurons in TSD patients appears to be the limiting factor. Although enzyme replacement methods are successful in β-glucocerebrosidase replacement in Gaucher disease patients, they are expensive and are also associated with problems of targeting the enzymes to specific tissues.

Some pharmacological approaches have been taken to induce G_{M2} ganglioside hydrolysis. A large number of the drugs used to treat late-onset TSD patients are

amphiphilic, weak base compounds (such as imipradine) that have shown to induce lipidosis (Palmeri *et al.*, 1992). These compounds cause a depletion of residual lysosomal activity and deterioration in a patient's condition. Treatment of cells with dexamethasone has been shown to induce mannose receptor synthesis (Shepherd et al., 1985) and consequently counteract the effect of amphiphilic compounds (Navon *et al*, 1987). If the mechanism of how these compounds are interrelated could be understood, it would be easier to identify biochemical mechanisms that could be used as targets for therapeutic intervention. HSC3236 fibroblasts and others with residual Hex A levels are valuable to determine the effect of potential drugs in the treatment of late-onset TSD.

REFERENCES

Agmon V, Khosravi R, Marchesini S, Dinur T, Dagan A, Gatt S, Navon R (1996) Intracellular degradation of sulforhodamine-GM1: use for a fluorescence-based characterization of G_{M2}-gangliosidosis variants in fibroblasts and white blood cells. *Clin Chim Acta* 247: 105-120

Akalin N, Shi H-P, Vavougios G, Hechtman P, Lo W, Scriver CR, Mahuran D, *et al* (1992) Novel Tay-Sachs disease mutations from China. *Hum Mutat* 1: 40-46.

Akerman BR, Zielenski J, Triggs-Raine BL, Prence EM, Natowicz M, Lim-Steele JST, Kaback MM, Mules EH, Thomas GH, Clarke JTR, Gravel RA (1992) A mutation common in non-Jewish Tay-Sachs disease: frequency and RNA studies. *Hum Mutat* 1, 303-309.

Akli S, Chelly J, Mezard C, Gandy S, Kahn A, Poenaru L (1990) A "G" to "A" mutation at position -1 of a 5' splice site in a late infantile form of Tay-Sachs disease. *J Biol Chem* 265: 7324-7330

Akli S, Chelly J, Lacorte Jean-M, Poenaru L, Kahn A (1991) Seven novel Tay-Sachs mutations detected by chemical mismatch cleavage of PCR-amplified cDNA fragments. *Genomics* 11: 124-134

Arpaia E, Dumbrille-Ross A, Maler T, Neote K, Tropak M, Troxel C, Stirling JL, *et al* (1988) Identification of an altered splice site in Ashkenazi Tay-Sachs disease. *Nature* 333: 85-86

d'Azzo A, Proia RL, Kolodny EH, Kaback MM, Neufeld EF (1984) Faulty association of α- and β-subunits in some forms of β-hexosaminidase A deficiency. *J Biol Chem* 259: 11070-11074

Bapat B, Ethier M, Neote K, Mahuran D, Gravel RA (1988) Cloning and sequence analysis of a cDNA encoding the β-subunit of mouse β-hexosaminidase. *FEBS Letters* 237: 191-195

Bayleran J, Hechtman P, Saray W (1984) Synthesis of 4-methylumbelliferyl-β-D-N-acetylglucosamine-6-sulfate and its use in classification of G_{M2} gangliosidosis genotypes. *Clin Chim Acta* 143: 73-89

Beccari T, Hoade J, Orlacchio A, Stirling JL (1992) Cloning and sequence analysis of a cDNA encoding the α-subunit of mouse β-N-acetylhexosaminidase and comparison with the human enzyme. *Biochem J* 285: 593-596

Boles DJ, Proia RL (1995) The molecular basis of *HEXA* mRNA deficiency caused by

the most common Tay-Sachs disease mutation. *Am J Hum Genet* 56: 716-724,

Bradford MM (1976) A rapid and sensitive method for the quantitation of microgram quantities of protein utilizing the principle of protein-dye binding. *Anal Biochem* 72: 248-254

Breathnach R, Chambon P (1981) Organization and expression of eukaryotic split genes coding for proteins. *Annu Rev Biochem* 50: 349-383

Brown CA, Mahuran DJ (1993) β-Hexosaminidase isozymes from cells cotransfected with α and β cDNA constructs: analysis of the α-subunit missense mutation associated with the adult form of Tay-Sachs disease. *Am J Hum Genet* 53: 497-508

Cannon RD, Niimi K, Jenkinson HF, Shepherd MG (1994) Molecular cloning and expression of the *Candida albicans* β-N-acetylglucosaminidase (HEX1) gene. *J Bacteriol* 176: 2640-2647

Cao Z, Natowicz M, Kaback M, Lim-Steele J, Prence E, Brown D, Chabot T, *et al* (1993) A second mutation associated with apparent β-hexosaminidase A pseudodeficiency: identification and frequency estimation. *Am J Hum Genet* 53: 1198-1205

Cohen-Tannoudji M, Marchand P, Aklim S, Sheardown SA, Puech J-P, Kress C, Gressens P, *et al* (1995) Disruption of murine *Hexa* gene leads to enzymatic deficiency and to neuronal storage, similar to that observed in Tay-Sachs disease. *Mammalian Genome* 6: 844-849

Conzelmann E, Sandhoff K (1978) AB variant of infantile G_{M2} gangliosidosis: deficiency of a factor necessary for stimulation of hexosaminidase A-catalyzed degradation of ganglioside G_{M2} and glycolipid G_{A2}. *Proc Natl Acad Sci USA* 75: 3979-3983

Conzelmann E, Sandhoff K (1983-84) Partial enzyme deficiencies: residual activities and the development of neurological disorders. *Dev Neurosci* 6: 58-71

Conzelmann E, Sandhoff K, Nehrkorn H, Geiger B, Arnon R (1978) Purification, biochemical and immunological characterization of hexosaminidase A from variant AB of infantile G_{M2} gangliosidosis. *Eur J Biochem* 84: 27

Dlott B, d'Azzo A, Quon DVK, Neufeld EF (1990) Two mutations produce intron insertion in mRNA and elongated β-subunit of human β-hexosaminidase. *J Biol Chem* 26: 17921-17927

Doucet JP, Trifaro JM (1988) A discontinuous and highly porous sodium dodecyl

sulfate-polyacrylamide slab gel system of high resolution. *Anal Biochem* 168: 265-271

Doucet Jean-P, Murphy BJ, Tuana BS (1990) Modification of a discontinuous and highly porous sodium dodecyl sulfate-polyacrylamide gel system for minigel electrophoresis. *Anal Biochem* 190: 209-211

Dreyfus J, Poenaru L, Vibert M, Ravise N, Boue J (1977) Characterization of variant β-hexosaminidase: "hexosaminidase Paris". *Am J Hum Genet* 29:287

Emiliani C, Falzetti F, Orlacchio A, Stirling JL (1990) Treatment of HL-60 cells with dimethyl sulphoxide inhibits the formation of β-N-acetylhexosaminidase S. *Biochem J* 272: 211-215

Feinberg AP, Vogelstein B (1983) A technique for radiolabeling DNA restriction endonuclease fragments to high specific activity. *Anal Biochem* 132: 6-13

Fernandes MJG, Kaplan F, Clow CL, Hechtman P, Scriver CR (1992a) Specificity and sensitivity of hexosaminidase assays and DNA analysis for the detection of Tay-Sachs disease gene carriers among Ashkenazic Jews. *Genet Epidem* 9: 169-175

Fernandes M, Kaplan F, Natowicz M, Prence E, Kolodny E, Kaback M, Hechtman P (1992b) A new Tay-Sachs disease B1 allele in exon 7 in two compound heterozygotes each with a second novel mutation. *Hum Molec Genet* 1: 759-761

Fielder K, Simons K (1995) The role of N-glycans in the secretory pathway. *Cell* 81: 309-312

Fox MF, DuToit DL, Warnich L, Reteif AE (1984) Regional localization of alpha-galactosidase (*GLA*) to Xpter----q22, hexosaminidase B (*HEXB*) to 5q13----qter, and arylsulfatase B (*ARSB*) to 5pter----q13. *Cytogenet Cell Genet* 38: 45

Furst W, Sandhoff K (1992) Activator proteins and topology of lysosomal sphingolipid catabolism. *Biochim Biophys Acta* 1126: 1-16

Gething M-J, Sambrook J (1992) Protein folding in the cell. *Nature* 355: 33-45

Graham TR, Zassenhaus HP, Kaplan A (1988) Molecular cloning of the cDNA which encodes β-N-acetylhexosaminidase A from *Dictyostelium discoideum*. *J Biol Chem* 263: 16823-16829

Gravel RA, Clarke JTR, Kaback MM, Mahuran D, Sandhoff K, Suzuki K (1995) The G_{M2} Gangliosidoses. In Scriver CR, Beaudet AL, Sly WS, Valle D (eds.) The Metabolic Basis of Inherited Disease. 7th ed. Chapter 92. McGraw-Hill, Inc.,

New York

Grebner E, Tomczak J (1991) Distribution of three α-chain β-hexosaminidase A mutations among Tay-Sachs carriers. *Am J Hum Genet* 48: 604-607

Harmon DL, Gardner-Medwin D, Stirling JL (1993) Two new mutations in a late infantile Tay-Sachs patient are both in exon 1 of the β-hexosaminidase α gene. *J Med Genet* 30: 123-128

Hasilik A, Neufeld EF (1980) Biosynthesis of lysosomal enzymes in fibroblasts. *J Biol Chem* 255: 4937-4945

Hasilik A, Waheed A, Von Figura K (1981) Enzymatic phosphorylation of lysosomal enzymes in the presence of UDP-N-acetylglucosamine. Absence of the activity in I-cell fibroblasts. *Biochem Biophys Res Commun* 98:761,

Hechtman P (1977) Characterization of an activating factor required for hydrolysis of G_{M2} ganglioside catalyzed by hexosaminidase A. *Can J Biochem* 55: 315-324

Helenius A, Marquardt T, Braakman I (1992) The endoplasmic reticulum as a protein-folding compartment *Trends Cell Biol* 2: 227-231

Helenius A (1994) How N-linked oligosaccharide affect glycoprotein folding in the endoplasmic reticulum. *Mol Biol Cell* 5: 253-265

Higgins DG, Bleasby AJ, Fuchs R (1992) CLUSTAL V: improved software for multiple sequence alignment. *Comput Appl Biosci* 8: 189-191

Hille-Rehfeld A (1995) Mannose 6-phosphate receptors in sorting and transport of lysosomal enzymes. *Biochim Biophys Acta* 1241: 177-194

Hoflack B, Fujimoto K, Kornfeld S (1987) The interaction of phosphorylated oligosaccharides and lysosomal enzymes with bovine liver cation-dependent mannose 6-phosphate receptor. *J Biol Chem* 262:123-129

Hou Y, Tse R, Mahuran DJ (1996) Direct determination of the substrate specificity of the α-active site in heterodimeric β-hexosaminidase A. *Biochem* 35: 3963-3969

Hirschberg CB, Snider MD (1987) Topography of glycosylation in the rough endoplasmic reticulum and Golgi apparatus. *Annu Rev Biochem* 56: 63-87

Kaback MM (1972) Thermal fractionation of serum hexosaminidases: applications to heterozygote detection and diagnosis of Tay-Sachs disease. *Meth. Enzymol.* 28: 862-867.

Kaback MM, Shapiro LJ, Hirsch P (1977) Tay-Sachs disease heterozygote detection: a quality control study. In Kaback MM, Rimoin DL, O'Brien JLS (eds.) Tay-Sachs disease: Screening and prevention. Vol 18. A.R. Liss, New York.

Kaback M, Lim-Steele J, Dabholkar D, Brown D, Levy N, Zeiger K (1993) Tay-Sachs disease-carrier screening, prenatal diagnosis, and the molecular era. *JAMA* 270: 2307-2315

Kanfer JN, Spielvogel C (1973) Hexosaminidase activities of cultured human skin fibroblasts. *Biochim Biophys Acta* 193: 203-207

Klenk E (1939) Beitrage zur Chemie der Lipidosen. I. Niemann-Pick'shen Krankheit und amauritische Idiotie. *Hoppe Seyler's Z Physiol Chem* 262: 128

Klenk E (1935) Uber die natur der Phosphatide und anderer Lipoide des Gehirns und der Leber bei der Niemann-Pick'schen Krankheit. *Hoppe Seyler's Z Physiol Chem* 235: 24

Klenk E (1942) Uber die Ganglioside, eine neue Gruppe von zuckerhaltigen Gehirnlipoiden. *Hoppe Seyler's Z Physiol Chem* 273: 76

Korneluk RG, Mahuran DJ, Neote K, Klavins MH, O'Dowd BF, Tropak M, Willard H, Anderson M-J, Lowden JA, Gravel RA (1986) Isolation of cDNA clones coding for the α-subunit of human β-hexosaminidase. *J Biol Chem* 261: 8407-8413.

Kornfeld S (1990) Lysosomal enzyme targeting. *Biochem Soc Trans* 18: 367-374

Kornfeld S (1992) Structure and function of the mannose 6-phosphate/insulin like growth factor receptors. *Annu Rev Biochem* 61: 307-30.

Kornfeld R, Kornfeld S (1985) Assembly of asparagine-linked oligosaccharides. *Annu Rev Biochem* 54: 631-64

Krawczak M, Reiss J, Cooper DN (1992) The mutational spectrum of single base-pair substitutions in mRNA splice junctions of human genes: causes and consequences. *Hum Genet* 90: 41-54

Kuroki Y, Itoh K, Nadaoka Y, Tanaka T, Sakuraba H (1995) A novel missense mutation (C522Y) is present in the β-hexosaminidase β-subunit of a Japanese patient with infantile Sandhoff disease. *Biochem Biophys Res Commun* 212: 564-571

Kytzia H-J, Sandhoff K (1985) Evidence for two different active sites on human β-hexosaminidase A. *J Biol Chem* 260: 7568-7572

Laemmli UK (1970) Cleavage of structural proteins during assembly of the head of bacteriophage T4. *Nature* 227: 680-685

Landels EC, Ellis IH, Fensom AH, Green PM, Bobrow M (1991) Frequency of the Tay-Sachs disease splice and insertion mutations in the UK Ashkenazi Jewish population. *J Med Genet* 28: 177-180

Lau MM, Neufeld EF (1989) A frameshift mutation in a patient with Tay-Sachs disease causes premature termination and defective intracellular transport of the alpha-subunit of beta-hexosaminidase. *J Biol Chem* 264: 21376-80

Ledeen R, Salsman K (1965) Structure of the Tay-Sachs ganglioside. *Biochem* 4: 2225

Little LE, Lau MM, Quon DV, Fowler AV, Neufeld EF (1988) Proteolytic processing of the alpha-chain of the lysosomal enzyme, β-hexosaminidase, in normal human fibroblasts. *J Biol Chem* 263: 4288

MacGregor GR, Nolan GP, Fiering S, Roederer M, Herzenberg LA (1991) Use of *E.coli lacZ* (β-galactosidase) as a reporter gene. Methods in Molecular Biology 7: 217-235

Macleod PM, Wood S, Jan JE, Applegarth DA, Dolman CL (1977) Progressive cerebellar ataxia, spasticity, psychomotor retardation, and hexosaminidase deficiency in a 10-year-old child: juvenile Sandhoff disease. *Neurology* 27: 571-573

Mahuran D, Novak A, Lowden JA (1985) The lysosomal hexosaminidase isozymes. *Cur Top Biol Med Res* 12: 229-288

Mahuran DJ, Neote K, Klavins MH, Leung A, Gravel RA (1988) Proteolytic processing of pro-α and pro-β precursors from human β-hexosaminidase. *J Biol Chem* 263: 4612-4618

Mahuran DJ (1995) β-Hexosaminidase: Biosynthesis and processing of the normal enzyme, and identification of mutations causing Jewish Tay-Sachs disease. *Clin Biochem* 28: 101-106

Makita A, Yamakawa T (1963) The glycolipids of the brain of Tay-Sachs disease. The chemical structure of globoside and main ganglioside. *Jpn J Exp Med* 33: 361

Miranda AF, Duigou GJ, Hernandez E, Fisher PB (1988) Characterization of mutant human fibroblast cultures transformed with simian virus 40. *J Cell Sci* 89: 481-493

Mules EH, Dowling CE, Patersen MB, Kazazian HH, Thomas GH (1991) A novel mutation in the invariant AG of the acceptor splice site of intron 4 of the β-hexosaminidase α-subunit gene in two unrelated American Black G_{M2}-gangliosidosis (Tay-Sachs disease) patients. *Am J Hum Genet* 48: 1181-1185

Myerowitz R (1988) Splice junction mutation in some Ashkenazi Jews with Tay-Sachs disease: evidence against a single defect within this ethnic group. *Proc Natl Acad Sci USA* 85: 3955-3959

Myerowitz R, Costigan FC (1988) The major defect in Ashkenazi Jews with Tay-Sachs disease is an insertion in the gene for the α-chain of β-hexosaminidase. *J Biol Chem* 263: 18587-18589

Myerowitz R, Hogikyan ND (1986) Different mutations in Ashkenazi Jewish and non-Jewish French Canadians with Tay-Sachs disease. *Science* 232: 1646-1648

Myerowitz R, Hogikyan ND (1987) A deletion involving Alu sequences in the β-hexosaminidase α-chain gene of French Canadians with Tay-Sachs disease. *J Biol Chem* 262: 15396-15399

Myerowitz R, Piekarz R, Neufeld EF, Shows TB, Suzuki K (1985) Human β-hexosaminidase α chain: coding sequence and homology with the β chain. *Proc Natl Acad Sci USA* 82: 7830-7834

Nakano T, Suzuki K (1989) Genetic cause of a juvenile form of Sandhoff disease. Abnormal splicing of β-hexosaminidase β gene transcript due to a point mutation within intron 12. *J Biol Chem* 264: 5155-5158

Nakano T, Muscillo M, Ohno K, Hoffman AJ, Suzuki K (1988) A point mutation in the coding sequence of the β-hexosaminidase α gene results in defective processing of the enzyme protein in an unusual G_{M2}-gangliosidosis variant. *J Neurochem* 51: 984-987

Navon R, Argov Z, Brand N, Sandbank U (1981) Adult G_{M2} gangliosidosis in association with Tay-Sachs disease: a new phenotype. *Neurology* 31: 1397-1401

Navon R, Baram D (1987) Depletion of cellular β-hexosaminidase by imipramine is prevented by dexamethasone; implications for treating psychotic hexosaminidase-A deficient patients. *Biochem Biophys Res Commun* 13: 1098-1103

Navon R (1991) Molecular and clinical heterogeneity of adult G_{M2} gangliosidosis. *Dev Neurosci* 13: 295-298

Navon R, Kolodny EH, Mitsumoto H, Thomas GH, Proia RL (1990) Ashkenazi-Jewish

and non-Jewish adult G_{M2} gangliosidosis patients share a common genetic defect. *Am J Hum Genet* 46: 817-821

Neote K, Bapat B, Dumbrille-Ross A, Troxel C, Schuster SM, Mahuran DJ, Gravel RA (1988) Characterization of the human *HEXB* gene encoding lysosomal β-hexosaminidase. *Genomics* 3: 279-286

Neote K, McInnes B, Mahuran DJ, Gravel RA (1990) Structure and distribution of an Alu-type deletion mutation in Sandhoff disease. *J Clin Invest* 86: 1524-1531

Neufeld EF (1991) Lysosomal storage diseases. *Annu Rev Biochem* 60: 257-80.

Norfulus F, Yamanaka S, Proia RL (1996) Promoters for the human β-hexosaminidase genes, *HEXA* and *HEXB*. DNA *Cell Bio* 15: 89-97

O'Dowd BF, Quan F, Willard HF, Lamhonwah Anne-M, Korneluk RG, Lowden JA, Gravel R a, *et al* (1985) Isolation of cDNA clones coding for the β subunit of human β-hexosaminidase. *Proc Natl Acad Sci USA* 82: 1184-1188

O'Dowd BF, Klavins MH, Willard HF, Gravel R, Lowden JA, Mahuran DJ (1986) Molecular heterogeneity in the infantile forms of Sandhoff disease (O-variant G_{M2} gangliosidosis). *J Biol Chem* 261: 12680-12685

O'Dowd BF, Cumming DA, Gravel RA, Mahuran D (1988) Oligosaccharide structure and amino acid sequence of the major glycopeptides of mature human beta-hexosaminidase. *Biochem* 27: 5216-5226

Ohno K, Suzuki K (1988) A splicing defect due to an exon-intron junctional mutation results in abnormal β-hexosaminidase α chain mRNAs in Ashkenazi Jewish patients with Tay-Sachs disease. *Biochem Biophys Res Commun* 153: 463-469

Okada S, O'Brien JS (1969) Tay-Sachs disease: generalized absence of a beta-D-N-acetylhexosaminidase component. *Science* 165: 698-700

Orita M, Suzuki Y, Sekiya T, Hayashi K (1989) Rapid and sensitive detection of point mutations and DNA polymorphisms using the polymerase chain reaction. *Genomics* 5: 874-879

Palmeri S, Mangano L, Battisti C, Malandrini A, Federico A (1992) Imipramine induced lipidosis and dexamethasone effect: morphological and biochemical study in normal and chronic GM2 gangliosidosis fibroblasts. *J Neurol Sci* 110: 215-221

Paw BH, Kaback MM, Neufeld EF (1989) Molecular basis of adult-onset and chronic G_{M2} gangliosidoses in patients of Ashkenazi Jewish origin: substitution of serine

for glycine at position 269 of the α-subunit of β-hexosaminidase. *Proc Natl Acad Sci USA* 86: 2413-2417

Paw BH, Moskowitz SM, Urhammer N, Wright N, Kaback MM, Neufeld EF (1990a) Juvenile G_{M2} gangliosidosis caused by substitution of histidine for arginine at position 499 or 504 of the α-subunit of β-hexosaminidase. *J Biol Chem* 265: 9452-9457

Paw BH, Tieu P, Kaback MM, Lim J, Neufeld EF (1990b) Frequency of three *HEXA* mutant alleles among Jewish and non-Jewish carriers identified in a Tay-Sachs screening program. *Am J Hum Genet* 47: 698-705

Paw BH, Wood LC, Neufeld EF (1991) A third mutation at the CpG dinucleotide of codon 504 and a silent mutation at codon 506 of the HEX A gene. *Am J Hum Genet* 48: 1139-1146

Phaneuf D, Wakamatsu N, Huang J, Borowski A, Peterson AC, Fortunato SR, Ritter G, *et al* (1996) Dramatically different phenotypes in mouse models of human Tay-Sachs and Sandhoff diseases. *Hum Molec Genet* 5: 1-14

Pohlmann R, Boeker MWC, von Figura K (1995) The two mannose 6-phosphate receptors transport distinct complements of lysosomal proteins. *J Biol Chem* 270: 27311-27318

Proia RL (1988) Gene encoding the human β-hexosaminidase β chain: extensive homology of intron placement in the α- and β-chain genes. *Proc Natl Acad Sci USA* 85: 1883-1887

Proia RL, Soravia E (1987) Organization of the gene encoding the human β-hexosaminidase α chain. *J Biol Chem* 262: 5677-5681

Proia RL, d'Azzo A, Neufeld EF (1984) Association of α- and β-subunits during the biosynthesis of β-hexosaminidase in cultured human fibroblasts. *J Biol Chem* 259: 3350-3354

Quon DVK, Proia RL, Fowler AV, Bleibaum J, Neufeld EF (1989) Proteolytic processing of the β-subunit of the lysosomal enzyme, β-hexosaminidase, in normal human fibroblasts. *J Biol Chem* 264: 3380-3384

Rapoport TA (1990) Protein transport across the endoplasmic reticulum membrane.*Science* 258: 931-935

Rattazzi MC, Brown JA, Davidson RG, Shows TB (1976) Studies on complementation of β-hexosaminidase deficiency in human G_{M2} gangliosidosis. *Am J Hum Genet*

28: 143-154

Reitman ML, Varki A, Kornfeld S (1981) Fibroblasts from patients with I-cell disease and pseudohurler polydystrophy are deficient in uridine 5'-diphosphate-N-acetylglucosamine: glycoprotein N-acetylglucosaminyl-phosphodiesterase activities. *J Clin Invest* 67:1574.

Richard MM, Erenberg G, Triggs-Raine BL (1995) An A-to-G mutation at the +3 position of intron 8 of the *HEXA* gene is associated with exon 8 skipping and Tay-Sachs disease. *Biochem Mol Med* 55: 74-76

Robberson BL, Cote GJ, Berget SM (1990) Exon definition may facilitate splice site selection in RNAs with multiple exons. *Mol Cell Bio* 10: 84-94.

Robinson D, Stirling JL (1968) N-acetyl-beta-glucosaminidases in human spleen. *Biochem J* 107: 321

Rosebush PI, MacQueen GM, Clarke JTR, Callahan JW, Strasberg PM, Mazurek MF (1995) Late-onset Tay-Sachs disease presenting as catatonic schizophrenia: diagnostic and treatment issues. *J Clin Psychiatry* 56:8: 347-353

Rothman JE, Wieland FT (1996) Protein sorting by transport vesicles. *Science* 272: 227-234

Sachs B (1887) On arrested cerebral development with special reference to its cortical pathology. *J Nerv Ment Dis* 14: 541

Sambrook J, Fritsch EF, Maniatis T (Eds.) (1989) Molecular Cloning: a Laboratory Manual. 2nd ed. Cold Spring Harbour Laboratory Press, USA.

Sandhoff K (1969) Variation of beta-N-acetyl-glucosaminidase-pattern in Tay-Sachs disease. *FEBS Letters* 4: 351

Sandhoff K, Andreae U, Jatzkewitz H (1968) Deficient hexosaminidase activity in an exceptional case of Tay-Sachs disease with additional storage of kidney globoside in visceral organs. *Pathol Eur* 3: 278

Sandhoff K, Harzer K, Wasle W, Jatzkewitz H (1971) Enzyme alterations and lipid storage in three variants of Tay-Sachs disease. *J Neurochem* 18: 2469

Sandhoff K, Harzer K, Furst W (1995) Sphingolipid activator proteins. In Scriver CR, Beaudet AL, Sly WS, Valle D (eds.) The Metabolic Basis of Inherited Disease. 7th ed. Chapter 76. McGraw-Hill Inc., New York

Sanger F, Nicklen S, Coulson AR (1977) DNA sequencing with chain terminating inhibitors. *Proc Natl Acad Sci USA* 74: 5463-5467

Sango K, Yamanaka S, Hoffman A, Okuda Y, Grinberg A, Westphal H, McDonald MP, *et al* (1995) Mouse models of Tay-Sachs and Sandhoff disease differ in neurologic phenotype and ganglioside metabolism. *Nat Genet* 11: 170-176

Sathyamoorthy N, Wang TTY, Phang JM (1994) Stimulation of pS2 expression by diet-derived compounds. *Cancer Res* 54: 957-961

Seglen PO (1983) Inhibitors of lysosomal function. Methods Enzymol 96: 737-64

Shepherd V, Konish MG, Stahl P (1985) Dexamethasone increases expression of mannose receptors and decreases extracellular lysosomal accumulation in macrophages. *J Biol Chem* 260: 160-164

Somerville CC, Colwell RR (1993) Sequence analysis of the β-N-acetylhexosaminidase gene of *Vibrio vulnificus*: Evidence for a common evolutionary origin of hexosaminidases. *Proc Natl Acad Sci USA* 90: 6751-6755

Sonderfeld-Fresko S, Proia RL (1989) Analysis of the glycosylation and phosphorylation of the lysosomal enzyme, β-hexosaminidase B, by site-directed mutagenesis. *J Biol Chem* 264: 7692-7697

Sorge JA, West C, Kuhl W, Treger L, Beutler E (1987) The human glucocerebrosidase gene has two functional ATG initiator codons. *Am J Hum Genet* 41: 1016-1024

Soto-Gil RW, Zyskind JW (1989) N,N'-diacetylchitobiase of *Vibrio harveyi*. *J Biol Chem* 264: 14778-14783

Srivastava SK, Wiktorowicz J, Klebe R, Awasthi YC (1975) Studies on β-D-N-acetylhexosaminidase: Various isozymes in tissues of normal subjects and Sandhoff disease patients. *Biochim Biophys Acta* 397: 428-436

Suzuki K, Chen GC (1967) Brain ceramide hexosides in Tay-Sachs disease and generalized gangliosidosis. *J Lipid Res* 8: 105

Suzuki K, Vanier MT (1991) Biochemical and molecular aspects of late-onset GM2-gangliosidosis: B1 variant as a prototype. *Dev Neurosci* 14:288

Svennerholm L (1962) The chemical structure of normal human brain and Tay-Sachs gangliosides. *Biochem Biophys Res Commun* 9: 436

Takeda K, Nakai H, Hagiwara H, Tada K, Shows TB, Byers MG, Myerowitz R (1990)

Fine assignment of beta-hexosaminidase A alpha-subunit on 15q23-24 by high resolution in situ hybridization. *Tohoku J Exp Med* 160: 203

Talerico M, Berget SM (1990) Effect of 5' splice site mutations on splicing of the preceding intron. *Mol Cell Biol* 10:6299-6305.

Tallman JF, Brady RO, Navon R, Padeh B (1974) Ganglioside catabolism in hexosaminidase A-deficient adults. *Nature* 252: 254-255

Taniike M, Yamanaka S, Proia RL, Langaman C, Bone-Turrentine T, Suzuki K (1995) Neuropathology of mice with targeted disruption of Hexa gene, a model of Tay-Sachs disease *Acta Neuropathol Berl* 89: 296-304

Tay W (1881) Symmetrical changes in the region of the yellow spot in each eye of an infant. *Trans Opthalmol Soc* 1: 155

Terry RD, Weiss M (1963) Studies on Tay-Sachs disease: II. Ultrastructure of the cerebrum. *J Neuropathol Exp Neurol* 22: 18

Tews I, Perrakis A, Oppenheim A, Dauter Z, Wilson KS, Vorgias CE (1996) Bacterial chitobiase structure provides insight into catalytic mechanism and the basis of Tay-Sachs disease. *Nature Struct Biol* 3: 638-648.

Triggs-Raine BL, Feigenbaum ASJ, Natowicz M, Skomorowski Marie-A, Schuster SM, Clarke JTR, Mahuran DJ, *et al* (1990) Screening for carriers of Tay-Sachs disease among Ashkenazi Jews. *New Engl J Med* 323: 6-12

Triggs-Raine BL, Akerman BR, Clarke JTR, Gravel RA (1991) Sequence of DNA flanking the exons of the *HEXA* gene and identification of mutations in Tay-Sachs disease. *Am J Hum Genet* 49: 1041-1054

Triggs-Raine BL, Mules EH, Kaback MM, Lim-Steele JST, Dowling C, Akerman B, Natowicz M, *et al* (1992) A pseudodeficiency allele common in non-Jewish Tay-Sachs carriers: implications for carrier screening. *Am J Hum Genet* 51: 793-801

Triggs-Raine BL, Benoit G, Salo TJ, Trasler JM, Gravel RA (1994) Characterization of the murine β-hexosaminidase (*HEXB*) gene. *Biochim Biophys Acta* 1227: 79-86

Trop I, Kaplan F, Brown C, Mahuran D, Hechtman P (1992) A glycine 250 to aspartate substitution in the α-subunit of hexosaminidase A causes juvenile-onset Tay-Sachs disease in a Lebanese-canadian family. *Hum Mutat* 1: 35-39

Tse R, Vavougious G, Hou Y, Mahuran DJ (1996) Identification of an active acidic residue in the catalytic site of β-hexosmaminidase. *Biochem* 35: 7599-7607

Von Heijne G (1990) The signal peptide. *J Membr Biol* 115:195

Wahl GM, Stern M, Stark GR (1979) Efficient transfer of large DNA fragments from agarose gels to diazobenzyloxymethyl-paper and rapid hybridization by using dextran sulfate. *Proc Natl Acad Sci USA* 76: 3683

Warburg O, Christian W (1942) Isolation and crystallization of enolase. *Biochem. Z.* 310, 384.

Weitz G, Proia RL (1992) Analysis of glycosylation and phosphorylation of the α-subunit of the lysosomal enzyme, β-hexosaminidase A, by site-directed mutagenesis. *J Biol Chem* 267: 10039-10044

Wenger DA, Okada S, O'Brien JS (1972) Studies on the substrate specificity of hexosaminidase A and B from liver. *Arch Biochem Biophys* 153: 116

Wiktorowitcz JE, Awashti YC, Kurosky A, Srivastava SK (1977) Purification and properties of human kidney-cortex hexosaminidase A and B. *Biochem J* 165: 49

Williams GM, Stromberg K, Kroes R (1973) Cytochemical and ultrastructural alterations associated with confluent growth in cell cultures from epithelial-like cells from rat liver. *Lab Invest* 29: 293-300

Williams JG, Mason PJ (1985) Hybridisation in the analysis of RNA In Hanes DD, Higgins J (eds.) Nucleic Acid Hybridisation, IRL Press Limited, Oxford

Wood S (1978) Juvenile Sandhoff disease: Complementation tests with Sandhoff and Tay-Sachs disease using polyethylene glycol- induced cell fusion. *Hum Genet* 41: 325-329

Wood S, MacDougall BG (1976) Juvenile Sandhoff disease: Some properties of the residual hexosaminidase in cultured fibroblasts. *Am J Hum Genet* 28: 489-495

Yamanaka S, Johnson MD, Grinberg A, Westphal H, Crawley JN, Taniike M, Suzuki K, *et al* (1994) Targeted disruption of the *Hexa* gene results in mice with biochemical and pathologic features of Tay-Sachs disease. *Proc Natl Acad Sci USA* 91: 9975-9979

Yoo Han-W, Astrin KH, Desnick RJ (1993) Comparison of enzyme and DNA analysis in a Tay-Sachs disease carrier screening program. *J Kor Med Sci* 8: 84-91

Zokaeem G, Bayleran J, Kaplan P, Hechtman P, Neufeld EF (1987) A shortened β-hexosaminidase α-chain in an Italian patient with infantile Tay-SAchs disease. *Am J Hum Genet* 40: 537-47

Zühlsdorf M, Imort M, Hasilik A, von Figura K (1983) Molecular forms of β-hexosaminidase and cathepsin D in serum and urine of healthy subjects and patients with elevated activity of lysosomal enzymes. *Biochem. J.* 213, 733-740